The role of Serum amyloid A in NLRP3 inflammasome activation in breast and colon cancer

By

Carla Fourie

Thesis presented in fulfilment of the requirements
for the degree of Doctor of Philosophy
in the Faculty of Science at Stellenbosch University

Supervisor: Prof AM Engelbrecht

Co-Supervisor: Prof WJS de Villiers

Co-Supervisor: Dr T Davis

April 2022

Declaration of originality

By submitting this dissertation electronically, I declare that the entirety of the work contained therein is my own original work, that I am the sole author thereof (save to the extent explicitly otherwise stated), that reproduction and publication thereof by Stellenbosch University will not infringe any third-party rights and that I have not previously in its entirety or in part submitted it for obtaining any qualification.

This dissertation includes one original paper published in a peer-reviewed journal. The development and writing of the paper was the principal responsibility of myself.

Date: April 2022

Acknowledgements

I would like to sincerely express my gratitude towards the following people:

To the kindest person I know, my supervisor Prof Engelbrecht. Thank you for all the guidance and advice, for believing in me and for providing me with the countless opportunities to become a better researcher. It has been a huge privilege to be part of CRG for all these years and I look forward to future opportunities that we may have together.

The biggest thank you to my co-supervisor Tanja Davis. Without your support since my honours, I would not be the researcher I am today. Thank you for always having an open-door, and for the assistance and guidance in and out of the lab. You and Prof have been my greatest role models. Thank you for all the help this year, even when you were 13 222 km away. A big thank you for also providing me with the animal tissues to perform my experiments.

My co-supervisor, Prof Wim de Villiers, thank you for all the support and for always taking time out of your busy schedule to stay updated with our research.

My parents, thank you for being patient with my studies while I pursue my dreams as a researcher. Words can never describe how grateful I am. Thank you for all the support, encouragement, and motivation all these years. A big thank you to my sister, Heike, for always being interested and helping me through the frustrating times. I appreciate all your support, having you nearby and all the spontaneous adventures.

My PhD-office partner in crime and friend, Manisha, for all the support, motivation in and out of the lab, inspiration, daily Mybrew walks and running last minute gels. I look forward to our future adventures as researchers together. A big thank you also to Dirk, who always willingly listened and motivated us and for lighting a braai fire during the frustrating times.

Christo, thank you for all your love, patience, encouragement, IT skills and motivation the past couple of months. Thank you for always listening and for being my best friend. Thank you for inspiring me to believe in me.

My friends, Nandri, Wian, Daleen and Jurgen, thank you for all the late-night chats, motivation, and support, it means a lot.

To the Veldsman's, thank you for being my biggest supporters for the duration of my postgraduate studies. I am forever grateful for all the motivation and encouragement. Thank you for also inviting us into your home and for taking care of us during the Covid-19 lockdown.

CRG and DSG, thank you for all the guidance and assistance during these years. A big thank you to Manisha and Niel for providing me with the tissues to perform my experiments. Thank you to Sholto, our PhD office companion, for all the advice, assistance and coffee runs.

To the staff of the Physiology department, thank you for always having an open door and providing me with the guidance and facilities to complete my studies. Thank you to Andre for also always taking time out of his busy day to assist with any problems in the lab.

Candice Snyders, from Tygerberg Medical School at Stellenbosch University, thank you for helping us with the Milliplex assay. Reggie Williams from the Division of Clinical Anatomy at Stellenbosch University, thank you for assisting us with the histopathology. Lize Engelbrecht and Kerishnee Naicker from Central Analytical Facilities (CAF) at Stellenbosch university for helping us with the imaging of our histopathology samples.

Lastly, the National Research Foundation (NRF) for providing me with funding.

Abstract

Introduction:

Cancer is a complex disease with multiple interactions targeting the organism on cellular, tissue and systemic levels. The main research focus for the past decades has been on the genome and on the molecular level where signaling pathways were dissected for the development of targeted therapies. However, in order to develop more efficient therapeutic regimes, a better understanding on systemic level is required. Over the past few years, the role of serum amyloid A (SAA) has gathered significant evidence which highlights its role in the pathogenesis of several cancers, including breast and colorectum carcinomas. To date, SAA has been shown to bind to several pattern recognition receptors, which might suggest that inflammasomes play a role in the tumour-promoting properties of SAA. Inflammasomes are cytoplasmic multiprotein complexes characterized by a sensor protein, an adaptor protein, and inflammatory caspases. However, the role of inflammasomes in cancer remain controversial. The aim of this study was therefore to investigate the role of SAA in inflammasome signaling in breast and colon cancer.

Methods:

In this 3-part animal study, tissues were subjected to immunoblotting, real-time PCR, haematoxylin and eosin staining and immunohistochemistry. For the first inflammatory model, wild-type and SAA double knockout C57BL/6 mice received 2.5% dextran sulfate sodium, which was administered for a total of 5 days. To assess tumourigenesis, colitis-associated cancer and triple negative breast cancer models were used, respectively. For colitis-associated cancer, wild-type and SAA double knockout C57BL/6 mice received an intraperitoneal injection of 12.5 mg/kg azoxymethane. After one week, dextran sulfate sodium treatment was administered at a concentration of 2.5% for a total of 5 days, followed by a recovery period of 16 days. Dextran sulfate sodium treatment was administered for a total of 3 cycles. Triple negative breast tumours were established in wild-type and SAA double knockout C57BL/6 mice by injecting EO771 cells subcutaneously at the fourth mammary fat pad. The experimental endpoint was reached when tumour volumes reached 300-400 mm^3.

Results:

In this study we have showed that in an *in vivo* model of dextran sulfate sodium induced colitis, SAA ablation exerted pro-inflammatory properties independent of the NLRP3 inflammasome. The ablation of serum amyloid A1/2 was associated with the increased expression of pro-inflammatory cytokines. In contrast, in an *in vivo* colitis-associated cancer and in a triple negative breast cancer model, the ablation of SAA suppressed canonical NLRP3

inflammasome activation, which was associated with anti-inflammatory properties. These findings suggest that during tumourigenesis, SAA functions as an endogenous damage associated molecular pattern in the tumour microenvironment.

Conclusion:

Here we show for the first time, in models of CAC and TNBC, the novel role of SAA in the activation of the NLRP3 inflammasome and the generation of pro-inflammatory cytokines, two mechanisms known to promote tumour development and metastasis. This study emphasizes the notion that the tumour-induced systemic environment acts as a critical regulator of cancer progression and metastasis. In conclusion, simultaneously targeting SAA and NLRP3 components could be beneficial for cancer treatments.

Opsomming

Inleiding:

Kanker is 'n komplekse siekte met verskeie interaksies wat die organisme op sellulêre, weefsel- en sistemiese vlakke teiken. Die hoof navorsingsdoel vir die afgelope dekades was op die genoom sowel as seinoordragpaaie op molekulêre vlak te dissekteer vir die ontwikkeling van geteikende terapieë. Om meer doeltreffende terapeutiese prosedures te ontwikkel, is 'n beter begrip op sistemiese vlak egter nodig. Oor die afgelope paar jaar het die rol van serum amiloïed A (SAA), 'n akuut-fase proteïen, hoofsaaklik deur hepatosiete geproduseer, beduidende bewyse gelewer vir die rol daarvan in die patogenese van verskeie kankers, insluitend bors- en kolorektumkarsinome. Dit is al bewys dat SAA aan verskeie reseptore bind, soos TLRs, wat voorstel dat inflammasome 'n rol speel in tumorgenese. Inflammasome is sitoplasmiese multiproteïen-komplekse wat gekenmerk word deur 'n sensorproteïen, 'n adapterproteïen en inflammatoriese kaspases. Die rol van inflammasome in kanker bly egter omstrede. Die doel van hierdie studie was dus om die rol van SAA in inflammasoom aktivering in bors- en kolonkanker te ondersoek.

Metodes:

In hierdie 3-delige dierestudie is weefsels ondersoek deur gebruik te maak van qPCR, hematoksilien- en eosienkleuring en immunohistochemie. Vir die eerste inflammatoriese model het wilde-tipe (WT) asook muise wat nie SAA gene besit nie (SAADKO), 2.5% dekstraansulfaatnatrium (DSS) ontvang, wat vir 'n totaal van 5 dae toegedien is. Om tumorgenese te ondersoek, is kolitis-geassosieerde kanker- (CAC) en trippel negatiewe borskankermodelle (TNBC) onderskeidelik gebruik. Vir CAC het wilde-tipe en SAADKO C57BL/6 muise 'n intraperitoneale inspuiting van 12.5 mg/kg asoksimetaan ontvang. Na een week is DSS-behandeling toegedien in geoutoklaveerde drinkwater teen 'n konsentrasie van 2.5 % vir 'n totaal van 5 dae, gevolg deur 'n herstelperiode van 16 dae. DSS-behandeling is vir 'n totaal van 3 siklusse toegedien. TNBC gewasse is gevestig in WT en SAADKO C57BL/6 muise deur EO771 selle onderhuids in die vetweefsel van die vierde melkklier in te spuit. Die eksperimentele eindpunt is bereik toe tumorvolumes 300-400 mm3 bereik het.

Resultate:

In hierdie studie het ons getoon dat in 'n *in vivo* model van dekstraansulfaat natrium-geïnduseerde kolitis, SAA ablasie pro-inflammatoriese eienskappe uitgeoefen het onafhanklik van die NLRP3 inflammasoom. Die ablasie van SAA1/2 was geassosieer met die verhoogde uitdrukking van pro-inflammatoriese sitokiene. In teenstelling hiermee, in 'n *in vivo* kolitis-geassosieerde kanker en in 'n trippel negatiewe borskankermodel, het die ablasie van SAA

kanonieke NLRP3-inflammasoomaktivering onderdruk, wat geassosieer was met anti-inflammatoriese eienskappe. Hierdie bevindinge dui daarop dat SAA as 'n endogene skade-geassosieerde molekulêre patroon in die tumor mikro-omgewing tydens tumorgenese, funksioneer.

Gevolgtrekking:

Hier wys ons vir die eerste keer, in modelle van CAC en TNBC, die nuwe rol van SAA in die aktivering van die NLRP-inflammasoom en die generering van pro-inflammatoriese sitokiene, twee meganismes wat bekend is om tumorontwikkeling en metastase te bevorder. Hierdie studie beklemtoon die idee dat die tumor-geïnduseerde sistemiese omgewing optree as 'n belangrike reguleerder van kankerprogressie en metastase. Ten slotte, deur gelyktydig SAA en NLRP3-komponente te teiken deur reseptore te inhibeer of deur stroomafwaartse seinoordrag meganismes te voorkom, kan dit voordelig wees vir kankerbehandelings.

List of publications

- **Fourie C.**, Davis T., Kriel J & Engelbrecht A-M, 2018. The paracrine effects of fibroblasts on Doxorubicin-treated breast cancer cells. *Experimental cell Research*: 15; 381(2):280-287.

- **Fourie C**., Davis T., Shridas P., De Villiers WJS & Engelbrecht A-M., 2020. Serum amyloid A and inflammasome activation: a link to breast cancer progression? *Cytokine and Growth factor reviews*; 59:62-70.

- Van der Merwe M., Van Niekerk G., **Fourie C.**, Du Plessis M & Engelbrecht A-M, 2021. The impact of mitochondria on cancer treatment resistance. *Cellular Oncology*; 44:983-995.

- Du Plessis M., **Fourie C**., Riedemann J., De Villiers WJS & Engelbrecht A-M, 2021. Cancer and Covid-19: Collectively catastrophic. *Cytokine and Growth factor reviews*; https://doi.org/10.1016/j.cytogfr.2021.10.005.

Table of Contents

List of Figures

List of Tables

List of Abbreviations

A

AIM-	Absent in melanoma-2
AOM-	Azoxymethane
APP-	Acute phase protein
APR-	Acute phase response
ASC-	Apoptosis-associated speck-like protein containing a CARD
ATP-	Adenosine triphosphate

B

BMDM-	Bone marrow-derived macrophages

C

CAC-	Colitis-associated cancer
CAF-	Cancer associated fibroblast
CANTOS-	Canakinumab Anti-inflammatory Thrombosis Outcomes Study
CAPS-	Cryopyrin-associated periodic syndromes
COX2-	Cyclooxygenase 2
CRC-	Colorectal cancer

D

DAMP-	Damage associated molecular pattern
DNA-	Deoxyribonucleic acid
DSS-	Dextran sodium sulfate

E

ECM-	Extracellular matrix
EMT-	Epithelial to mesenchymal transition
ER-	Endoplasmic reticulum
ERK-	Extracellular signal-regulated kinase

F

FDA-	US Food and Drug administration
FGF-	Fibroblast growth factor

G

GI- Gastrointestinal tract
GSDMB- Gasdermin B

H

HCC- Hepatocellular carcinoma
HER2- Human epidermal growth factor receptor 2
HMGB1- High mobility group box 1
HNSCC- Head and neck squamous cell carcinomas

I

IBD- Inflammatory bowel disease
IκB- Nuclear factor of kappa light polypeptide gene enhancer in B-cells inhibitor
IL- Interleukin
IL-1R- Interleukin-1 receptor
IRAK- Interleukin-1 receptor-associated kinases

K

KO- Knock-out

L

LPS- Lipopolysaccharide

M

MAPK- Mitogen-activated protein kinase
MMP- Matrix metalloproteinases
MRI- Magnetic resonance imaging
MYD88- Myeloid differentiation factor 88

N

NFκB- Nuclear factor kappa beta
NLR- NOD-like receptor
NO- Nitric oxide
NOD- Nucleotide-binding and oligomerization domain
NSCLC- Non-small cell lung cancer

P

PAMP- Pathogen associated molecular pattern

PRR-	Pattern recognition receptor

R

RAGE-	Receptor for advanced glycation end products
RNA-	Ribonucleic acid
ROS-	Reactive oxygen species

S

SAA-	Serum amyloid A
SAADKO-	Serum amyloid A double knockout

T

TIR-	Toll/IL-1 receptor domain
TIRAP-	Toll/interleukin-1 receptor domain-containing adapter protein
TLR-	Toll-like receptor
TME-	Tumour microenvironment
TNF-	Tumour necrosis factor
TRAF-	TNF receptor-associated factor
TRAM-	TRIF-related adaptor molecule
TRIF-	TIR-domain-containing adapter-inducing interferon

V

VEGF-	Vascular endothelial growth factor

W

WT-	Wild-type

Units of measurement

A	–	Amps
Bp	–	base pairs
g	–	gram
g/mL	–	grams per millilitre
Hrs	–	hours
Kb	–	kilobases
kDa	–	kilodalton
l	–	litre
min	–	minute
mg	–	milligram
ml	–	millilitre
mm^3	–	cubic millimetre
mM	–	millimolar
ng	–	nanogram
nM	–	nanomolar
nm	–	nanometre
^oC	–	degree Celsius
µg/µl	–	microgram per microlitre
µl	–	microlitre
µM	–	micromolar

Chapter 1

Literature Review

1.1 Introduction: The Hallmarks of Cancer

Cancer is a complex disease with multiple interactions targeting the organism on cellular, tissue and systemic levels. The main research focus for the past decades has been on the genome and on signaling pathways which were dissected for the development of targeted therapies. However, in order to develop more efficient therapeutic regimes, a better understanding at systemic level is also required. Hanahan and Weinberg first described the hallmarks of cancer that provided a logical framework for understanding the diversity of neoplastic diseases: the hallmarks include sustaining proliferative signaling, evading growth suppressors, resisting cell death, enabling replicative immortality, inducing angiogenesis, and activating invasion and metastasis (Hannahan & Weinberg, 2011). Underlying these hallmarks are genome instability, which generates the genetic diversity that expedites their acquisition, and inflammation, which fosters several hallmark functions. Although the interaction between stromal inflammation and cancer progression is well known, the systemic link driving the activation of the molecular pathways in these processes remains to be elucidated. Further contributing to the complex dynamics of inflammation and cancer, local inflammation is present in the stroma of many tumours and inflammatory cells and cytokines may be involved in almost every aspect of cancer progression, including the ability of cancer cells to metastasize to other parts of the body. High serum concentrations of inflammatory cytokines are also involved in systemic inflammation and play an important role in the metastatic process, especially in cancers of the lung, breast, colon-rectum and pancreas (Hoshino *et al*., 2020). For the purpose of this study, inflammatory mechanisms in breast and colon associated cancers will be elaborated on.

1.2 An introduction to Breast cancer

Breast cancer is the most frequently diagnosed cancer and the leading cause of cancer-related deaths in women worldwide (DeSantis *et al*., 2019). Breast cancer is often metastatic and can spread to distant organs such as bone, lungs, liver and the brain, which mainly contributes to the difficulty to develop successful treatment options. Early diagnosis of this disease can result in a good prognosis and high survival rate. A mammogram is widely used as a screening approach to detect breast cancer, but other screening methods such as Magnetic Resonance Imaging (MRI), which is more sensitive than a mammogram, is also

utilized. Risk factors to develop breast cancer include sex, age, family history, gene mutations and unhealthy lifestyle habits (Drukteinis *et al*., 2013).

Breast cancer was formerly classified based on available histopathological and molecular characteristics such as tumour size, tumour staging and phenotypic characteristics. However, these classifications are limited in their prognostic value since these factors do not always correlate with disease progression, therapy and recurrence. Since tumour growth, invasion, motility, recurrence and treatment resistance all depend on different metabolic pathways in breast cancer, classification based on molecular characterization, such as genetic profiling and biomarker identification, provides a more accurate assessment of the prognosis and guides the development of optimal treatment strategies (Reis-Filho *et al*., 2010; Weigelt *et al*., 2010). Molecular classification based on disease-related aberrant receptor expression has guided the molecular categorization of breast cancers into the following broad subtypes (Figure 1.1):

Estrogen-receptor (ERα) positive – 80% of breast cancers
Overexpressed ERα and increased blood estrogen levels are the main driving forces of these cancers, contributing to hyperplasia of mammary cells. ERα-positive breast cancers are classified as Luminal subtype and further subclassified as Luminal 1 or Luminal 2, based on the expression of human epidermal growth factor receptor 2 (HER2) (Bardou *et al*., 2003; Cui *et al*., 2005).

Progesterone-receptor (PR) positive – 30% of breast cancers
In PR-positive cancers, the binding of either of two progesterone isoforms to PR regulates the expression of several genes implicated in carcinogenesis of the breast and other tissues (Daniel *et al*., 2011). PR-positive breast cancers are classified as Luminal subtype and further subclassified as Luminal 1 or Luminal 2, based on the expression status of HER2.

HER2 over-expressing – 22% of breast cancers
HER2 or also referred to as ErbB2, is a receptor tyrosine kinase and an activator of cell proliferation and de-differentiation (Ross *et al*., 2009). Overexpression, or the lack of HER2 has been reported as one of the most effective prognostic indicators for early-stage or metastatic breast cancer (Slamon *et al*., 2001). Cancers with HER2 overexpression are classified as Luminal or non-Luminal, depending on the expression status of ERα and PR.

Triple negative (TN) – 16% of breast cancers

Triple-negative expression status, which features no detectable or abnormal over-expression of ERα, PR or HER2, is associated with relatively poor prognosis and frequently presents at an advanced stage of progression (Bauer *et al*., 2007). These tumours are challenging to target, often develop therapeutic resistance and have high chances of recurrence. The TN subtype typically features a poorly differentiated, basal-like phenotype (TNBC), but a non-basal subtype is also observed (Ovcaricek *et al*., 2011).

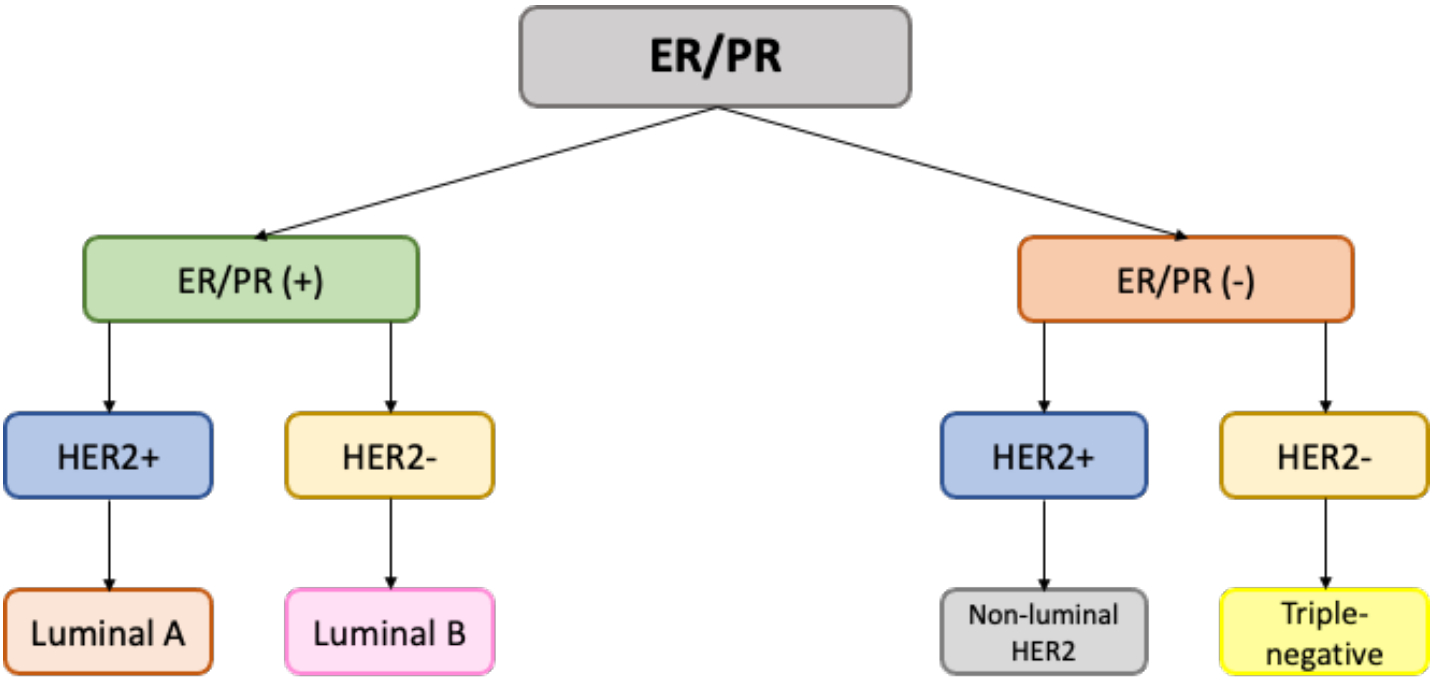

Figure 1.1: **Simplified classification of breast cancer subtypes.**

Abbreviations: ER: Estrogen receptor; **HER2**: Human epidermal growth factor receptor 2; **PR**: Progesterone receptor

Taking the above into consideration, it is clear that breast cancer is a complex disease, which makes the development of targeted therapies difficult, and is also the reason why treatment resistance often occurs. Despite all the research, it is surprising how little is known about the role of the immune system in breast cancer development, as compared to other cancers, especially since cancer-related inflammation has emerged as one of the hallmarks of cancer. In contrast to breast cancer, the connection between inflammation and colon-associated

cancers are well established where inflammatory bowel disease (IBD) is an important risk factor for the development of colon cancer (Eaden *et al*., 2001). However, the molecular mechanisms by which inflammation promotes cancer development are still being investigated and could differ between colitis-associated and other forms of colorectal cancer.

1.3 An introduction to Colon cancer

As mentioned above, it is now commonly accepted that inflammation contributes to the initiation, promotion and progression of tumour development in colon-associated cancers. In fact, one of the best clinically characterized examples of the association between inflammation and carcinogenesis is the development of colon cancer in patients suffering from ulcerative colitis, which is a common form of inflammatory bowel disease (IBD) (Eaden *et al*., 2001).

Colorectal cancer (CRC) is the third most common cancer diagnosed in both men and women worldwide and presents with a high mortality rate, which is attributed to rapid cancer progression with late diagnosis at an advanced tumour stage (Siegel *et al*., 2017). The prognosis of CRC patients is generally good for early-stage cancer; however, most cases are diagnosed at later stages, and it is estimated that 40% of CRCs progress to fatal metastases (Tsikitis *et al*., 2014). It is estimated that in 2021, 104 270 new cases of colon cancer and 45 230 cases of rectal cancer will be diagnosed in the US (Siegel *et al*., 2021). One of the predisposing factors for CRC is chronic non-resolving IBD, such as Crohn's disease and ulcerative colitis, which is usually associated with the duration and degree of mucosal inflammation. Colitis-associated cancer (CAC), an inflammation-associated form of CRC has been recognized as a form of IBD. Although it is rare (2-3% of all CRC cases), it represents an important mechanistic link between inflammation and cancer (Parian and Lazarev, 2015). The exact etiology of CAC is not known, it has however been hypothesized that a defective innate immune response might be a primary etiological factor (Asquith and Powrie, 2010). The innate immune response plays an important role in controlling the intestinal microbiota, maintaining homeostasis and provides initial resistance to invading pathogens (Ignacio *et al*., 2016). Various cellular components of the innate immune system such as epithelial cells, neutrophils and macrophages are located within the intestinal wall. These cellular populations as well as cytosolic pattern recognition receptors (PRRs) are responsible for the surveillance of microbial occupants of the intestine.

Several mouse models currently exist for the study of colitis-associated cancer. Dextran sulfate sodium (DSS), an agent with direct toxic effects on the colonic epithelium, can be administered to mice in their drinking water in multiple cycles to create a chronic inflammatory state. Tumour development in this DSS model can be accelerated if administered in a pro-carcinogenic setting, where the mice are pre-treated with azoxymethane (AOM) (Tanaka *et*

al., 2003). In the acute DSS colitis model (referred to as acute colitis in this study), mice are fed with DSS polymers in their drinking water which induces a colitis characterized by diarrhea, bloody feces, weight loss and a histological picture of inflammation and ulceration, similar to human IBD.

Chronic, idiopathic inflammatory disorders such as IBDs are characterized by significant inflammation of the small intestine as well as the colon. Increased levels of pro-inflammatory cytokines such as interleukin-1β (IL-1β), IL-6, IL-18, and tumour necrosis factor-alpha (TNF-α) are detected in plasma of IBD patients and correlate with the severity of inflammation (Ishiguru, 1999). It has been suggested that IL-1β is essential in the early phase of the inflammatory cascade, which results in an inflamed colon. IL-1β, which is regulated by inflammasomes for secretion, is therefore an important pro-inflammatory cytokine that contributes to the pathogenesis of IBD.

Furthermore, increased plasma concentrations of the above mentioned pro-inflammatory cytokines induce the secretion of serum amyloid A (SAA), an acute phase protein, which is most commonly produced in the liver. Apart from the increased expression of pro-inflammatory cytokines associated with cancer development, SAA also possesses pro-inflammatory properties that induce the release of several cytokines from different cell types, including cancer cells, into the tumour microenvironment (TME).

1.4 The expression and regulation of Serum amyloid A (SAA) in cancer

Inflammation is implicated in the etiology of many cancers, where several inflammatory molecules are associated with cancer growth and development. One of these inflammatory molecules is serum amyloid A (SAA), an acute phase protein (APP) primarily produced by hepatocytes and adipose tissue in the liver (Uhlar & Whitehead, 1999). These APPs are endogenous molecules that amplify innate immune responses (Uhlar & Whitehead, 1999). SAA proteins are encoded by four separate genes on chromosome 11. In humans, SAA exists in an acute phase form, *SAA1* and *SAA2*, while human *SAA3* is a pseudogene and *SAA4* is constitutively expressed at lower levels (Uhlar *et al*., 1994) (Table 1.1). In humans, the expression of SAA1 and SAA2 can be induced by several inflammatory signals, including pro-inflammatory cytokines such as IL-1β, IL-6 and gram-negative bacteria such as *lipopolysaccharides* (LPS). In mice, SAA1 and SAA2 are predominantly produced by hepatocytes, SAA3 encodes a functional SAA protein and is also one of the major forms of SAA in inflammatory tissues (Gabay & Kushner, 1999). It was initially thought that the liver was the only site of SAA synthesis, but a variety of extrahepatic tissues including the breasts,

stomach, small and large intestine, prostate, lung, pancreas, kidney, tonsil, thyroid, pituitary gland, placenta, skin epidermis and brain neurons also express SAAs (Urieli-Shoval, 1998).

Table 1.1: SAA variants in humans and mice.

SAA Variants	**Function**	
	Human	**Mice**
SAA1	APR protein; inducible	APR protein; inducible
SAA2	APR protein; inducible	APR protein; inducible
SAA3	Pseudogene	APR protein; inducible
SAA4	Constitutively expressed	Constitutively expressed

Abbreviations: APR: acute phase protein; **SAA**: serum amyloid A

At the primary sequence level, the human and mouse SAA proteins share high sequence homology, which suggests that these proteins may have similar functions, but their modes of expression vary. Although mouse SAA3 has a different expression profile from that of SAA1 and SAA2, its sequence is as homologous to human SAA1 as mouse SAA1 and SAA2. The sequence homology suggests that the functions of SAA3, expressed upon induction by inflammatory cues in various mouse tissues, may be similar to those of human SAA1 and SAA2 (Figure 1.2) (Fan *et al*., 2019).

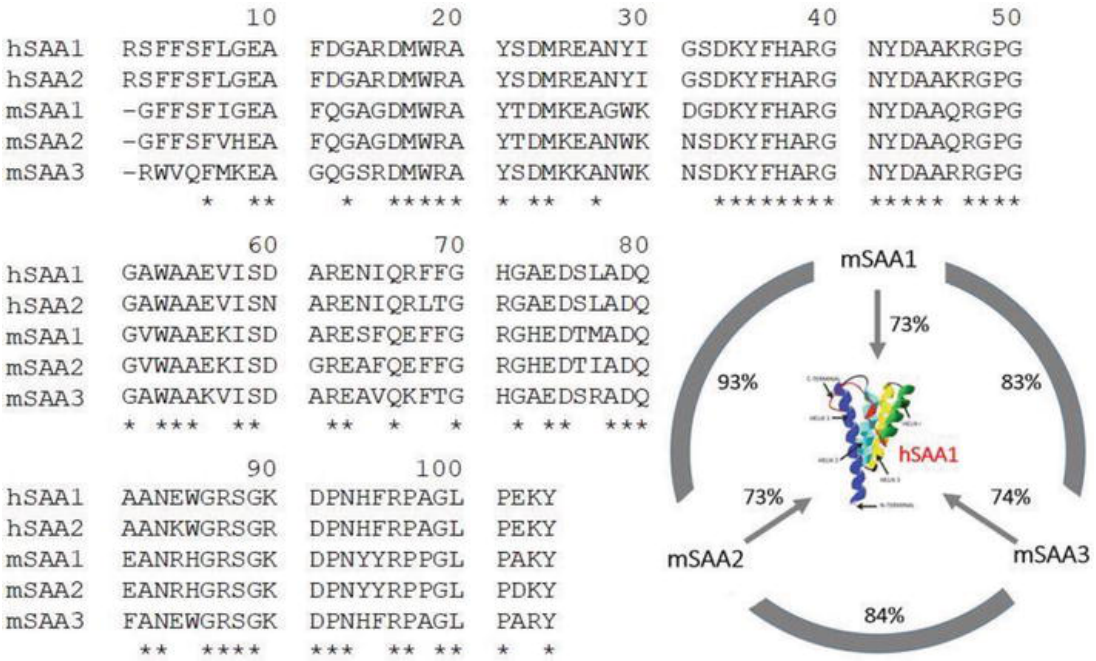

Figure 1.2: Comparison of the amino acid sequence of human and mouse inducible SAA proteins. The amino acid sequences of mature SAA protein without signal peptides are shown and identical amino acids are marked with asterisks (*). Inset shows the percent of sequence homology between the 3 inducible mouse SAA proteins and human SAA1 (Fan *et al*., 2019).

The expression of SAA is primarily regulated at transcriptional level by cytokines such as TNF-α, IL-1 and IL-6 or by glucocorticoids that bind to their corresponding receptors to induce a series of transcription factors. To date, SAAs have been shown to bind to toll-like receptors2/4 (TLR2/4), formyl peptide receptor 2 (FPR2), scavenger receptor B1 (SR-B1) and receptor for advanced glycation end products (RAGE) on immune cells, endothelial cells and macrophages (Figure 1.3). Consequently, these cells secrete a variety of cytokines and chemokines, which can induce cancer promoting effects. One example includes the ability of purified SAA from plasma to exert cytokine-like properties by promoting the secretion of IL-1β from lymphocytes, granulocytes, monocytes and macrophages (Patel *et al*., 1998; Preciado-Patt *et al*., 1998; Furlaneto & Campa, 2000; He *et al*., 2006).

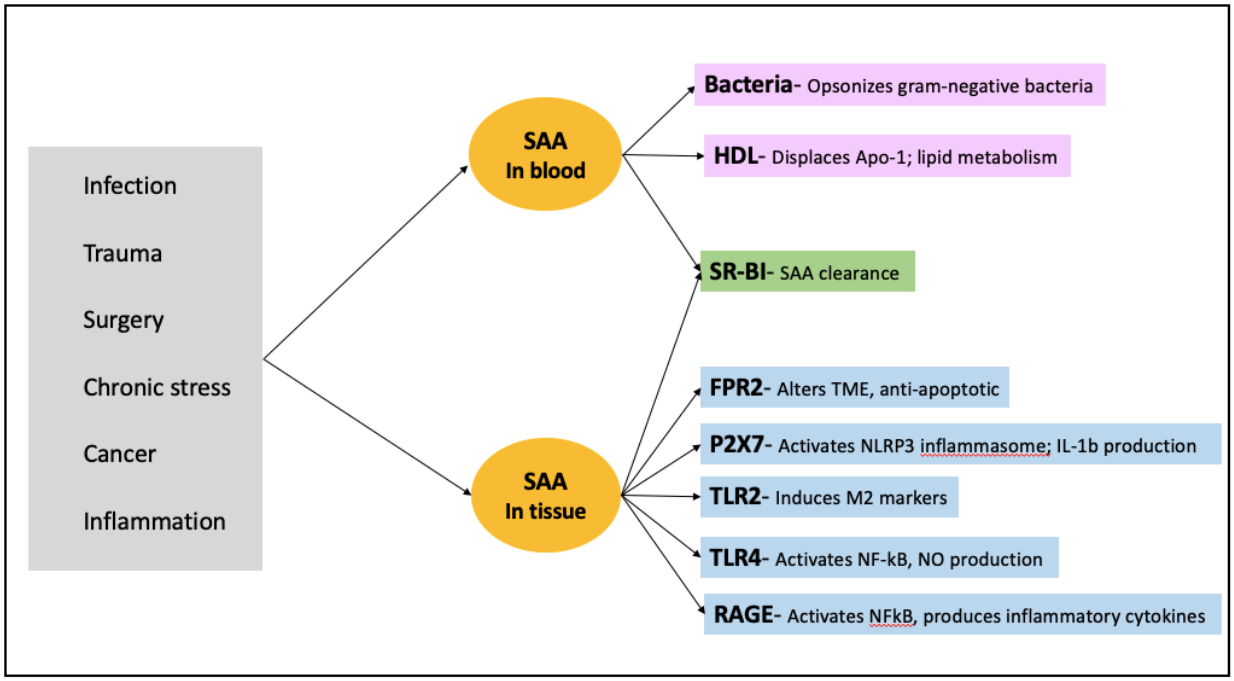

Figure 1.3: A summary of SAA synthesis and its associated receptors. SAA is secreted into the blood or produced by tissue in response to various stimuli, such as inflammation and cancer. Once it binds to its associated receptors, it can induce several effects including alteration of the TME and NLRP3 inflammasome activation. **Abbreviations: FPR**: Formyl peptide receptor; **HDL**: High density lipoprotein; **P2X7**: P2X purinoceptor 7; **RAGE**: Receptor for advanced glycation end products; **TLR**: Toll-like receptor

Other biological activities of SAA in inflammation include acting as an extracellular matrix (ECM) adhesion protein, enhancing the production of matrix metalloproteinases (MMPs), promoting the migration and infiltration of leukocytes, angiogenesis stimulation and the production of inflammatory cytokines (Badolato *et al*., 1994; Migita *et al*., 1998; Lee *et al*., 2005). It has been proposed that a direct relationship exists between SAA concentrations and tumour grading where increased SAA levels are observed in stage IV patients with lung, breast and melanoma cancer when compared to stage I and benign tumours (Rayne & Cooper, 1983; O'Hanlon *et al*., 2003). SAA is therefore considered as a marker to monitor tumour progression (Vlasova & Moshkovskii, 2006). One theory which explains SAA's contribution to tumour pathogenesis suggests that SAA can act as an ECM adhesion protein (Malle *et al*., 2010). The ECM is a highly organized network of proteins, proteoglycans and glycoproteins, which form a molecular scaffold to provide binding sites for cells. SAA has binding sites for ECM components such as heparin/heparan sulfate and has YIGSR-like (the Tyr-Ile-Gly-Ser-Arg

peptide derived from laminin) and RGD-like (Arg-Gly-Asp) adhesion epitopes (residues 29–42) that correspond to laminin and fibronectin cell-binding domains, respectively. SAA can interact with the ECM and change its affinity to different cell types and therefore also plays an important role in cancer metastasis (Ancsin & Kisilevsky, 1999).

1.5 Metastasis of tumour cells

Metastasis is often the primary cause of mortality in cancer patients and treatment strategies are limited once this occurs (Siegel *et al*., 2021). Metastasis is defined as the development of a secondary malignant growth at a distance from the primary site of cancer and is therefore a multi-step process (Hanahan & Weinberg, 2000). Tumour cells are able to exit the primary tumour and invade into the surrounding tissue, enter blood or lymphatic vessels, be carried to a distant site, exit the vessel and re-establish a tumour mass in a new environment. This process requires the interaction of many cell types as well as extracellular environments. Several studies have indicated that breast cancer metastasizes to many distant organs, including bone, liver, lung and brain (Dent *et al*., 2009; Kennecke *et al*., 2010). Early in malignant cell transformation, disseminating tumour cells (DTCs) intravasate into the local vasculature at the primary tumour site. Once these DTCs enter circulation, they can extravasate into distant tissues or organs. Once lodged into these tissues/organs, DTCs are influenced by their microenvironment, which supports DTC survival. The formation of a pro-metastatic niche in distant organs/tissues plays a key role in DTC survival and can also signal for latent metastatic outgrowth in dormant cancer cells (Lambert *et al*., 2017; Doglioni *et al.*, 2019). However, the mechanisms that direct the formation of a pro-metastatic niche is dependent on cancer type. For example, S100a9, a Ca^{2+} binding protein belonging to the S100 family, regulates metastatic outgrowth in the lung and SAA regulates the formation of a pro-metastatic niche in the liver. Furthermore, ECM deposition within the pro-metastatic niche supports enhanced DTC migration across the endothelial layer to extravasate into the tissue parenchyma, which can also be influenced by SAA. Michaeli and co-authors reported that SAA enhances plasminogen activation in colon cancer (HT-29 cells) (Michaeli *et al*., 2008). Plasminogen activation can result in ECM degradation and tissue remodeling, which is associated with inflammation and tumour metastasis. One of the main causes of ECM alterations during cancer development is its degradation by MMPs, which promotes epithelial-mesenchymal transition (EMT) and genomic instability. This newly acquired phenotype is characterized by the acquisition of fibroblast-like elongated morphology, loss of cell polarity, enhanced migratory and invasive capacity, downregulation of epithelial markers such as adherens and tight junctions (E-cadherin and claudins) and the upregulation of genes normally expressed by mesenchymal cells such as α-smooth muscle actin (α-SMA), vimentin,

collagens, fibronectin, and the EMT-orchestrating transcription factors, such as Twist, Snail and Slug (Kalluri & Weinberg, 2009) (Figure 1.4).

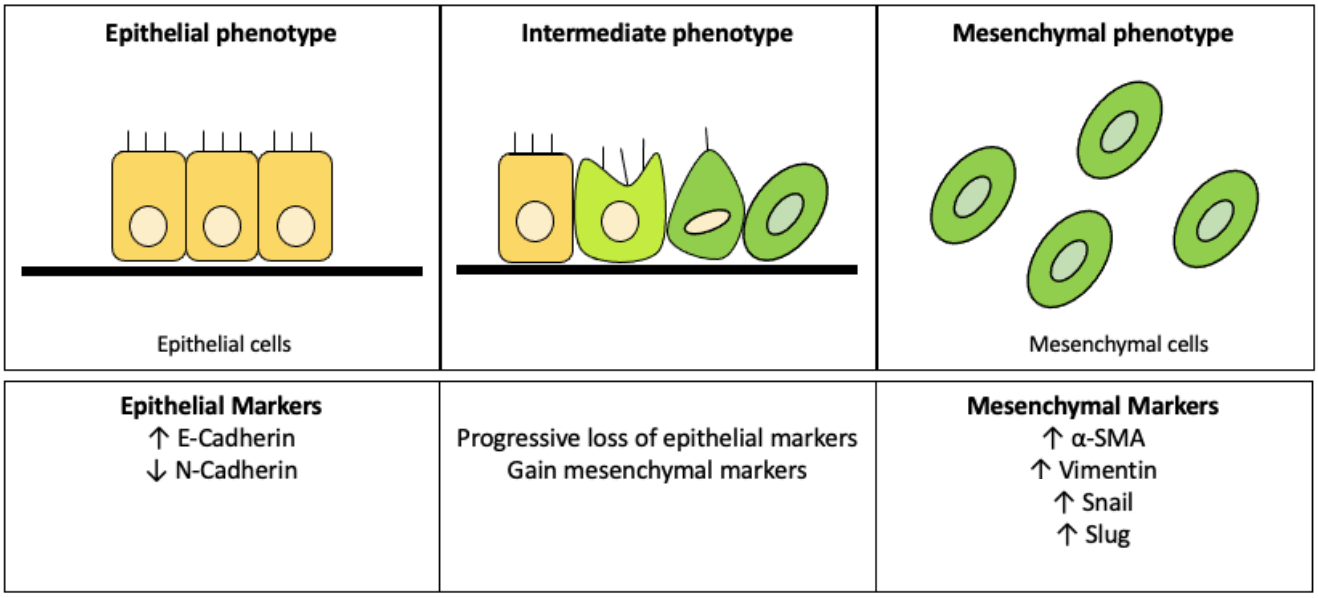

Figure 1.4: Epithelial to mesenchymal transition in cells (adapted from Wu *et al*., 2016).

EMT can therefore promote the invasion and metastasis of a variety of cancer cells, including colorectal cells. Different inflammatory cytokines secreted during IBD, such as IL-1β, mediates the activation of EMT through several pathways, which can promote the occurrence and development of CAC. This once again highlights the complex link between inflammation and inflammatory associated cancers. As mentioned earlier, the exact etiology of CAC is unknown, but several studies have implicated the inflammasome pathway in the progression of colitis and CAC, where TLRs and NOD-like receptor (NLR) proteins have emerged as important mediators of gastrointestinal inflammation and homeostasis (Allan *et al*., 2010; Lee *et al*.,2018). NLRs are highly conserved cytosolic pattern recognition receptors (PRRs) that plays an important role in surveying the intracellular environment for the presence of infection, noxious substances, and metabolic perturbations. Sensing of these danger signals by NLRs leads to their oligomerization into large macromolecule scaffolds, referred to as inflammasomes.

1.6 Mechanisms of inflammasome activation

The inflammasome is a multi-protein complex characterized by a nucleotide-binding and oligomerization domain (NOD)-like receptor (NLR), an adaptor protein ASC (apoptosis-associated speck-like as protein containing a CARD domain) and procaspase-1 (Karan, 2018). Surveillance of homeostatic parameters by NLRs allows the inflammasome to respond to a wide range of stimulatory pathogen associated molecular patterns (PAMPs) and damage associated molecular patterns (DAMPs), including microbial deoxyribonucleic acid (DNA), ribonucleic acid (RNA), cell wall components, endogenous factors and environmental contaminants. While several NLRs have been identified, inflammasomes containing the NLR family pyrin domain containing 3 (NLRP3) are the best characterized.

NLRP3 Inflammasome activation is a two-step process triggered by various PAMPs and DAMPs. The first step, referred to as the "**priming signal**", is when toll-like receptors (TLRs) are auto phosphorylated by exposure to PAMPs or DAMPs, which results in nuclear factor kappa beta (NFκB) activation. This nuclear factor stimulates the transcription and expression of NLRP3 inflammasome components, pro-IL-1β and pro-IL-18, the level of which is otherwise relatively low in many cell types. The second step, referred to as "**activation**" is where the functional NLRP3 inflammasome is activated by initiating the assembly of the multi-protein complex in the cytosol, leading to caspase-1 activation and IL-1β and IL-18 maturation (Jo *et al*., 2016). Caspase-1 also cleaves gasdermin D (GSDMD), generating a N-terminal fragment that translocates from the cytosol to the plasma membrane and forms pores through which IL-1β and IL-18 are secreted. However, excessive pore formation during infectious and sterile conditions can also result in cell rupturing (referred to as pyroptosis), resulting in cell death and the release of pro-inflammatory contents such as IL-1β, IL-18 and certain DAMPs into the extracellular environment (Ding *et al*., 2016). Other IL-1 family members can potentially be secreted following inflammasome activation, including IL-1α and IL-37, which is supported by the finding that a caspase-1 site also exists for IL-33 and IL-37 precursors. However, non-caspase mechanisms have shown to generate active forms of these cytokines (Dinarello *et al*., 2018; Chan & Schroder, 2020). In contrast to IL-1β, not much is known about the activation and secretion of IL-1α, a close homologue to IL-1β. It is suggested that IL-1α serves as a danger signal which is passively released from dying cells, but it has also been shown that NLRP3 inflammasome agonists such as uric acid crystals induce IL-1α cleavage and secretion, resulting in the co-secretion of both IL-1β and IL-1α (Yazdi & Drexler, 2013).

The main mechanisms that control NLRP3 inflammasome activation are as follows: the **channel model**, which is triggered by extracellular ATP that is released at the site of cellular

injury. Adenosine triphosphate (ATP) activates the P2X7 ATP-gated ion channel, causing a rapid K^+ efflux from the cell, which is a requirement for inflammasome activation (Katsnelson *et al*., 2015; Broz & Dixit, 2016). The **lysosome rupture model**, which is relevant for inflammasome activation by large particulate activators such as alum and silica crystals, which can often be inhaled. Inefficient clearance of such particulate matters leads to lysosome rupture, resulting in the release of cathepsin-B into the cytoplasm which will trigger the activation of the inflammasome (Tschopp & Schroder, 2010). The third model involves the **generation of reactive oxygen species (ROS)**. All NLRP3 inflammasome activators, including ATP and particulate matters, trigger the generation of short-lived ROS, while treatment with ROS scavengers has been shown to block the activation (Figure 1.5). These mechanisms are not exclusive from each other, for example, lysosomal rupture could result in the generation of ROS and there could be other yet unknown mechanisms leading to the activation of the inflammasome.

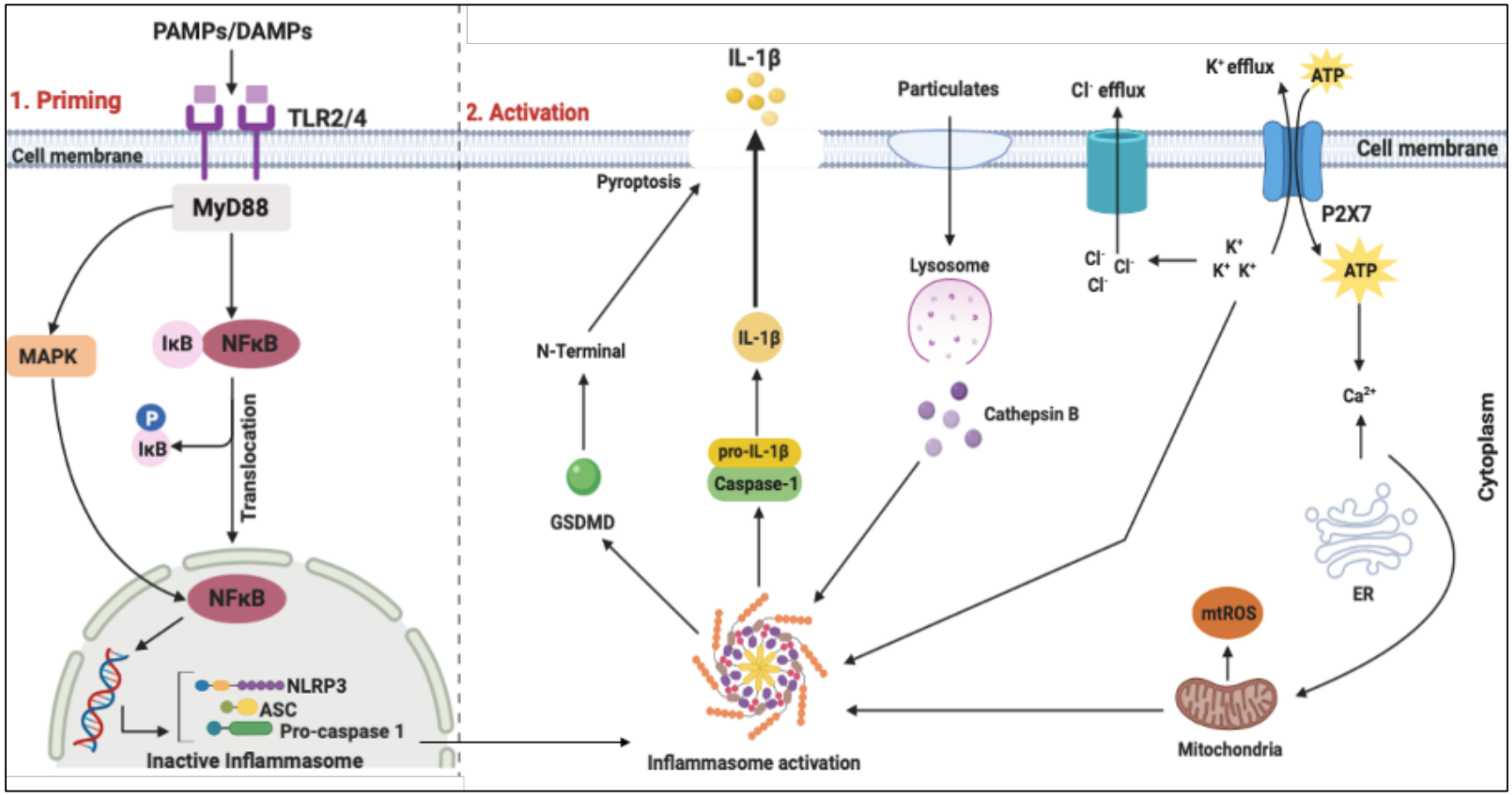

Figure 1.5: Priming and activation of the NLRP3 inflammasome. During the priming step, PAMPs or DAMPs bind to TLRs on the cell membrane. Once binding occurs, it induces the downstream activation of NFκB via MyD88, either by phosphorylating IκB or by activating MAPKs, resulting in transcriptional upregulation of inflammasome components including NLRP3 and procaspase-1. During the activation step, oligomerization of the inflammasome into its active state takes place through various signaling pathways, allowing pro-IL-β to bind to caspase-1, resulting in the production and secretion of IL-1β (Jo *et al*., 2016). **Abbreviations: DAMP**: Damage associated molecular pattern; **ER**: Endoplasmic reticulum; **GSDMD**: Gasdermin D; **MAPK**: Mitogen activated protein kinase; **P**: Phosphorylate; **PAMP**: Pathogen associated molecular pattern; **TLR**: Toll-like receptor

IL-1 cytokines play important roles in regulating the inflammatory processes by binding to IL-1Rs on most cell types (Garlanda *et al*., 2013). Upon activation, mature secreted IL-1β binds to and activates IL-1R1 on cell surfaces (such as immune and cancer cells) in an autocrine or paracrine manner (Boraschi *et al*., 2018). Activation of cytosolic toll- and IL-1R-like domains result in the recruitment of MyD88 and interleukin-1 receptor associated kinase-4 (IRAK4). IRAK4 undergoes autophosphorylation, which results in the phosphorylation of IRAK1 and IRAK2 and the recruitment of TNF receptor-associated factor 6 (TRAF6). IRAK1/2 and TRAF6 then dissociate from the receptor complex and activate NFκB. Once NFκB has translocated to the nucleus, it can induce the transcription of other inflammatory genes, such as *interleukin-6* (*IL-6*), *interleukin-8* (*IL-8*) and *cyclooxygenase-2* (*COX2*) (Brough *et al*., 2011) (Figure 1.6).

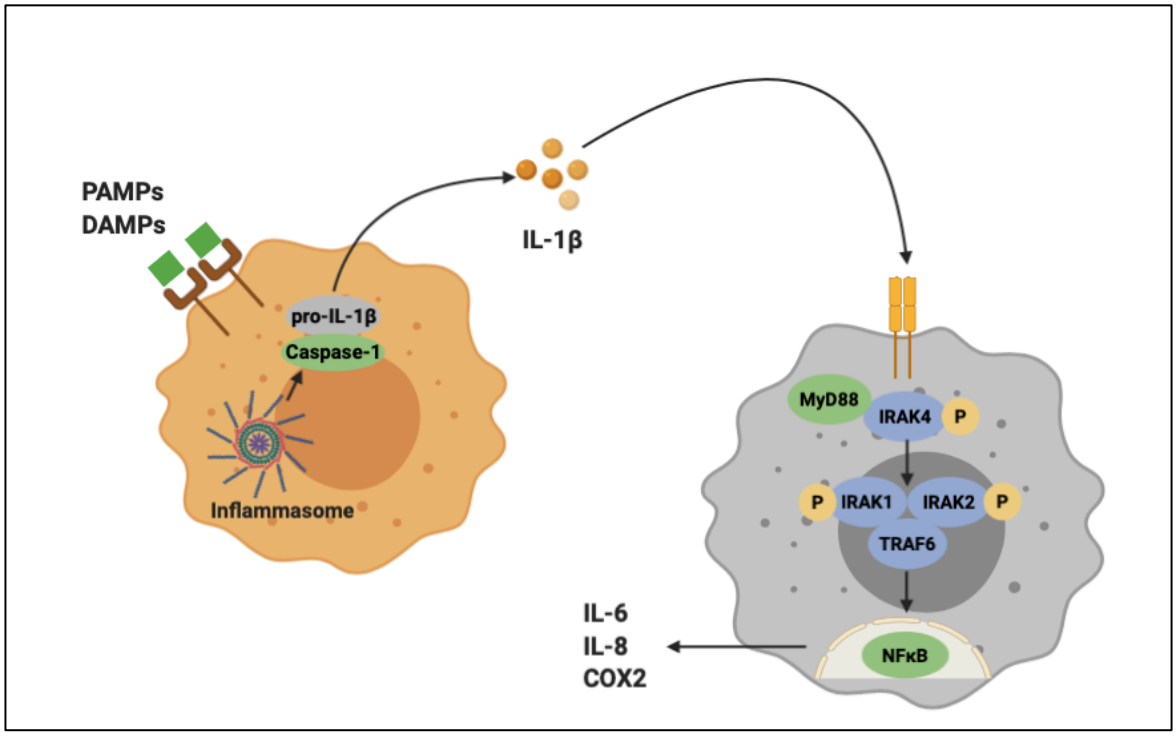

Figure 1.6: IL-1β signaling in cells. IL-1β signaling is initiated by the binding of PAMPs and DAMPs to receptors on the cell membrane, resulting in the activation of the NLRP3 inflammasome. Following cleavage and activation, IL-1β is then released by the cell and binds to IL-1R1 on another cell, inducing NFκB-mediated transcription of pro-inflammatory cytokines (Fourie *et al*., 2021). **Abbreviations: COX**: Cyclo-oxygenase; **DAMP**: Damage associated molecular pattern; **P**: Phosphorylate; **PAMP**: Pathogen associated molecular pattern

Studies have reported that epithelial activation of NFkB is critical for the development of CAC, resulting in a pro-inflammatory environment (Greten, 2004). It is also well documented that NLRP3 is an aggravating factor for inflammation and induces damage of the intestinal mucosa in IBD (Zhen *et al*., 2019)

1.6.1 Inflammasome activation in colon cancer

Polymorphisms of the *NLRP3* gene has been associated with poor survival in CAC patients, but the processes and specific role of NLRP3 in colon tumourigenesis is not well understood. In DSS/AOM murine models of CAC, genetic ablation of the inflammasome suggests that these inflammasomes act to suppress intestinal inflammation associated tumourigenesis by inhibiting cellular proliferation and promoting cell death (Karki *et al*., 2017). In fact, mice deficient in inflammasome components including ASC and caspase-1 exhibit increased colitis and tumourigenesis when compared to wild-type mice.

As mentioned, IL-1β and IL-18 play important roles as mediators of the mucosal inflammatory response. As such, CAC is characterized by the increased expression of IL-1β and IL-18, which is secreted after NLRP3 inflammasome activation. The role of IL-1β in the pathogenesis of colitis has been well established where IL-1β can induce several cellular activities such as proliferation, differentiation and apoptosis of immune and non-immune cells (Ning *et al*., 2015). Studies have shown that IL-1β secretion is upregulated in the sera of patients with IBD as well as in mice subjected to DSS-induced colitis (Bauer *et al*., 2010). Evidently, during chronic administration of DSS over four weeks, caspase-1 knockout mice presented with an almost complete absence of colitis. This was accompanied by a significant reduction of IL-18 and IL-1β in the colon (Siegmund, 2002).

Interestingly, in contrast to IL-1β, it has been reported that IL-18 suppresses colitis and CAC. IL-18 signaling therefore limits the development of intestinal inflammation. Takagi and authors reported that mice deficient for IL-18 were more susceptible to DSS-induced colitis and was associated with higher mortality rates and more severe histopathological changes (Takagi *et al*., 2003). MyD88 KO mice, which are defective in IL-1β and IL-18, showed increased colonic epithelial proliferation and colorectal tumourigenesis (Salcedo *et al*., 2010). In an acute colitis model induced by a 5-day treatment with 5% DSS, IL-18$^{-/-}$ mice had a higher inflammatory histology score when compared to wild-type controls. Increased frequency of tumour growth was also observed in IL-18$^{-/-}$. However, similarly to IL-1β, IL-18 performs dual functions in tumourigenesis and the topic remains controversial.

The function of the NLRP3 inflammasome in human cancers vary according to tumour type, where protective anti-tumourigenic as well as a pro-tumourigenic roles have been reported.

The role of NLRP3 in CAC is mainly reported as a negative regulator (Allen *et al*., 2010) (Table 1.2).

Table 1.2: The contrasting roles of the NLPR3 inflammasome in cancer.

Pro-tumourigenic	Mechanism of action	Anti-tumourigenic	Mechanism of action
Breast cancer	Increased NLRP3 and IL-1β promotes an inflammatory microenvironment (Guo *et al*., 2016).	**Colitis-associated cancer (CAC)**	Deficiencies in NLRP3 and caspase-1 causes increased morbidity by increased IL-1β and IL-18 secretion (Allen *et al*., 2010).
Colon cancer	Increased NLRP3 during EMT (Wang *et al*., 2016).	**Colorectal cancer (CRC)**	Decreased NLRP3 or caspase-1 causes reduced tumor burden due to decreased levels of IL-18 (Zaki *et al*., 2010).
Colorectal cancer (CRC)	Increased IL-18 results in decreased IL-22 which contributes to tumour development (Ungerback *et al*., 2012).	**Hepatocellular carcinoma (HCC)**	NLRP3 components are significantly downregulated in human HCC and is correlated with advanced stages (Wei *et al*., 2014).
Epithelial skin cancer	Increased IL-1β and caspase-1 promotes tumourigenesis (Drexler *et al*., 2012).		
Head and neck squamous cell carcinoma (HNSCC)	Increased IL-1β contributes to inflammatory-induced carcinoma and increased NLRP3 promotes		

	survival and invasiveness of HNSCC (Bae *et al*., 2017).		
Lung cancer	NLRP3 activation promotes proliferation and metastasis via Akt and ERK1/2 (Wang *et al*., 2016).		
Prostate cancer	Hypoxia increased NLRP3 and pro-IL-1β expression via NFkB activity (Veeranki, 2013).		

As seen in Table 1.2, the role of NLRP3 and breast cancer progression has also been reported. Although not well documented, recent evidence has suggested that NLRP3 and IL-1β production in breast tissue provides an inflammatory microenvironment favourable for tumour growth (Moossavi *et al*., 2018).

1.6.2 Inflammasome activation in breast cancer

As mentioned in the previous section, activation of NLRP3 inflammasome has been reported to occur in several malignancies including head and neck carcinoma, glioblastoma, lung, colon and breast cancer (Moossavi *et al*., 2018; Zahid *et al*., 2019). In breast cancer patients, IL-1β levels positively correlate with a high rate of cancer recurrence, where it is believed to promote tumour growth, angiogenesis, invasion and metastasis (Soria *et al*., 2011). In support of these findings, Guo *et al* reported that the inflammasome as well as IL-1β play important roles in the promotion of tumour growth and metastasis in breast cancer (Guo *et al*., 2016). In this study, they showed that in both NLRP3-deficient and caspase-1-deficient tumour mouse models, primary tumour growth was significantly reduced when compared to the wild-type controls which had high circulating IL-1β levels. These findings suggest that inflammasome activation and IL-1β production may create favourable microenvironments for tumour metastasis, contradicting the reported association between NLRP3 and CAC.

Although the association between the NLRP3 inflammasome and cancer progression is not well documented, the activation of the NLRP3 inflammasome is associated with increased IL-1β production and inflammatory cell infiltration in cardiac fibroblasts (Kawaguchi *et al*., 2011). More recently, evidence to support the role of the NLRP3 inflammasome in cancer associated fibroblasts (CAFs) has emerged. Ershaid and colleagues reported that the NLRP3 inflammasome is upregulated in human breast CAFs and that these fibroblasts can function as DAMP sensors. The authors also observed that multiple genes involved in the NLRP3 inflammasome pathway, including *caspase-1* and *IL-1β*, were upregulated in CAFs but not in fibroblasts isolated from normal mammary tissue. Apart from breast cancer cells, NLRP3 inflammasome components (NLRP3, caspase-1 and IL-1β) were also upregulated in breast stroma. The authors further indicated that CAF-derived inflammasome signaling promoted tumour growth in an *in vivo* mouse model (Ershaid *et al*., 2019). Based on the observations that IL-1β and its associated signaling pathways is upregulated in several models, it is plausible that NLRP3 inflammasome activation promotes tumourigenesis in breast cancer, however, the exact mechanisms as to how this occurs is not well understood.

Taking the above findings into consideration, the NLRP3 inflammasome has differential effects in the development and progression of tumourigenesis, depending on cancer type. Although multiple receptors have been implicated in activating the inflammasome, the involvement of TLR4 in breast and colon cancer has been reported (Table 1.3).

Table 1.3. TLRs and associated cancers (Pandey *et al*., 2015).

TLRs	Cancer
TLR1	Prostate cancer
TLR2	Breast cancer, hepatocarcinoma
TLR3	Esophageal squamous cell carcinoma
TLR4	Colorectal, bladder, ovarian, prostate, breast, lung and pancreatic cancer
TLR6	Prostate cancer
TLR7	Pancreatic carcinogenesis
TLR9	Lung cancer and esophageal squamous cell carcinoma
TLR10	Prostate cancer

Further contributing to the complexity of tumourigenesis, clinical studies have suggested that the expression of PRRs such as TLRs are not limited to immune cells but are also found to be elevated in various human epithelial cancers, which trigger the expression of several genes that are involved in various inflammatory and immune responses (Sato *et al*., 2009). Chronic activation of TLRs therefore promote tumourigenesis through pro-inflammatory responses such as the secretion of pro-inflammatory cytokines as described earlier, to augment the proliferative and anti-apoptotic signals in the TME as well as in the tumour cells.

1.7 Toll-like receptor activation in cancer

TLRs belong to a family of receptors that are expressed on antigen presenting cells, such as macrophages and dendritic cells, as well as on fibroblasts and epithelial cells and play an important role in immune responses against infection (Bhatelia *et al*., 2014). As mentioned above, recent evidence indicates that TLRs are also expressed in cancer cells where it is linked to tumour proliferation and survival and the ability to alter the TME to promote tumourigenesis (Huang *et al*., 2005). However, the role of TLRs in cancer development remain controversial since both anti- and pro-tumour responses are reported in literature.

Ten TLRs (TLR1-10) have been identified in humans and are classified into two subgroups, depending on their cellular localisation (Kawai & Akira, 2005). TLRs 1, 2, 4, 5, 6 and 10 are located on the cell surface and respond to PAMPs from micro-organisms, including lipids and bacterial proteins, or DAMPs from damaged tissues to activate innate and adaptive immune responses. TLRs 3, 7, 8 and 9 are located intracellularly in endosomes and primarily respond to nucleic acids (Maglione *et al*., 2015). Mammalian TLRs are comprised of an extracellular domain that contains leucine-rich repeats (for ligand binding), a transmembrane region and a cytoplasmic toll/interleukin-1 receptor (TIR) domain, which is required for intracellular signaling (Rakoff-Nahoum & Medzhitov, 2009). Receptor activation bridges two TLR molecules at the ectodomain to form a dimer with the TIR domain to activate downstream signaling. This TIR-mediated signaling involves TLR adaptor proteins, including MyD88, toll/interleukin-1 receptor domain-containing adapter protein (TIRAP), TIR-domain-containing adapter-inducing interferon-β (TRIF) and TRIF-related adaptor molecule (TRAM). TLR-ligand binding activates NFκB through the IKK complex, but various other signaling pathways capable of inducing pro-tumourigenic responses can also be activated upon ligand binding, including p38 and extracellular signal-regulated kinase1/2 (ERK1/2) (Lee & Kim, 2007; Chatuverdi, 2009).

As described earlier, diverse conditions can promote NLRP3 inflammasome assembly and many receptors, including PRRs, control NLRP3 priming. Among the PRRs, TLRs, NOD2 and RAGE can prime NLRP3 for further activation, where the overexpression of TLRs has been reported in colon, breast, prostate, lung as well as in ovarian cancer (Fukata *et al*., 2007; Sato *et al*., 2009; Zhou *et al*., 2009).

1.7.1 Toll-like receptor activation in colon cancer

In the GI tract, TLRs function as key modulators of the immune system by maintaining homeostasis and suppressing immune responses to commensal bacteria (Cario, 2010). Once these modulators are disrupted in diseases such as Crohn's disease and ulcerative colitis, chronic inflammation is induced. Generally, inflammation is linked to cancer via two pathways, namely: **extrinsic inflammation** induced by non-transformed cells (invading pathogens or auto-immune diseases) and **intrinsic inflammation** induced by transformed cells. In CRC, TLRs are involved in both. Autoimmune diseases cause chronic levels of inflammation that predisposes individuals to developing CRC. Tumours can then intrinsically activate inflammation through TLR binding via cancer related DAMPs. This binding results in tumour-promoting inflammation through NFκB signaling and the production of inflammatory cytokines (IL-1β, TNF-α and IL-6) (Tang *et al*., 2010).

Furthermore, TLR signaling can result in the acquisition of invasive and metastatic tumour phenotypes and the ability of tumour cells to detach from its epithelial neighbours, breaking through the basement membrane and the invasion of nearby tissues. In CRC, TLR-mediated changes in components of the immune system in the TME can change intracellular signaling (NFκB) and motility. For example, activation of TLR4 by LPS *in vivo* and *in vitro* induces epithelial to mesenchymal transition (EMT) and invasive phenotypes. Furthermore, the TLR/MyD88 pathway plays an important role in microbiota-induced development of CAC. It is therefore accepted that the severity of chronic colitis directly correlates with CRC tumour development and bacterial-induced inflammation drives the progression from adenoma to invasive carcinoma. Similarly, the increased expression of TLR2 and TLR4 has been reported in breast cancer (as indicated by Table 1.3), which is associated with cancer progression (Yang *et al*., 2010).

1.7.2 Toll-like receptor activation in breast cancer

Although the association between TLRs and breast cancer has not been thoroughly investigated, previous studies have highlighted the link between these two factors. Studies also suggest that the activation of TLRs expressed on breast tumour cells may enhance tumour growth by increasing several signaling pathways including pro-survival signals, anti-apoptotic signals, pro-inflammatory cytokines, angiogenesis and invasiveness (Yang *et al*., 2010). Evidence suggests that TLRs contributes to apoptosis and tumour cell resistance and increased invasiveness in the human breast cancer cell line, MDA-MB-231, which expresses TLR1-TLR10 at both the mRNA and protein level. TLR4 was found to be the highest expressed TLR in these cells. By knocking down *TLR4* in these cells, breast cancer cell viability was reduced, and the secretion of IL-6 and IL-8 was inhibited (Hang *et al*., 2010). The role of TLR9 in MDA-MB-231 cells has also been highlighted, which promotes cell invasion by increasing the activity of MMP-13. Furthermore, mammary carcinomas with recurrence also had a significant increase in the expression of mRNA TLR3, TLR4 and TLR9 (Merrel *et al*., 2006).

When we consider these findings, TLR activation by DAMPs can initiate positive feedback loops to promote chronic inflammation. The TLR4 signaling pathway can be stimulated by various ligands, including PAMPs and DAMPs. It has been suggested that DAMPs, such as high mobility group box 1 (HMGB1), play a large role in activating TLR4 which is an important factor to consider in breast cancer development because of its highly pro-inflammatory TME, where various DAMPs are constantly secreted (Fang *et al*., 2014). DAMPs are released in response to different modes of cell death such as apoptosis, necroptosis and necrosis and their release is regulated by different mechanism at different stages of cell death. Although the release of DAMPs is much better documented during anti-tumour therapy in breast cancer,

it has been observed that cancer cells also release DAMPs through stress pathways not related to cell death mechanisms (Sims *et al*., 2010). DAMPs, including HMGB1 and heat-shock proteins, act via PRRs such as TLRs and RAGE in several tumour types, which are also implicated in NLRP3 priming (Table 1.4). These receptors therefore activate a shared set of inflammatory pathways, including NFkB, p38, ERK, inflammasome assembly and the release and secretion of several cytokines such as IL-1β, IL-6 and TNF-α to promote the recruitment of inflammatory cells to the breast TME.

Table 1.4*:* Damage-associated molecular patterns (DAMPs) act via Pattern Recognition Receptors (PRRs) to promote tumourigenesis in several cancer types.

Abbreviations: **HMGB1**: High mobility group box 1; **RAGE**: Receptor for advanced glycation end products; **TLR4**: Toll-like receptor 4

DAMP	Receptor	Tumour	Main effect	Targeted cell	Effect on tumour
HMGB1	RAGE	Colon and lung carcinoma	Tumour growth and metastasis of remnant cancer cells after chemotherapy	Tumour cells	Tumour regrowth and metastasis
		Pancreatic adenocarcinoma	Decreased apoptosis	Tumour cells	Tumour survival
	TLR4	Mammary carcinoma Colon carcinoma	Anti-cancer immune evasion	Dendritic cells	Tumour survival
Heat shock proteins	RAGE	Breast carcinoma	NFkB activation and cell growth	Tumour cells	Tumour growth
		Colon carcinoma Colorectal adenocarcinoma	Pro-tumourigenic gene activation, invasion and metastasis	Tumour cells	Metastasis and tumour progression

As seen in Table 1.4, DAMPs are also implicated in colon tumour growth and metastasis. Even though DAMPs are generally retained within a healthy cell and are released upon cellular stress or cell death, it has been shown that DAMPs are also released from breast, lung and ovarian tumours into the TME (Hernandez *et al*., 2016). Although it remains to be elucidated, SAA which is highly upregulated in a pro-inflammatory TME (Mallea *et al*., 2009), has been proposed to function as an endogenous DAMP to promote cancer growth and development because of its ability to bind to TLRs (Cheng *et al*., 2008; O'Reilly *et al*., 2014).

1.8 Serum amyloid A as an endogenous DAMP

Inflammatory-related diseases such as cancer is associated with the expression of pro-inflammatory cytokines, which is enhanced by the presence of SAA as described earlier. Cells within the TME can utilize inflammasome activation to promote this response (Malle *et al*., 2009). It has been reported that several types of amyloids can activate the NLRP3 inflammasome, including SAA and amyloid-β, but the role of SAA signaling in NLRP3 activation in cancer is limited and not well documented (Halle *et al*., 2008; Ather *et al*., 2011).

To support the above-mentioned, there is evidence to support the binding of SAA to TLRs and its downstream signaling effects. In immune cells, Sandri and colleagues showed that macrophage activation by SAA is TLR4-dependent (Sandri *et al*., 2008). In mice, macrophages from TLR4-deficient strains did not produce significant amounts of nitric oxide (NO) upon SAA stimulation when compared to wild-type mice. The authors concluded that SAA acts as an endogenous TLR4 ligand (Sandri *et al*., 2008). Similarly, in neutrophils, SAA induced the release of IL-1β in cell culture supernatants. However, in the presence of a caspase-1 inhibitor, SAA-induced IL-1β processing and secretion was abrogated (Migita *et al*., 2014). In cancer, Cheng *et al.* observed that SAA stimulates TLR2 activation in HeLa (cervical cancer) cells, and this was associated with the degradation of Iκβ and an increase in NFκB activity (Cheng *et al*., 2008). Furthermore, relatively low concentrations of SAA induced robust phosphorylation of ERK1/2 and p38 in the Hela cells. These results suggest the involvement of TLR2 in SAA signaling. Ather and colleagues exposed peritoneal macrophages from TL2/4$^{-/-}$ and Myd88$^{-/-}$ mice to SAA and found that IL-1β secretion was primarily dependent on TLR2 and MyD88, both in the presence and absence of ATP or aluminum crystals (Ather *et al*., 2011). As some of these studies date back to more than ten years ago, a gap in research with regards to cancer cells exist, which therefore emphasizes the importance to define the role of SAA in NLRP3 signaling in cancer.

To further support the hypothesis that SAA can function as an endogenous DAMP that activates the NLRP3 inflammasome, Shridas and colleagues more recently observed that in J774 macrophages, SAA treatment activates caspase-1, as evidenced by cleavage of pro-caspase-1 to active caspase-1 and this significantly increases IL-1β protein secretion from the cells compared to untreated controls. Furthermore, SAA-induced IL-1β secretion was blocked in the presence of a caspase-1 inhibitor. When bone marrow-derived macrophages (BMDMs) isolated from wild-type and NLRP3$^{-/-}$ mice were treated with SAA, IL-1β secretion was decreased by more than 10-fold in BMDMs from NLRP3$^{-/-}$ mice compared to the cells from wild-type mice. These results indicate that SAA stimulates IL-1β secretion in macrophages, likely by activating NLRP3 inflammasome mediated caspase-1 activation. The authors concluded that SAA acts as an "endogenous" danger signal with the ability to stimulate both essential steps (priming and activation) of NLRP3 inflammasome-mediated IL-1β secretion (Shridas *et al*., 2018). Similarly, Yu and authors cultured keratinocytes in the presence of SAA and found that mRNA expression of caspase-1 and NLRP3 was significantly upregulated. Blocking TLR2 and TLR4 in these cells, respectively, decreased IL-1β mRNA expression by almost 75%. The authors also concluded that SAA could be one of the DAMPs in psoriasis, which induces IL-1β via the NLRP3 inflammasome (Yu *et al*., 2015).

Taken together, these results highlight the SAA-mediated activation of several important steps in inflammasome signaling. SAA's ability to activate the inflammasome priming step (via NFκB pathways) by signaling through PRRs has been documented and Shridas *et al.* demonstrated that SAA upregulates NLRP3 mRNA expression, which is consistent with inflammasome priming (Shridas *et al*., 2018). In macrophages, SAA had the ability to prime and activate the NLRP3 inflammasome (supported by K^+ efflux in SAA-mediated IL-1β release) to stimulate IL-1β secretion, which distinguishes it from numerous compounds such as ATP, pore-forming toxins, β-amyloid and crystals that are incapable of inducing IL-1β secretion in the absence of a priming stimulus. SAA therefore seems to represent as an endogenous danger signal with the unique ability of stimulating both essential steps of NLRP3 inflammasome mediated IL-1β secretion. The support for SAA-mediated inflammasome activation originates from studies using different cellular models, suggesting that this effect is not cell-type specific. This is particularly relevant in an environment such as the TME, which consists of a multitude of cell types and where SAA could potentially activate the inflammasome in several, if not all, of these cell types. It should however also be considered that the propensity of a particular cell type for inflammasome activation could affect the extent of the SAA-induced effects. Future studies comparing SAA-mediated inflammasome activation in the different cell types present in the TME would shed light on this intriguing question.

1.9 Inflammasome inhibition and SAA as a potential therapeutic target

Excessive inflammation induced by the inflammasome is a detrimental factor in many types of cancer and inflammasome inhibitors are therefore considered a promising approach for cancer prevention and treatment by targeting upstream and downstream molecules in the inflammasome activation pathway (Xu *et al*., 2019). SAA plays an important role in chronic inflammation, where it contributes to tumour initiation and progression via multiple signaling pathways, as well as interacting with the ECM. Inhibiting the secretion of SAA from tumour cells or inhibiting its downstream activity, could have beneficial therapeutic outcomes. This may be achieved by reducing the production of SAA inducers, such as IL-1, IL-6 and TNF-α. Antagonists or inhibitors for these cytokines are currently being used clinically (De Buck *et al*., 2016).

Thalidomide, a drug that targets and inhibits the activation of caspase-1, has showed anti-tumour effects in patients with advanced myeloma (Xu *et al*., 2019). In a randomised phase II trial, thalidomide combined with docetaxel (chemotherapeutic agent) resulted in the increased median survival rate in patients with metastatic androgen-independent prostate cancer. It has also been demonstrated that thalidomide reduces high levels of angiogenic factors such as fibroblast growth factor (FGF) and vascular endothelial growth factor (VEGF). However, its antitumour activity has a moderate effect on other types of cancer and increases the risk of thrombotic events (Lee *et al*., 2009).

Anakinra is a recombinant form of IL-1Ra and is commonly used to treat autoinflammatory diseases such as rheumatoid arthritis (Dinarello, 2009). In a breast cancer mouse model, anakinra decreased metastatic tumour growth to bone (Holen *et al*., 2016). The study also showed that anakinra failed to increase tumour cell death but suppressed cancer cell proliferation and angiogenesis. Previous studies with myeloma cells have shown that anakinra significantly reduces IL-6 levels but does not increase myeloma cell death. However, a combination therapy of anakinra and dexamethasone can induce myeloma cell death. Due to anakinras' clinical and safety record and short half- life, it is an ideal drug to be combined with chemotherapy. In breast cancer, Wu and authors identified an IL-1-associated inflammatory signature in primary tumours and if validated in follow-up clinical studies, could be used to stratify patients at diagnosis and justify the use of IL-1 targeting therapies (Wu *et al*., 2018). Although anakinra has been approved by the US Food and Drug administration (FDA) as treatment for rheumatoid arthritis, the anti-tumour effects await further studies.

Additionally, parthenolide, a sesquiterpene lactone compound found in a herb named feverfew, is used as an anti-inflammatory medicine (Kwok *et al*., 2001). Parthenolide is

considered as a potential anti-tumour therapeutic drug that inhibits NFκB signaling and which can also inhibit caspase-1 activation. In gastric and breast cancer, parthenolide inhibits tumour cell growth by downregulating NFκB phosphorylation (Sohma *et al*., 2011). However, its anti-cancer potential is limited by poor solubility and bioavailability (D'anneo *et al*., 2013).

In contrast to IL-1β, the development of IL-18 inhibitors is less advanced. One agent that targets IL-18 is the GSK-1070806 antibody, however it has not been evaluated in a cancer setting. Kang and authors observed that IL-18 is secreted by B16 murine melanoma cells and enhanced IL-18 expression was positively correlated with the pathogenesis and metastasis of malignant skin tumours. These effects were reduced in the presence of IL-18-binding protein (IL-18BP), which inhibits IL-18 receptor binding (Kang *et al*., 2009).

Blocking the binding of SAA to its receptors will prevent the resulting downstream pro-inflammatory processes. When focusing on TLR4, TAK242 is an effective and specific TLR4 inhibitor that binds to the Cys-747 intracellular domain and blocks interactions with downstream effectors (Li *et al*., 2006). Zandi and authors demonstrated that TLR4 inhibition by TAK242 significantly decreased the viability of ovarian and breast cancer cells (Zandi *et al*., 2019). TAK242 also inhibited the activity of MMP-2 and MMP-9 in ovarian and breast cancer cells. Another TLR4 antagonist, C34, inhibits TLR4 *in vivo* and *in vitro* (Neal *et al*., 2013). C34 inhibits TLR4 signaling *in vivo* in the presence of LPS in a NFκB-luciferase transgenic mouse strain. To determine the *in vitro* effect of C34, the authors treated macrophages and enterocytes with LPS. In these cells C34 significantly reduced the LPS-induced NFκB translocation from the cytoplasm to the nucleus.

Developing inhibitors for TLRs remain challenging due to the large number of cell surface TLRs (TLR1, TLR2, TLR4, TLR5, TLR6, and TLR10,) and the significant homology shared with the IL-1R-family. Furthermore, TLRs may also require dimerisation either as homo- or heterodimers for functional activity. Heterodimerisation appears to substantially influence the potency of ligand binding (eg. TLR1/2 and TLR2/6) and should be taken into consideration. Cheng and colleagues tested CU-CPT22, a TLR2 antagonist against a panel of homologous TLRs and found that CU-CPT22 only inhibits TLR1/2 signaling without affecting other TLRs (Cheng *et al*., 2013). CU-CPT22 also inhibited downstream signal transduction; NO production was suppressed as well as the release of IL-1β. Additionally, MMG-11, a potent TLR1/2 and TLR2/6 antagonist, inhibits NFκB activation induced by TLR2 ligands in mouse macrophages and ultimately prevents the secretion of pro-inflammatory cytokines, including TNF and IL-1β (Grabowskia *et al*., 2019). Thus SAA, being an activator of both TLR2 and 4,

could potentially serve as a therapeutic target for chronic inflammatory diseases including cancer.

Neutralizing monoclonal antibodies that target SAA could be utilized to prevent its inflammatory effects. Similar products to target pro-inflammatory cytokines such as IL-1 and IL-6 has been developed. To date, canakinumab, an IL-1β neutralizing human monoclonal antibody is used to treat cryopyrin-associated periodic syndromes (CAPs) in children and adults (Kuemmerle-Deschner & Huag, 2013). During a randomized, double-blinded, placebo-controlled trial of patients with lung cancers and atherosclerosis, researchers found that canakinumab significantly decreased lung cancer mortality by targeting the IL-1β innate immunity pathway (Ridker *et al*., 2017). Currently, canakinumab is being tested in clinical trials that focus on non-small cell lung cancer (NSCLC), triple negative breast cancer (TNBC), metastatic melanoma and colorectal cancer. In another phase III clinical trial, Canakinumab Anti-inflammatory Thrombosis Outcomes Study (CANTOS), it was demonstrated that canakinumab significantly reduced the incidence and mortality of lung cancer. Goh and authors investigated a similar product, P2D7, which blocks IL-1β from binding to IL-1R (Goh *et al*., 2016). The engineered antibody had a higher affinity for IL-1β than canakinumab and potently neutralized human and mouse IL-1β.

Anti-IL-6 therapies have also been developed to treat cancer. Current IL-6 inhibitors include siltuximab, a humanized monoclonal antibody which is used in clinical trials for myeloma and prostate cancer (Rossi *et al*., 2015). It binds to and neutralizes human IL-6 directly and decreases the levels of unbound IL-6 and prevents receptor binding, thereby exerting its anti-cancer effects (Deisseroth *et al*., 2015). Blocking SAA could also limit metastasis. Double-knockout $Saa1^{-/-}$ $Saa2^{-/-}$ mice implanted with pancreatic adenocarcinoma cells failed to show features of a pro-metastatic niche in the liver (Lee *et al*., 2019). Similarly, mice inoculated with lung Lewis carcinoma cells transfected with SAA1 or SAA2, resulted in metastasis and colonization to the lung (Sung *et al*., 2010). This indicates that in *in vivo* models, SAA1 and SAA2 contributes to cancer metastasis.

Taken together, several possible therapeutic approaches to prevent SAA binding and downstream activity such as receptor inhibitors and neutralizing antibodies exist, however these effects have mostly only been observed in immune cells and evidence for the inhibition of signal transduction in cancer cells remains limited. By targeting SAA through the development of neutralizing monoclonal antibodies and limiting its function as an endogenous DAMP could potentially be used as a therapeutic strategy for treating chronic inflammatory diseases. Targeting inflammasome activation in cancer could be a promising approach for

cancer therapy, but the contrasting roles of inflammasomes suggest that due to the heterogeneity of cancer, specific treatment approaches depending on the type of cancer should be considered. A useful approach to consider may be to target TLRs, SAA, IL-1β and components of the inflammasome simultaneously. By neutralizing SAA, several downstream effects might be observed, which includes NLRP3 inflammasome inhibition, but it is still possible that other DAMPs in the TME could bind to TLRs and result in inflammasome activation. Therefore, blocking TLRs might prevent this from occurring and could also limit the production of other pro-inflammatory cytokines in the TME including IL-6 and TNF-α. Inhibiting components of the NLRP3 inflammasome like caspase-1 will result in the decreased production and secretion of IL-1β into the TME. Taking the above-mentioned into consideration, a recommended therapeutic approach could be to neutralize SAA and inhibit TLRs simultaneously or to neutralize SAA along with inhibiting components of the inflammasome.

1.10 Problem statement

Although there have been many significant advances made in the diagnosis and treatment of cancer, numerous unresolved challenges remain, which include prevention, early diagnosis, metastasis, and recurrence. As previously established, chronic inflammation is a major driving force for cancer development and progression in several organs and tissue, including colorectal associated cancers and breast cancer. Although the disease-promoting role of IL-1β has been well established, the function of the NLRP3 inflammasome in human cancers is still controversial. While there have been several studies that investigate the molecular mechanisms of SAA in both tumour and non-tumour cells, the mechanism of action of SAA in cancer progression remains to be elucidated.

1.10.1 Hypothesis

Serum amyloid A acts as an endogenous damage associated molecular pattern in the tumour microenvironment to promote cancer growth by activating the NLRP3 inflammasome.

1.10.2 Aims

We aimed to identify the role of serum amyloid A in NLRP3 inflammasome activation in breast and colon cancer by:

1. Determining whether the NLRP3 inflammasome is activated in models of acute colitis (AC), colitis-associated cancer (CAC) and triple negative breast cancer (TNBC).
2. Determining whether the inflammasome promotes a pro-inflammatory environment favorable for cancer growth.
3. Determining whether SAA activates NLRP3 signaling to promote tumourigenesis.
4. Determining the role of SAA in inflammasome activation in an inflammatory (AC) versus tumour (CAC and TNBC) setting.

1.10.3 Objectives

To achieve our aims, we established the following objectives:

In vivo

1. To establish a physiologically relevant tumour-bearing mouse model using wild-type and double knockout of SAA1 and SAA2 (SAADKO) mice for acute colitis (AC), colitis-associated cancer (CAC) and breast cancer.
2. To investigate whether SAA plays a role in NLRP3 inflammasome activation through Western blotting and qPCR experiments, respectively.
3. To determine whether SAA and the NLRP3 inflammasome alters the inflammatory profile in blood plasma by using a Milliplex kit.

4. To assess structural and morphological changes in the tumours of SAADKO and wild-type (WT) mice by using H&E stains.
5. To assess proliferation in tumours of SAADKO and WT mice by using Ki67 immunohistochemistry.
6. To assess NLRP3 expression in WT and SAADKO tumours by using NLRP3 immunohistochemistry.

Chapter 2

Materials and Methods

2.1 *In vivo* acute colitis (AC) and colitis-associated cancer (CAC) model

Human inflammatory bowel disease (IBD) such as ulcerative colitis, is a chronic, relapsing and remitting inflammatory condition that results from chronic dysregulation of the mucosal immune system of the GI tract and can lead to the development of colon cancers, however, the precise pathogenesis is not completely understood (Eaden *et al*., 2001). Therefore, animal models of experimental colitis have been developed to investigate the molecular and cellular mechanisms that lead to IBD. In the acute DSS-colitis model, mice are fed with dextran sulfate sodium (DSS) polymers in their drinking water which induce a colitis often characterized by bloody faeces, diarrhoea, weight loss and a histological picture of inflammation and ulceration. Strictly speaking, DSS does not directly cause intestinal inflammation per se, but rather induces chemical injury to the intestinal epithelium, resulting in exposure of the lamina propria and submucosal compartment to luminal antigens and enteric bacteria, which triggers inflammation. The effectiveness of DSS-induced colitis depends on many factors including dosage (usually 1-5%), duration (acute or chronic), strain of DSS, sex of animals (males are often more susceptible) and microbial environment of animals.

Consequently, low replicability of animal experiments is perceived as a major hurdle in the field of biomedicine. Therefore, many attempts to enhance replicability and reduce variability has led to the recommendation to use isogenic mice. The C57BL/6 strain has evolved as the gold standard strain for this purpose and is widely used in knockout and transgenic research. As the C57BL/6J mouse was the first strain to have its genomic sequence published, it is widely used in biomedical research for immunology, nutrition, and human diseases such as obesity and cancers (Song & Hwang, 2017). This mouse strain is also frequently used in DSS-induced IBD models and is more appropriate for inducing chronic colitis compared to the BALB/c mouse strain (Melgar *et al*., 2005). For this study, wild-type (WT) and serum amyloid A double knockout (SAADKO) C57BL/6 mice were used to assess acute DSS-induced colitis. Targeted deletion of the SAA1.1 and SAA2.1 genes was performed by InGenious Targeting Laboratory, Inc. (Stony Brook, NY) using embryonic stem cells derived from C57BL/6N and 129SVEV mice. SAA1.1 and SAA2.1 are located approximately 9 kb apart in opposite orientation on chromosome 7. An approximate 21.3 kb region was used to construct the targeting vector, which contains a short homology arm extending ~2.8 kb and a long homology arm extending ~8.4 kb on the 5′ and 3′ sides, respectively, of a Lox/FRT-flanked neocassette. The neocassette replaced ~10.1 kb of the SAA1.1 and SAA2.1 genes, including exons 1 and

2 of each gene. Heterozygote animals were received and bred to generate the SAA1.1/SAA2.1$^{+/+}$ (WT) and SAA1.1/SAA2.1$^{-/-}$ (SAADKO) mice (De Beer *et al*., 2010)

Subsequently, the acute-colitis (AC) model was established with 8-week-old, sex-matched, WT and SAADKO mice. For this study, 6 male and 6 female SAADKO (SAA1$^{-/-}$ and SAA2$^{-/-}$) were used along with 12 age- and sex-matched WT control mice. Mice received 2.5% DSS, a chemical colitogen with anticoagulant properties (40 kilodaltons; Alfa Aesar, Ward Hill, MA), which was administered for a total of 5 days in autoclaved drinking water, prior to euthanasia and sample collection (Figure 2.1.2).

As IBDs, such as ulcerative colitis, are characterized by long-lasting and relapsing intestinal inflammation, colitis-associated cancer (CAC) has been described as one of the most serious complications of long-term IBD. Therefore, a CAC model using WT and SAADKO C57BL/6 mice (as described above) was also used for this study. Mice received an intraperitoneal injection of 12.5 mg/kg AOM, which is a carcinogenic chemical compound (Sigma-Aldrich, St. Louis, MO), prepared in saline. AOM is metabolized by cytochrome p450, isoform CYP2E1, converting it into methylazocylmethanol (MAM), a highly reactive alkylating species which induces O^6 methylguanine adducts in DNA resulting in G-A transitions. After it is secreted into the bile, it is taken up by colonic epithelium and induces mutagenesis (Thaker *et al*., 2012). After one week, DSS (40 kilodaltons; Alfa Aesar, Ward Hill, MA) treatment was administered in autoclaved drinking water at a concentration of 2.5% for a total of 5 days, followed by a recovery period of 16 days. DSS is a heparin-like polysaccharide that is dissolved in the drinking water and inflicts colonic epithelial damage, which mimics some of the features of IBD (Thaker *et al*., 2012). Combining AOM and DSS provides a two-step tumour model of CAC. DSS treatment was administered for a total of 3 cycles (Figure 2.1.4). The disease activity score (DAI) was previously assessed in our group and Figure 2.1.1 shows that SAADKO mice had a lower DAI score compared to WT mice ($p<0.05$) (Davis *et al*., 2021).

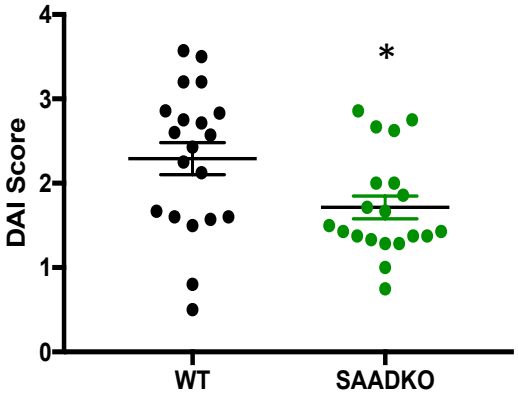

Figure 2.1.1: **Average disease activity score (DAI) score of animals during DSS cycle 1**. Scoring the disease activity index (DAI) was calculated as the sum of individual scores for weight loss (0=0%; 1=0-4.99%; 2=5-9.99%; 3=10-14.99%; and 4=15-20%), stool consistency (0=normal stool; 2=loose/pasty stool; 3=delayed defecation, and 4=diarrhea), and rectal bleeding (0=negative, 2=positive for occult blood; and 4=gross rectal bleeding). **Abbreviations**: **DAI**: Disease activity index; **DSS**: Dextran sulfate sodium

2.1.1 Timeline and study design for acute colitis (AC)

2.1.1 Timeline for AC

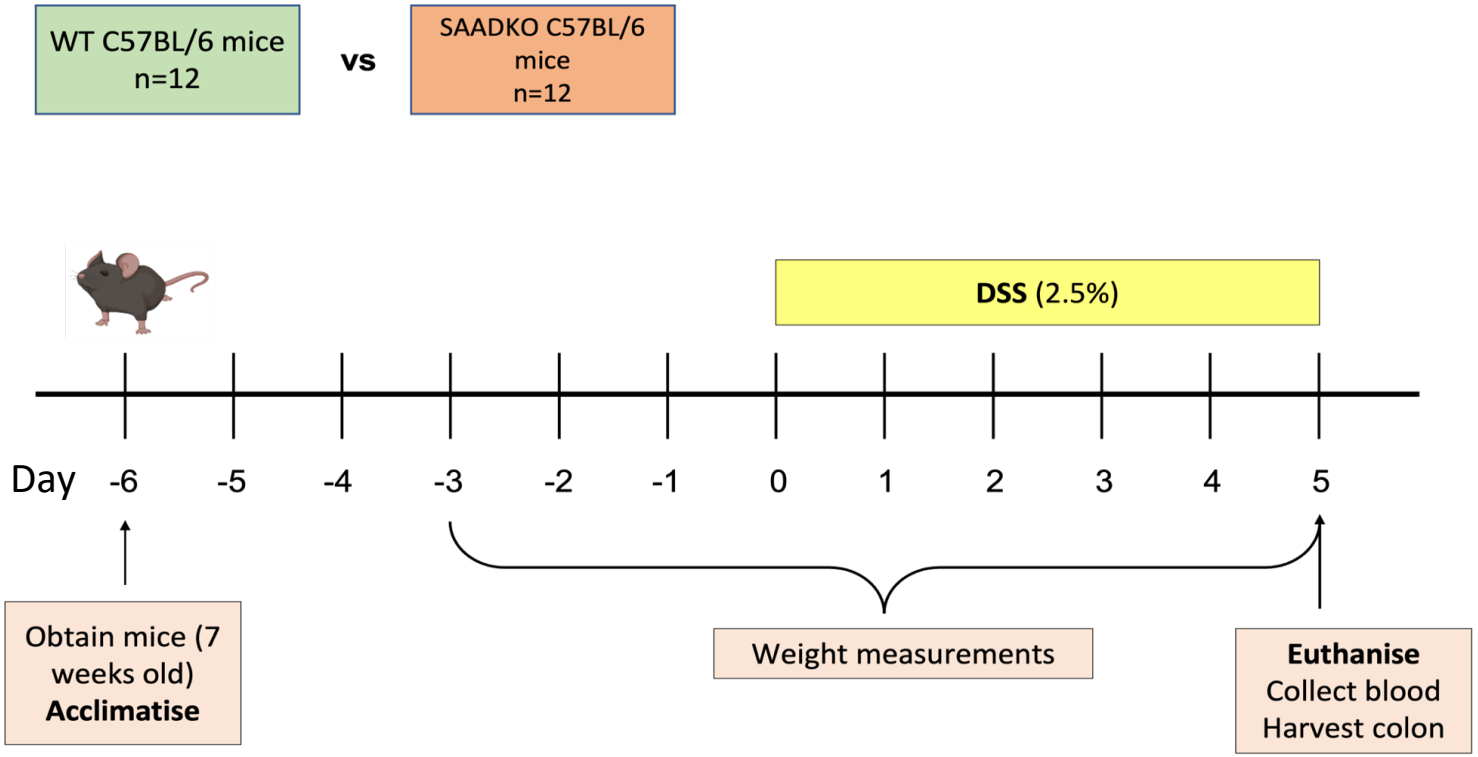

Figure 2.1.2: Timeline for acute colitis induction in WT and SAADKO mice. **Abbreviations**: **DSS**: dextran sulfate sodium; **SAADKO**: SAA-double knockout; **WT**: Wild-type

2.1.1 Study design for AC

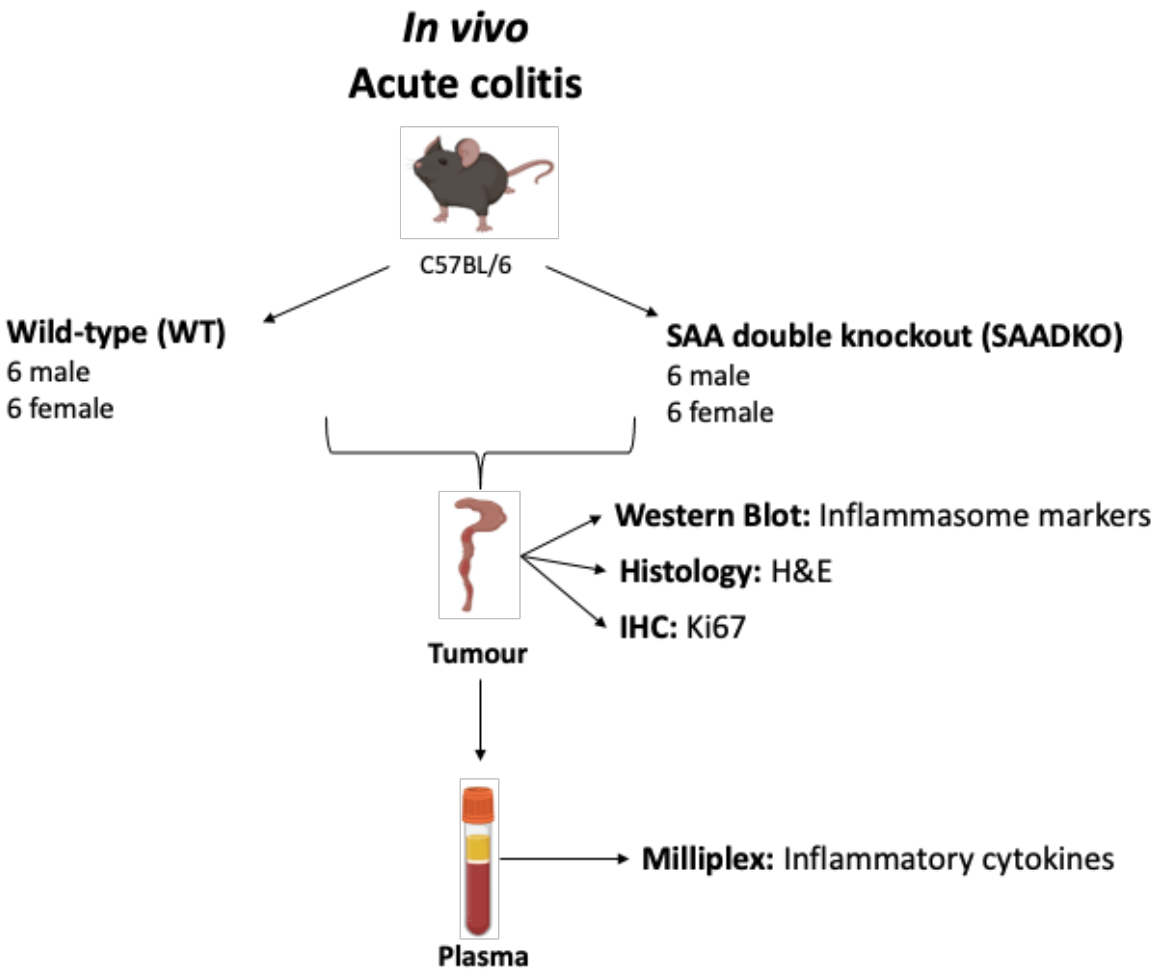

Figure 2.1.3: Study design for DSS-induced colitis in WT and SAADKO mice. **Abbreviations**: **H&E**: Haematoxylin and eosin; **IHC**: Immunohistochemistry; **SAADKO**: SAA-double knockout; **WT**: Wild-type

2.1.2 Timeline and study design for colitis-associated cancer (CAC)

2.1.2 Timeline for CAC

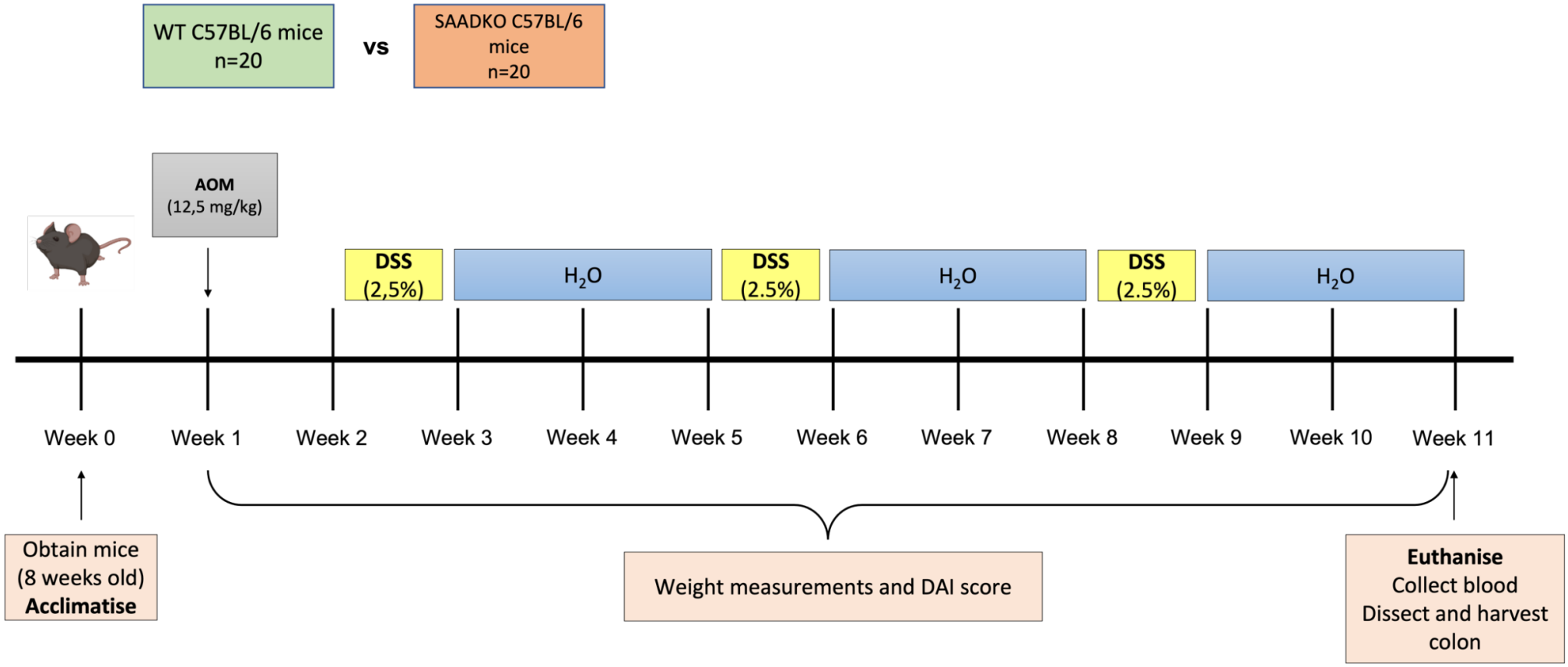

Figure 2.1.4: Timeline for AOM/DSS-induced CAC in WT and SAADKO mice. **Abbreviations**: **AOM**: Azoxymethane; **DAI**: Disease activity index; **DSS**: dextran sulfate sodium; **SAADKO**: SAA-double knockout; **WT**: Wild-type

2.1.2 Study design for CAC

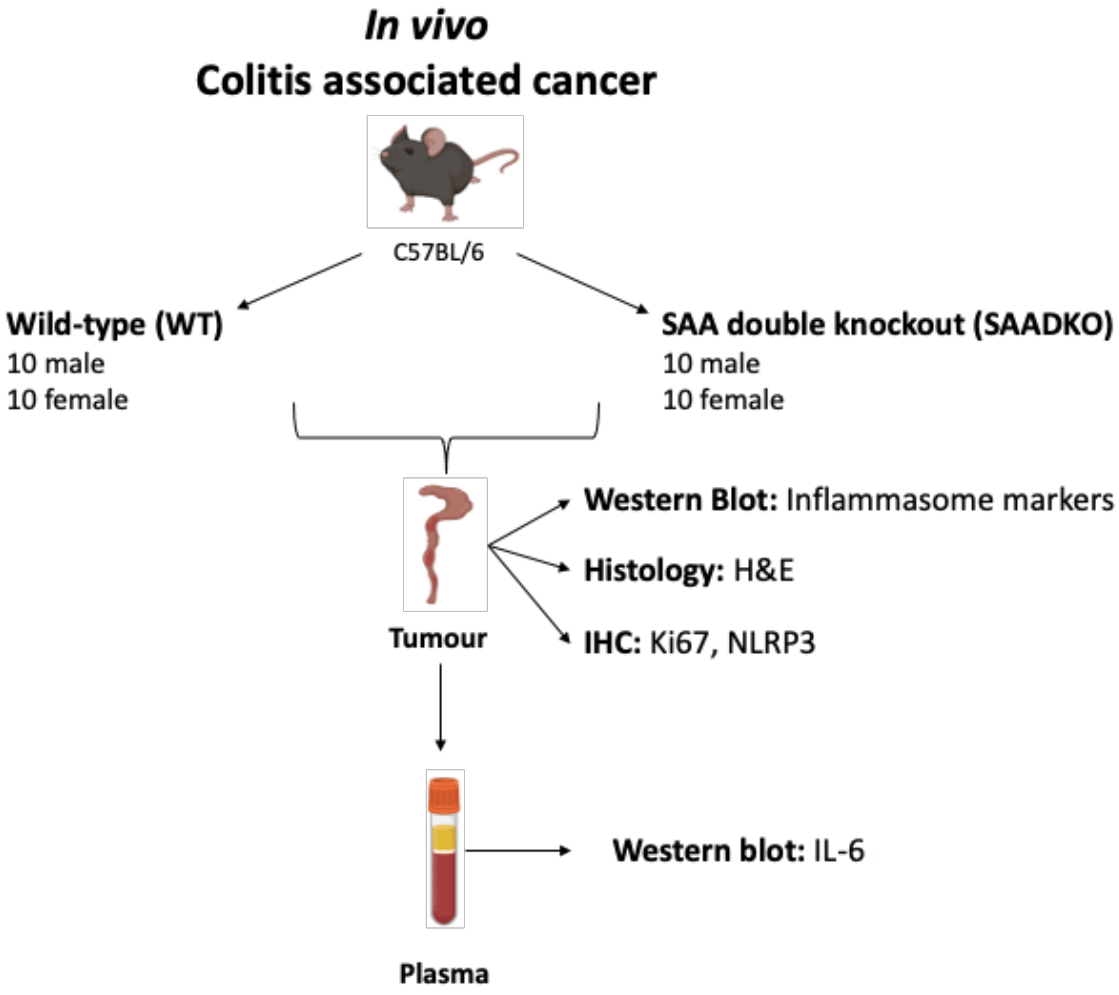

Figure 2.1.5: Study design for AOM/DSS-induced CAC in WT and SAADKO mice. **Abbreviations**: **H&E**: Haematoxylin and eosin; IHC: Immunohistochemistry **SAADKO**: SAA-double knockout; **WT**: Wild-type

2.1.3 Ethical clearance, animals and housing

Ethical clearance

Ethical clearance was obtained from the Stellenbosch University Research Ethics committee according to the approved protocol (ACU-2019-6307) to identify the role of SAA in AC and CAC respectively, by using the DSS and AOM/DSS model in C57BL/6 Wild-type (WT) mice and C57BL/6 mice that lack the *SAA1* and *SAA2* genes (SAADKO).

Animals and housing

For the CAC study, ten male and 10 female SAADKO ($SAA1^{-/-}$ and $SAA2^{-/-}$) were used along with 20 age- and sex-matched WT control mice. The mice were housed at the Stellenbosch University animal facility in individually ventilated cages with autoclaved bedding and standard chow and water, ad libitum.

2.1.4 Acute Colitis (AC) and Colitis-associated Cancer (CAC) induction, monitoring and assessment

CAC was induced by following the AOM/DSS protocol modified from Thaker *et al.* (Thaker *et al*., 2012). Mice received an intraperitoneal injection of 12.5 mg/kg AOM (Sigma-Aldrich, St. Louis, MO) prepared in saline. After one week, DSS (40 kilodaltons; Alfa Aesar, Ward Hill, MA) treatment was administered in autoclaved drinking water at a concentration of 2.5% for a total of 5 days, followed by a recovery period of 16 days. DSS treatment was administered for a total of 3 cycles. Animals were monitored daily, and weight measurements and stool samples were collected every day during DSS treatment as well as the first four days of the recovery period. At the end of the third DSS cycle, the mice were euthanized, and the samples were collected.

The acute-colitis (AC) model was established with 8-week-old, sex-matched, WT and SAADKO mice. For this study, 6 male and 6 female SAADKO ($SAA1^{-/-}$ and $SAA2^{-/-}$) were used along with 12 age- and sex-matched WT control mice. Mice received 2.5% DSS, which was administered for a total of 5 days in autoclaved drinking water, prior to euthanasia and sample collection.

To measure colon length, images of the excised colons were taken, and the lengths were measured from the caeco-colic junction to the rectum on scaled images with Fiji (Madison, WI) software. Scoring the disease activity index (DAI) was calculated as the sum of individual scores for weight loss (0=0%; 1=0-4.99%; 2=5-9.99%; 3=10-14.99%; and 4=15-20%), stool

consistency (0=normal stool; 2=loose/pasty stool; 3=delayed defecation, and 4=diarrhea), and rectal bleeding (0=negative, 2=positive for occult blood; and 4=gross rectal bleeding).

2.1.5 Blood plasma inflammatory profiling

SAA1 and SAA2

Plasma SAA1/2 levels were assessed with Western blotting, using rabbit anti-mouse SAA antisera (De Beer laboratory, University of Kentucky, USA). The protocols are set out in section 2.1.6.

IL-1β, IL-6, IL-10, MCP-1 and TNF-α

The inflammatory profiles of the mice were assessed for IL-1β, IL-6, IL-10, MCP-1 and TNF-α for the acute colitis model. The day before analysis, plasma samples were transferred from -80°C to -20°C. The samples were subjected to a Milliplex MAP Mouse cytokine/chemokine magnetic bead panel (MCYTOMAG-70K, Merck) according to the manufacturer's protocol and detected by Luminex. In short, analytes from test samples are captured by beads coated with specific capture antibodies (e.g., anti-IL-1β or anti-IL-6). Thereafter, biotinylated detection antibodies are introduced, and the mixture incubated with Streptavidin-PE, a reported molecule, to complete the reaction on the surface of each bead. Finally, each individual bead is identified using flow cytometry and the result quantified based on the fluorescent reporter signals.

2.1.6 Protein harvest and quantification

Protein harvest

Colonic tumours were snap-frozen in liquid nitrogen after harvest and stored at -80°C until further analysis. Tumour tissue was cut into smaller pieces, followed by incubation and sonication in RIPA buffer supplemented with a protease inhibitor cocktail (Roche, Basel Switzerland).

Protein quantification and sample preparation

Protein concentration was determined with a Bradford assay. A standard curve using six incremental concentrations was prepared from a 2 mg/ml bovine serum albumin (BSA) solution. The optical density was measured at 595 nm on a Cecil Aurius CE 2021 spectrophotometer. The measured absorbances were plotted on a graph in Microsoft excel to determine the standard curve. Protein quantification results were used to calculate the amount of sample needed for 35 μg protein. The lysates were diluted in Laemmli sample buffer (150

µl β-mercaptoethanol and 850 µl Laemmli sample buffer) at a 1:2 ratio. Samples were stored at -80°C until further analysis by Western blot.

TCA Protein Precipitation

An equal volume of 40% Trichloroacetic acid (TCA) (Sigma-Aldrich) was added to 50 µL plasma samples and incubated on ice for 30 minutes. After the incubation period, plasma samples were centrifuged at 4500 x g for 8 minutes at 4°C. The supernatant was removed, and the pellet was washed in 100% ice-cold ethanol. This was followed by centrifugation at 13 000 rpm for 5 minutes at 4°C. The pellet was then air-dried on ice for 90 minutes. RIPA buffer was added to the pellet and the samples were incubated overnight at 4°C. The following day a Bradford assay was performed to prepare samples for electrophoresis (section 2.1.7).

2.1.7 SDS-PAGE and Western blotting

Prepared samples were separated on 12% gels by sodium dodecyl sulfate polyacrylamide gel electrophoresis (SDS-PAGE) (TGX Stain-Free™ FastCast™ Acrylamide kit, BioRad). The molecular weights of specific bands were determined by loading 3 µL of a protein marker ladder into the first lane of each gel. The samples were dry boiled for five minutes at 95°C and loaded into each well. Proteins were separated at 90 V for the first 10 minutes, followed by 110 V for approximately 90 minutes (Mini Protean System, BioRad, Hercules). Following electrophoresis, separated proteins were transferred onto nitrocellulose membranes (Trans-blot Turbo™ RTA Transfer Kit, PVDF BioRad). Membranes were blocked in blocking buffer (BioRad) for 5 minutes with gentle agitation at room temperature, before overnight incubation with primary antibodies. The following antibodies were used: NLRP3 (Cell Signaling Technology; 1:1000 or 1:500); Caspase-1 (Abcam; 1:1000); NFkB (Cell Signaling Technology; 1:1000); phosphorylated NFkB (Cell Signaling Technology; 1:1000), total ERK (Abcam; 1:1000); phosphorylated ERK (Cell Signaling Technology; 1:1000); p38 (Cell Signaling Technology; 1:1000); phosphorylated p38 (Cell Signaling Technology; 1:1000) and MCM2 (Abcam; 1:1000) (Table 2.1). All antibodies were diluted in TBS-T, except NLRP3, which was diluted in blocking buffer.

Table 2.1*:* Primary antibodies and concentrations used for Western blotting to assess NLRP3 inflammasome signaling.

Antibody	Concentration	Size (kDa)
Inflammasome activation		
NLRP3	1:1000	110
Caspase-1	1:1000	45, 20, 12
Signaling pathways		
Total NFkB	1:1000	65
Phosphorylated NFkB	1: 1000	65
Total ERK	1:1000	44/42
Phosphorylated ERK	1:1000	44/42
Total p38	1:1000	38
Phosphorylated p38	1:1000	38
Proliferation		
MCM2	1:1000	102
SAA overexpression		
Serum amyloid A	1:1000	12
Metastasis		
E-cadherin	1:1000	135
Vimentin	1:1000	57
Snail	1:1000	29

The following day, membranes were washed in TBS-T (3 x for 5 minutes). Afterwards, membranes were incubated in anti-rabbit horseradish peroxidase-conjugated secondary antibody for one hour at room temperature on a roller. Once this step was complete, membranes were washed with TBS-T (3 x 5 minutes). Antibodies were detected using the ECL (BioRad) detection kit. Exposed bands were quantified using ImageLab software™ (BioRad). The exposed bands were quantified relative to the total protein present in each lane. A stain free total protein analysis was used. The technology uses a tri-halo compound that is

directly incorporated into the gel. After UV exposure, the compound modifies tryptophan residues in proteins which cause them to fluoresce. This fluorescent signal was then detected by a CCD camera, after the gel was transferred to the nitrocellulose membrane.

2.1.8 RNA extraction and qPCR

Harvested tissues were placed in RNAlater (Sigma-Aldrich) immediately after harvest and then stored at -80°C before RNA extraction. Tissues were cut into smaller pieces and the RNA was extracted with TRIzol Reagent (Thermofisher Scientific). According to the manufacturer's protocol, 1 mL of TRIzol reagent was added per 50-100 mg of tissue and was homogenized with a homogenizer. The samples were centrifuged for 5 minutes at 12 000 x g at 4°C and the clear supernatant was transferred to a new tube. After 5 minutes of incubation, 0.2 mL of chloroform per 1 mL of TRIzol reagent was added to each tube and was further incubated for another 2-3 minutes. After the mixture has separated (a lower red phenol-chloroform and colourless upper aqueous phase), the aqueous phase was transferred to a new tube. Afterwards, 0.5 mL of isopropanol per 1 mL TRIzol was used for lysis by incubating the samples for 10 minutes and then centrifuged for 10 minutes at 12 000 x g at 4°C. The supernatant was discarded. As a wash step, 1 mL of 75% ethanol per 1 mL of TRIzol was added to the samples and resuspended, followed by a brief vortex and centrifugation at 7500 x g at 4°C. The supernatant was discarded, and the RNA pellet air-dried at room temperature for 10-15 minutes. The pellets were resuspended in 20 μl dH_20 and was incubated in a heating block for 12 minutes at 57°C. The RNA yield was determined with a nanodrop.

For qPCR, the RNA was incubated with DNase I (Thermofisher Scientific) before being reverse-transcribed with the LunaScript RT mix (New England Biolabs, Ipswitch, MA). Complementary DNA (5 ng) was used as a template for qPCR reactions performed with the Luna Universal qPCR Master Mix (New England Biolabs) on a StepOnePlus instrument (Applied Biosystems, Waltham, MA). The following primers were used for amplification: **SAA3** (NM_011315.3) forward: 5'-ACAGCCAAAGATGGGTCCAG-3', reverse: 5'-CTGGCATCGCTGATGACTTT-3' (amplicon length, 190 bp); **SAA1** (NM_009117.4) forward: 5'-CATTTGTTCACGAGGCTTTCC-3', reverse: 5'- GTTTTTCCAGTTAGCTTCCTTCATGT-3' (amplicon length, 80 bp); **SAA2** (NM_001357491.1) forward: 5'-TCTTCTGCTCCCTGCTCCT-3', reverse: 5'- AGCCAGCTTCCTTCATGTCA-3' (amplicon length, 190 bp); **IL-1β** (NM_008361.4) forward: 5'-CCCAAAAGATGAAGGGCTGC-3', reverse: 5'-TGATACTGCCTGCCTGAAGC-3' (amplicon length, 113 bp); **NLRP3** (NM_001359638.1) forward: 5'-TTGCAGAAGCTGGGGTTGG-3', reverse: 5'- GTGTCTCCAAGGGCATTGCT-3' (amplicon length, 125 bp); **Eef2** (NM_007907.2) forward: 5'- AGTGTCCTGAGCAAGTGGTG-

3', reverse: 5'-CGGTGAAGC- CAAAGGACTCA-3' (amplicon length, 144 bp) and **GusB** (NM_001357026.1) forward: 5'-CGGGACTTTATTGGCTGGGT-3', reverse: 5'-CCATTCACCCACACAACTGC-3' (amplicon length, 131 bp). All primers were designed to span exon-exon boundaries. The quantitation cycle values of SAA1, SAA2, SAA3, IL-1β and NLRP3 were normalized to the values of Eef2 and GusB reference genes and gene expression was quantified using the delta-delta quantitation cycle method.

2.1.9 Histology

Colon tissues were rolled by means of the Swiss-roll method before being formalin-fixed and wax-embedded (see section 2.2.9). The tissue sections were cut at 5 μM. Thereafter, standard haematoxylin and eosin (H&E) staining was performed to assess tissue morphology. H&E stains were performed to assess ultrastructural changes. Prior to the staining protocol, samples were deparaffinized and rehydrated through incubating the slides 5 minutes each in the following order; twice in xylene, twice in 100% ethanol, twice in 95% ethanol and once in 70% ethanol. Cells were then stained in Mayer's Haematoxylin for 11 minutes each, rinsed in tap water for 2 minutes and Scott's water for 1 minute and stained with eosin for 30 seconds. Slides were then dipped 10 times each in the following order, once in 70% ethanol, twice in 95% ethanol, twice in 100% ethanol and 1 minute in xylene. Slides were mounted with coverslips using DPX mounting media.

2.1.9.1 Immunohistochemistry

For immunohistochemistry, the sections underwent deparaffinization and rehydration as mentioned above before heat-mediated antigen retrieval in sodium citrate buffer. Sections were blocked in 5% goat serum for 90 minutes before overnight primary antibody incubation. The following primary antibodies were used: NLRP3 (Cell Signaling Technology) and Ki67 (Abcam). The next day, sections were blocked in 3% hydrogen peroxide for 10 minutes and incubated in goat anti-rabbit secondary for 45 minutes. Sections were developed with 3,3' -diaminobenzidine tetra hydrochloride chromogen (Abcam) for 10 minutes and counter- stained with haematoxylin for 1 minute. Slides were then dipped 10 times each in the following order, once in 70% ethanol, twice in 95% ethanol, twice in 100% ethanol and 1 minute in xylene. The slides were then mounted with DPX mounting media.

2.1.9.2 Image analyses

Image acquisition was performed on an ImageXpress® Pico (Molecular Devices) and CellReporterExpress® software (Molecular Devices), fitted with a 4x, 20x and 40x objective.

Whole section acquisition was performed on the 4x objective. Stained sections were qualitatively assessed for morphological differences.

2.1.10 Statistical analysis

Data was normalized using ImageLab software™ and Western blot values were expressed as a percentage of the wild-type (WT) group. Results are presented as mean ± Standard Error of the Mean (SEM). Graphpad Prism® version 7 (Graphpad Software, Inc, CA, USA) was used to perform statistical analysis. Groups were compared by using an unpaired T-test. A value of $p<0.05$ was regarded as statistically significant.

2.2 *In vivo* triple negative breast cancer (TNBC) model

Invasive breast cancer allografts were established in wild-type (WT) C57BL/6 mice and mice lacking *SAA1* and *SAA2* (SAADKO) (refer to section 2.1) for this model. EO771 cells were subcutaneously injected at the fourth mammary fat pad into 9-week-old C57BL/6 WT and SAADKO mice. The EO771 cell line is a spontaneously developing medullary breast adenocarcinoma from C57BL/6 mice and is therefore considered as a syngeneic triple negative breast cancer (TNBC) model to study pre-clinical immune-oncology (Johnston *et al*., 2015). Syngeneic models are allografts immortalized from mouse cancer cell lines, which are then engrafted back into the same inbred immunocompetent mouse strain. Beneficially, the identical host and cell line strain ensures that tumour rejection doesn't occur. Furthermore, subcutaneous injections can be carefully timed to synchronize tumour development and mimic xenograft study designs. For this model, the experimental endpoint was reached when tumour volumes reached 300-400 mm^3. Figure 2.2.1 shows the study design for the TNBC model.

2.2.1 Study design for triple negative breast cancer (TNBC)

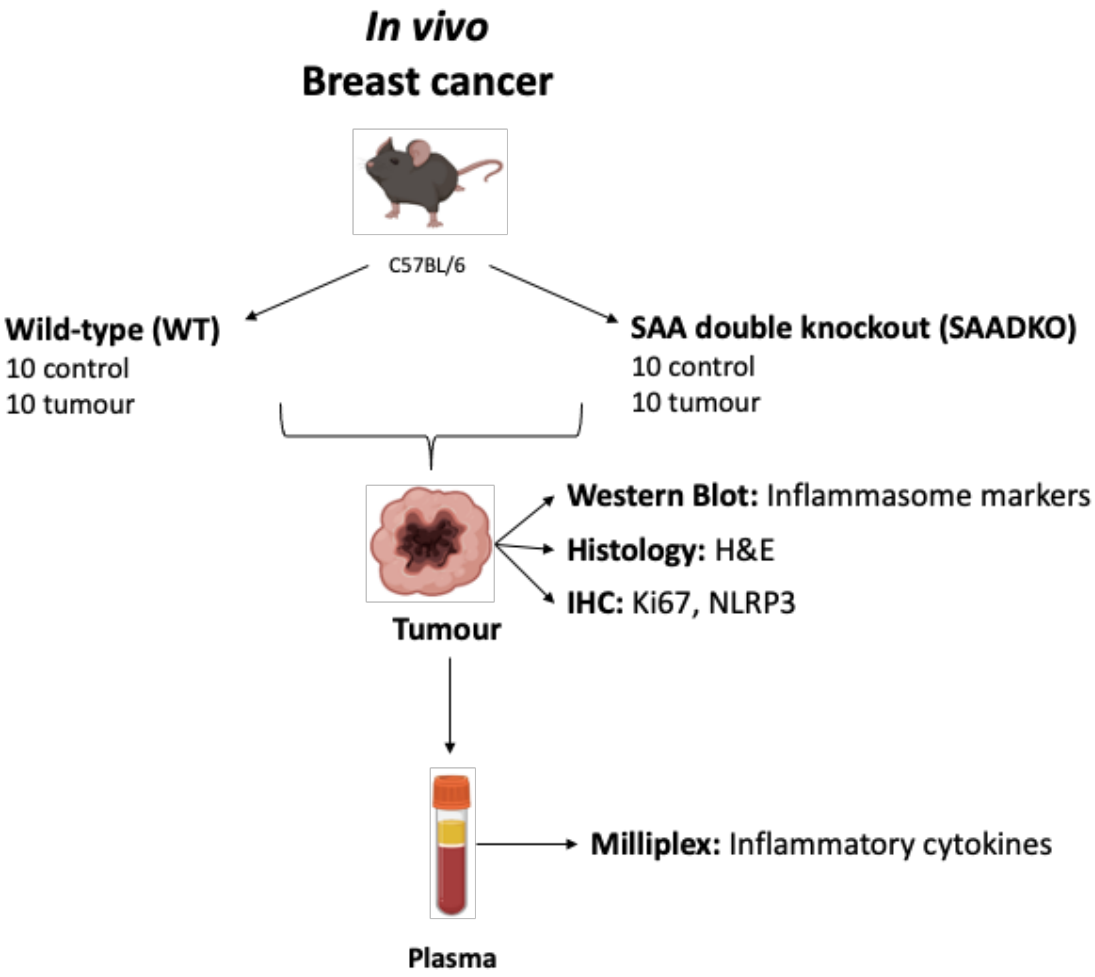

Figure 2.2.1: Study design for TNBC in WT and SAADKO mice. **Abbreviations**: **H&E**: Haematoxylin and eosin; **IHC**: Immunohistochemistry; **SAADKO**: SAA-double knockout; **WT:** Wild-type

2.2.2 Ethical clearance, animals and housing

Ethical clearance

Ethical clearance was obtained from Stellenbosch University Ethical committee (Project ID: 6426) to assess tumour growth as well as the role of SAA in C57BL/6 Wild-type (WT) mice and C57BL/6 mice that lack the *SAA1* and *SAA2* genes, referred to as SAA double knockout (SAADKO) according to the approved protocol (ACU-2019-6426).

Animals and housing

Maria Cecilia de Beer (University of Kentucky, USA) generously donated SAADKO breeding pairs that were bred alongside WT mice at the Tygerberg Animal Facility (Stellenbosch University). The mice were housed under temperature-controlled conditions in a 12-hour reversed dark-light cycle. A standard chow diet and distilled water were available to all mice, ad libitum. A total of 40 mice were used in the study (20 WT mice and 20 SAADKO mice). The mice were then further divided into two groups: control and EO771 tumour-induced mice.

2.2.3 Tumour induction, monitoring and tumour assessment

Cell culture

The EO771 breast cancer cell line (C57BL/6 syngeneic murine breast cancer cell line) was cultured in Dulbecco's Modified Eagle Medium (DMEM), supplemented with 10% FBS and 1% PenStrep. The cells were subcultured with Trypsin and maintained in a humidified incubator at 37°C with 5% CO_2. Before injecting the mice, the cells were detached with Trypsin, pelleted, and washed three times with Hank's Balanced Salt Solution (HBSS, Sigma Aldrich). The HBSS suspended cells were diluted to 1.5 x 10^6 cells/100 μL and aliquoted into syringes fitted with a 23-gauge needle.

Tumour establishment

EO771 cells were subcutaneously injected at the fourth mammary fat pad of 9-week-old WT and SAADKO mice under 3% Isoflurane (Isofor, Safeline Pharmaceuticals) sedation. Control mice were injected at the same site with 100 μL HBSS.

Assessment and measurements

Following injections, mice were monitored for three days to ensure that no physical deterioration had occurred. The mice were then weighed and assessed every second day. Once a palpable tumour in the tumour-bearing mice were observed, tumours were measured every second day with a digital caliper and tumour volumes were calculated as follows:

$$Tumour\ volume\ (mm^3) = \frac{W^2\ x\ L}{2}$$

Where W represents the width of the tumour and L the length. The experimental endpoint was reached when tumour volumes reached 300-400 mm^3. Humane endpoints were set at a weight loss of more than 10% of the previous measurement, bleeding ulcers or sudden physical deterioration based on the mouse grimace scale.

2.2.4 Sacrifice and sample collection

Upon reaching the experimental or humane endpoint, mice were euthanized under 3% Isoflurane sedation. Blood samples were collected by cardiac puncture with a 23-gauge needle and death was confirmed by cervical dislocation. Prior to cervical dislocation, each mouse was exsanguinated, and the blood was collected into citrate pediatric tubes (Pathcare). For plasma collection, blood samples were centrifuged at 1000 x g using a Labnet Prism Microcentrifuge for 10 minutes. Plasma samples were stored at -80°C in 50 µL aliquots until the day before analysis. Tumours were collected from tumour-bearing mice, weighed and divided into two sections. One sample was frozen with liquid nitrogen and stored at -80°C for further analysis (SDS-PAGE and Western blotting). The second section was stored in 4% neutral buffered formaldehyde (NBF, Merck) for histopathology and immunohistochemistry.

2.2.5 Tumour growth and species survival

Tumour growth

Tumour growth for each species was analyzed using a mixed model ANOVA in R (lmer package, Kenward-Roger's degrees of freedom) on the data of all mice in the study. Thereafter, tumour growth for each species was plotted as the least squares mean ± SEM.

Survival analysis

Mice that reached the experimental or humane endpoint were sacrificed and the date was recorded for survival analysis. The data was then statistically analyzed using a Cox-Mantel Test and the data plotted as a Kaplan-Meier cumulative proportional survival curves.

2.2.6 Blood plasma inflammatory profiling

SAA1 and SAA2

Plasma SAA1/2 levels were assessed with Western blotting, using rabbit anti-mouse SAA antisera (De Beer laboratory, University of Kentucky, USA). The protocols are set out in section 2.1.6 and 2.1.7.

IL-1β, IL-6, IL-10, MCP-1 and TNF-α

The inflammatory profiles of the mice were assessed for IL-1β, IL-6, IL-10, MCP-1 and TNF-α. Briefly, the day before analysis, plasma samples were transferred from -80°C to -20°C. The samples were subjected to a Milliplex MAP Mouse cytokine/chemokine magnetic bead panel (MCYTOMAG-70K, Merck) according to the manufactures protocol and detected by Luminex. In short, analytes from test samples are captured by beads coated with specific capture antibodies (e.g., anti-IL-1β or anti-IL-6). Thereafter, biotinylated detection antibodies are introduced, and the mixture incubated with Streptavidin-PE, a reported molecule, to complete the reaction on the surface of each bead. Finally, each individual bead is identified using flow cytometry and the result quantified based on the fluorescent reporter signals.

2.2.7 Protein harvest and sample preparation

Protein harvest from tumour tissue

Tumour tissue was cut into smaller pieces and homogenized in RIPA buffer with protease and phosphatase inhibitors for protein harvesting from cells. Subsequently, homogenates were incubated on ice for 2 hours before centrifugation (20 minutes at 4°C at 10 000 x g).

Protein quantification and sample preparation

Total protein was determined by means of a Bradford assay. Samples were diluted 40x before addition to Bradford reagent and spectrophotometric measurement at 595 nm on a Cecil Aurius CE 2021 spectrophotometer. A standard curve using six incremental concentrations was prepared from a 2 mg/ml bovine serum albumin (BSA) solution. The measured absorbencies were plotted on a graph in Microsoft excel to determine the standard curve. Protein quantification results were used to calculate the amount of sample needed for 50 μg protein. The lysates were diluted in Laemmli sample buffer (150 μl β-mercaptoethanol and 850 μl Laemmli sample buffer) at a 1:2 ratio. Samples were stored at -80°C until further analysis by Western blot.

TCA Protein precipitation

An equal volume of 40% Trichloroacetic acid (TCA) (Sigma-Aldrich) was added to 50 µL plasma samples and incubated on ice for 30 minutes. After the incubation period, plasma samples were centrifuged at 4500 x g for 8 minutes at 4°C. The supernatant was removed, and the pellet was washed in 100% ice-cold ethanol. This was followed by centrifugation at 13 000 rpm for 5 minutes at 4°C. The pellet was then air-dried on ice for 90 minutes. RIPA buffer was added to the pellet and the samples were incubated overnight at 4°C. The following day a Bradford assay was performed to prepare samples for electrophoresis (section 2.2.8).

2.2.8 SDS-PAGE and Western blot analysis

SDS-PAGE and Western blot analysis were carried out according to section 2.1.7. Briefly, protein samples were subjected to SDS-PAGE on TGX FastCast 12% Acrylamide gels (BioRad) and transferred onto nitrocellulose membranes. Membranes were blocked in 10 mL of Blocking buffer (BioRad) for five minutes and incubated with primary antibodies overnight at 4°C (Table 2.1). The following day, membranes were incubated with anti-rabbit secondary antibody (7074; Cell Signaling Technology) for 60 minutes before developing with Clarity ECL (BioRad). Analyses were performed with ImageLab software (BioRad), by using the total protein content on each membrane for normalization.

2.2.9 Tissue processing and sectioning

The formalin fixed tissue samples were processed by placing them into separate cassettes and underwent processing using the Leica HistoCORE PEARL automated tissue processor, following a 20-hour pre-programmed time-schedule. The processing consisted of dehydration, clearing and wax infiltration steps. The dehydration step ensured that all water was removed from the tissue through a series of increasing percentages of ethanol, namely two rounds of 70% (90 minutes each), one round of 90% (90 minutes), two rounds of 100% (90 minutes each) and a final round of 100% (120 minutes). The dehydration step was followed by the clearing of the tissue samples by removing the ethanol and replacing it with xylene. Tissues were incubated in xylene twice, once for 90 minutes and once for 120 minutes. Wax infiltration was done with two paraffin wax incubation steps, consisting of 120 minutes each. The processed tissues were then placed in individual cassettes, orientated to achieve longitudinal sections through each sample. The cassettes were filled with hot paraffin wax using the Leica EG1150H tissue embedder. The cassettes were cooled on the Leica 1150C cold block until the wax hardened. The samples were sectioned into 3 µm sections using a microtome (Leica Biosystems, #RM2235) due to the densely packed cellular nature of the tumour samples. The

sections were transferred to a pre-warmed water bath, after which they were placed on microscope slides and were placed on a pre-warmed heating plate to dry. The samples were then subjected to haematoxylin and eosin staining (H&E) and immunohistochemistry.

2.2.9.1 Histology

H&E stains were performed to assess ultrastructural changes. Prior to the staining protocol, samples were deparaffinised and rehydrated through incubating the slides 5 minutes each in the following order; twice in xylene, twice in 100% ethanol, twice in 95% ethanol and once in 70% ethanol. Cells were then stained in Mayer's Haematoxylin for 11 minutes each, rinsed in tap water for 2 minutes and Scott's water for 1 minute and stained with eosin for 30 seconds. Slides were then dipped 10 times each in the following order, once in 70% ethanol, twice in 95% ethanol, twice in 100% ethanol and 1 minute in xylene. Slides were mounted with coverslips using DPX mounting media.

2.2.9.2 Immunohistochemistry

The sections underwent deparaffinization and rehydration as mentioned in section 2.1.9.1 before heat-mediated antigen retrieval in sodium citrate buffer. Sections were blocked in 5% goat serum for 90 minutes before overnight primary antibody incubation. The following primary antibodies were used: NLRP3 (Cell Signaling Technology) and Ki67 (Abcam). The next day, sections were blocked in 3% hydrogen peroxide for 10 minutes and incubated with goat anti-rabbit secondary for 45 minutes. Sections were developed with 3,3' -diaminobenzidine tetra hydrochloride chromogen (Abcam) for 10 minutes and counter- stained with haematoxylin for 1 minute before dehydration (refer to section 2.1.9.1) and mounting with DPX mounting media.

2.2.9.3 Image analyses

Image acquisition was performed on an ImageXpress® Pico (Molecular Devices) and CellReporterExpress® software (Molecular Devices), fitted with a 4x, 20x and 40x objective. Whole section acquisition was performed on the 4x objective. Stained sections were qualitatively assessed for morphological differences.

2.2.10 Statistical analysis

Data was normalized using ImageLab software™ and Western blot values were expressed as a percentage of the WT group. Results are presented as mean ± Standard Error of the Mean (SEM). Graphpad Prism® version 7 (Graphpad Software, Inc, CA, USA) was used to perform statistical analysis. Groups were compared by using an unpaired T-test. A value of $p<0.05$ was regarded as statistically significant.

Chapter 3

Results

3.1 Introduction: The role of SAA in NLRP3 inflammasome activation in acute colitis (AC)

Chronic relapsing intestinal inflammation and a loss of homeostasis in the gut immune response characterizes inflammatory bowel diseases (IBDs) such as Crohn's disease and ulcerative colitis, where the most serious complication is the increased risk of developing colitis-associated cancer (CAC) (Fransescone *et al*., 2015). As mentioned previously, SAA1 and SAA2 are acute phase proteins (APPs) which are significantly upregulated systemically during an inflammatory response. SAA proteins are therefore implicated in chronic inflammatory states and inflammation-associated pathologies, including IBDs (Mullan *et al*., 2006). Hence, understanding the regulatory circuits that control innate immune responses in the intestine is critical to elucidate the pathogenesis of IBD. The NOD-like receptor (NLR)-family of inflammasomes have been identified as crucial regulators of intestinal homeostasis, by mediating the assembly of the inflammasome complex in the presence of microbial ligands (Sutterwala *et al*., 2006). This response triggers the activation of caspase-1 and the secretion of IL-1β and IL-18 in IBDs, however, the role of SAA and the NLRP3 inflammasome in acute colitis has not been elucidated. Here, we utilized a model of dextran sodium sulfate (DSS)-induced acute colitis as a model for IBD.

3.1.1 Confirmation of SAA1/2 knockout in DSS-induced acute colitis in SAADKO mice

Immunoblotting and qPCR was used to determine whether SAA1/2 expression was successfully knocked out in SAADKO mice (Figure 3.1.1 and Figure 3.1.2). In plasma samples from SAADKO mice, the expression levels of SAA1 and SAA2 were significantly decreased in the SAADKO group when compared to WT (100 ± 21.5 vs 7.73 ± 2.76, $p<0.05$) (Figure 3.1.1). To confirm these results, qPCR was performed by assessing *SAA1* and *SAA2* expression in these mice. Figure 3.1.2 shows that no expression of *SAA1* (1.02 ± 0.13 vs 0 ± 0, $p<0.001$) and *SAA2* (1.02 ± 0.12 vs 0 ± 0, $p<0.001$) were detected.

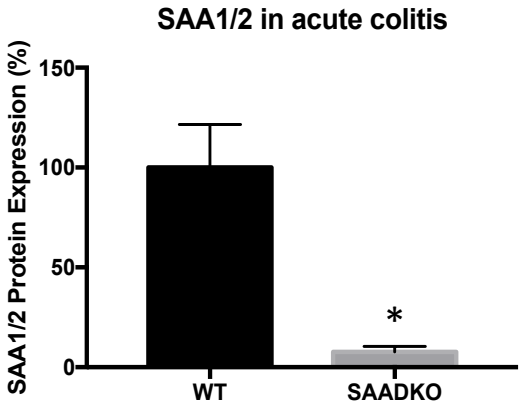

Figure 3.1.1: Western blot analysis to detect plasma SAA1/2 in DSS-induced colitis. Proteins were separated by SDS-PAGE and transferred to a nitrocellulose membrane for analysis. Results are presented as mean ± SEM (n=12). The asterisk (*) denotes a significant decrease in SAA1/2 in SAADKO mice compared to WT mice ($p<0.05$). Representative Western blot images can be found in Figure 3.1.7.

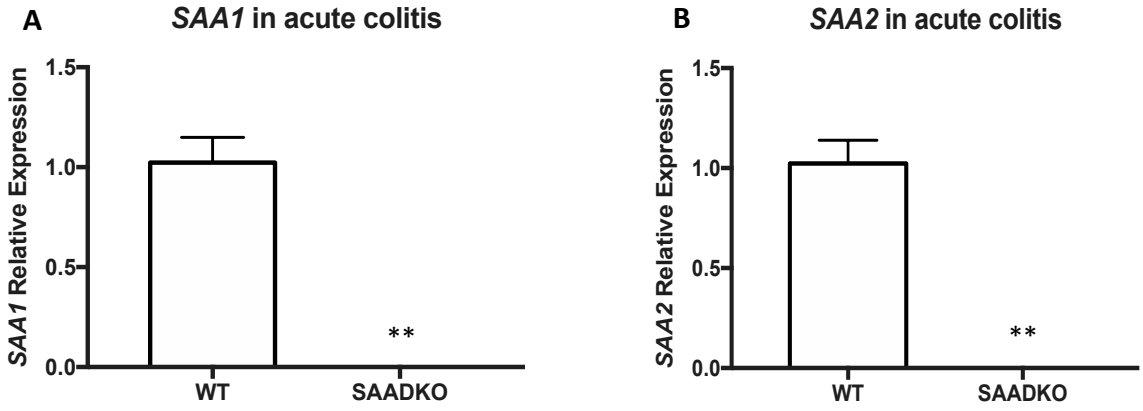

Figure 3.1.2: qPCR analysis to detect *SAA1/2* in DSS-induced colitis. The expression of *SAA1/2* was not detected in SAADKO mice. Results are presented as mean ± SEM (n=6). The asterisk (**) denotes a significant decrease in SAADKO mice compared to WT mice ($p<0.01$).

Furthermore, *SAA3*, which is also a functional and inducible protein in mice, was decreased in SAADKO compared to WT mice (1.22 ± 0.45 vs 0.17 ± 0.03, p=0.06) (Figure 3.1.3).

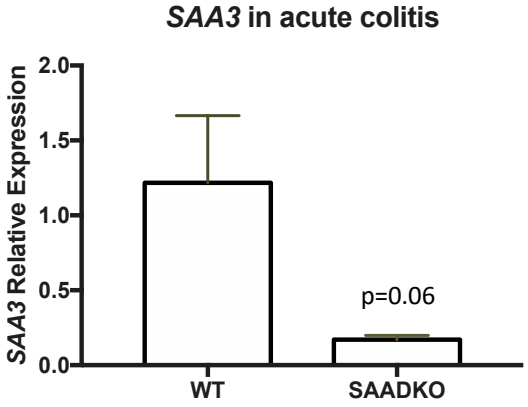

Figure 3.1.3: qPCR analysis to detect *SAA3* in DSS-induced colitis. The expression of *SAA3* was decreased in SAADKO mice compared to WT mice (p=0.06). Results are presented as mean ± SEM (n=6).

3.1.2 SAA1/2 and inflammation in DSS-induced acute colitis (AC)

3.1.2.1 SAADKO mice present with increased levels of pro-inflammatory cytokines

Blood plasma was analyzed for the inflammatory markers IL-1β, IL-6, IL-10, MCP-1 and TNF-α (Figure 3.1.4). Compared to WT mice, SAADKO mice had significantly increased IL-6 concentrations (6.36 ± 1.16 vs 13.52 ± 0.84, p<0.001). Although not significant, IL-1β (2.19 ± 0.14 vs 3.4 ± 0.76, p=0.05) and IL-10 (9.62 ± 1.73 vs 12.76 ± 3.12, p>0.05) were also increased in SAADKO mice compared to WT mice. No changes were observed in MCP-1 (26.65 ± 3.0 vs 31.58 ± 5.23, p>0.05) and TNF-α (5.8 ± 0.82 vs 5.8 ± 0.9, p>0.05) in SAADKO compared to WT mice.

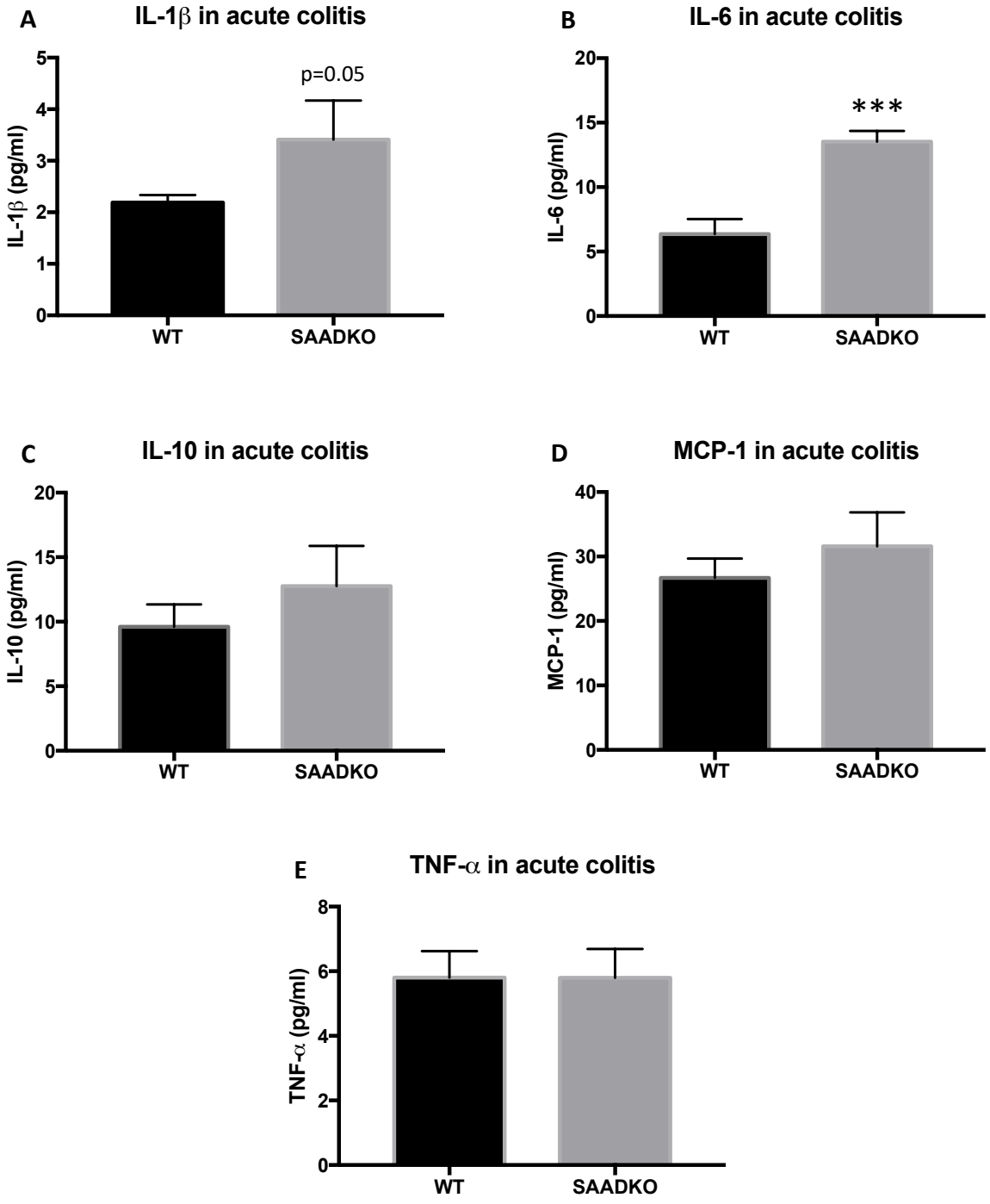

Figure 3.1.4*:* Inflammatory profile of WT and SAADKO mice in DSS-induced acute colitis. A Milliplex assay was used to assess the inflammatory profile (IL-1β, IL-6, IL-10, MCP-1 and TNF-α) of the plasma of acute colitis mice. Results are presented as mean ± SEM (n=10). The asterisk (***) denotes a significant increase in SAADKO compared to WT mice ($p<0.001$).

To support the results obtained by the Milliplex assay above, qPCR was also performed to determine the expression of *IL-1*β (Figure 3.1.5). These findings were not significant (1.31 ± 0.53 vs 1.9 ± 0.8, p>0.05).

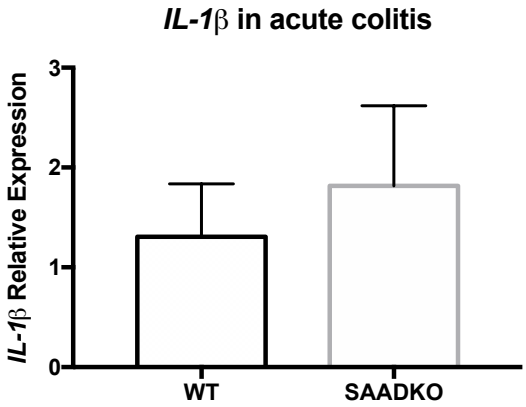

Figure 3.1.5: qPCR analysis to detect *IL-1*β in DSS-induced colitis. No significant changes were observed in SAADKO mice compared to WT mice (p>0.05). Results are presented as mean ± SEM (n=6).

3.1.3 SAADKO does not promote NLRP3 activation in DSS-induced acute colitis

Immunoblotting was used to characterize the biology of WT and SAADKO colons in a DSS-induced colitis mouse model (Figure 3.1.6). With regards to MCM2, a regulator of cell proliferation, no significant changes were observed (100 ± 13.99 vs 94.97 ± 12.43, p>0.05). In terms of the NLRP3 inflammasome complex, NLRP3 had no significant changes in SAADKO mice compared to WT mice (100 ± 30.3 vs 151.2 ± 51.91, p>0.05). There were also no changes in caspase-1 in SAADKO mice compared to WT mice and no cleaved caspase-1 bands were observed (100 ± 13.81 vs 94.31 ± 13.66, p>0.05). No significant change in NFkB expression was observed in SAADKO mice compared to WT mice (94.61 ± 21.98 vs 131.4 ± 30.26, p>0.05).

Several signaling pathways have been implicated in the priming step of the NLRP3 inflammasome, including MAPKs. Although no significant changes for ERK1/2 (94.83 ± 17.11 vs 70.66 ± 10.73, p>0.05) were observed, the MAPK, p38, was significantly increased in SAADKO mice compared to WT (95.23 ± 8.24 vs 197.2 ± 17.39, p<0.001).

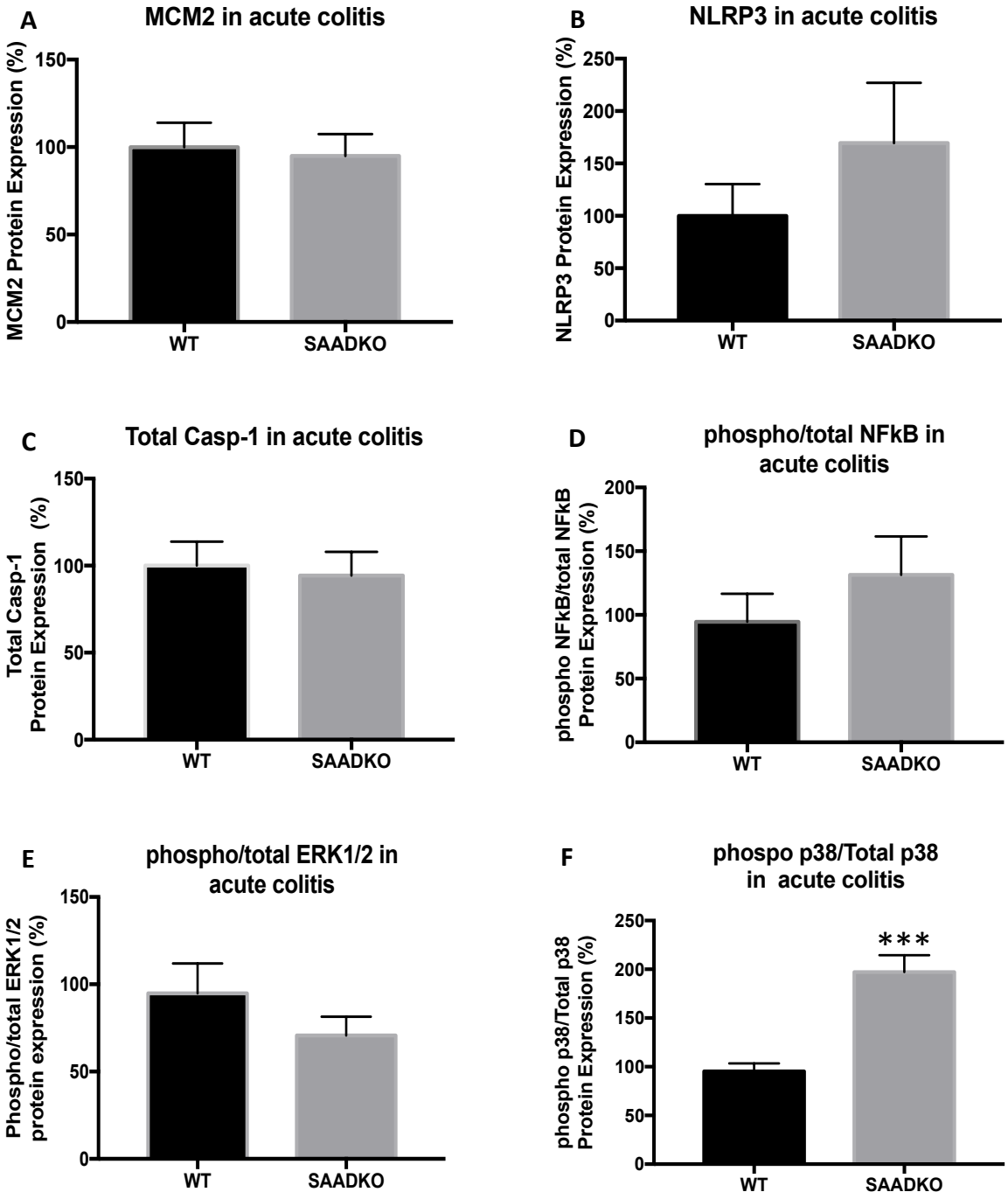

Figure 3.1.6: Western blot analysis to detect NLRP3 inflammasome components and signaling pathways in DSS-induced colitis. Proteins were separated by SDS-PAGE and transferred to a nitrocellulose membrane for analysis. Results are presented as mean ± SEM (n=12). The asterisk (***) denotes a significant increase in p38 in SAADKO mice compared to WT mice ($p<0.001$). Representative Western blot images can be found in Figure 3.1.7.

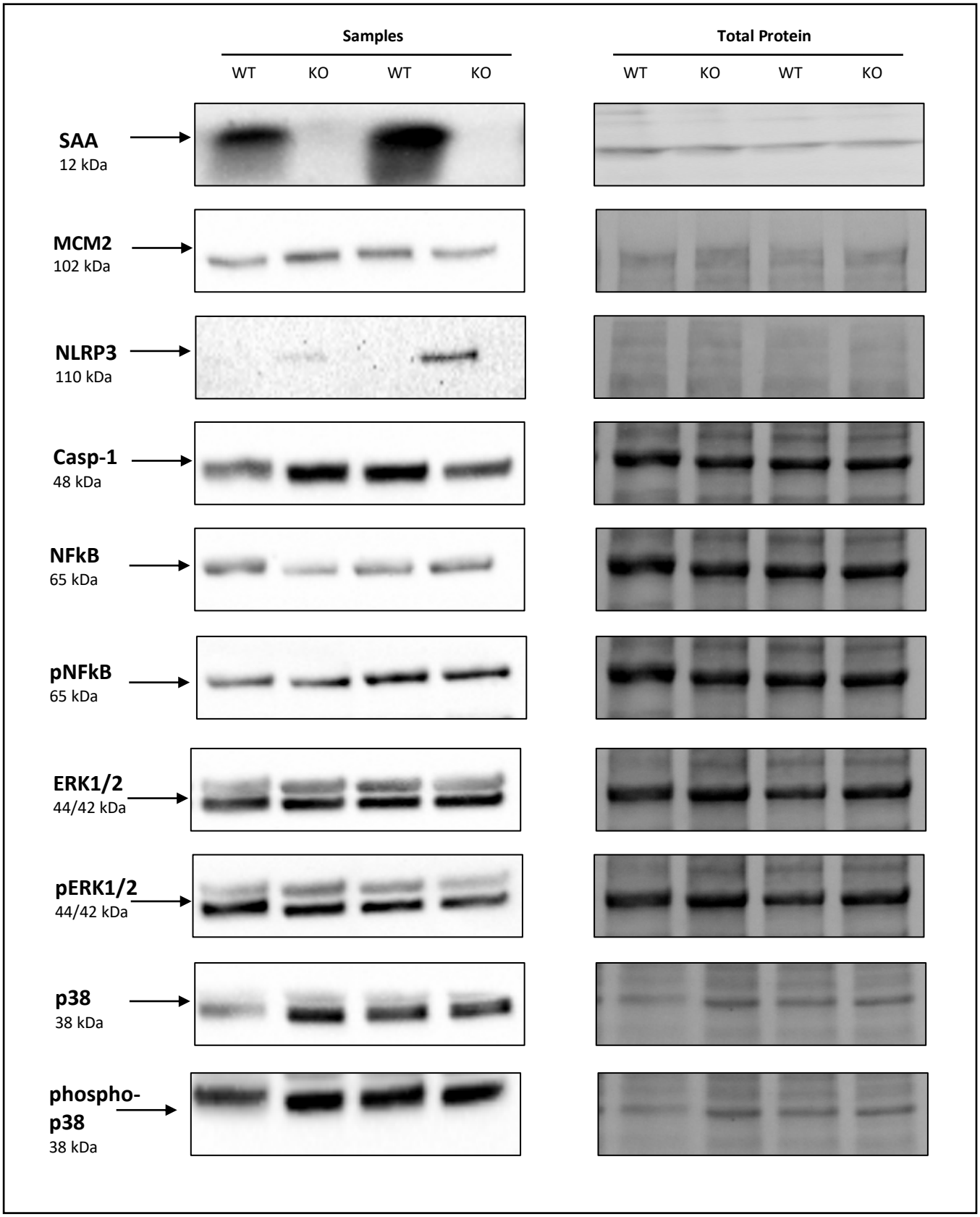

Figure 3.1.7: Representative images of Western blots for DSS-induced colitis. Proteins were separated by SDS-PAGE and transferred to a nitrocellulose membrane for analysis. **Abbreviations**: **KO**: knockout; **WT**: Wild-type

qPCR was also performed to determine the expression of *NLRP3* (Figure 3.1.8). No significance in *NLRP3* expression was detected in SAADKO mice compared to WT mice (1.16 ± 0.39 vs 1.96 ± 0.92; p>0.05).

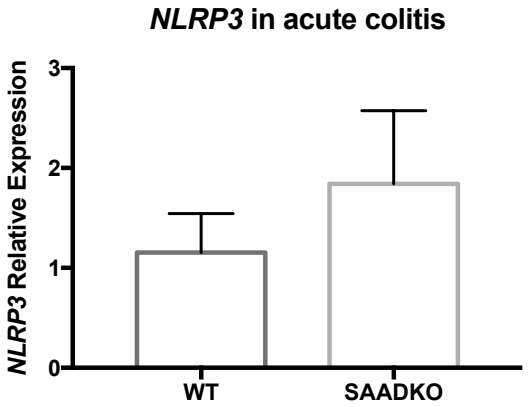

Figure 3.1.8: qPCR analysis to detect NLRP3 in DSS-induced colitis. No significant changes were observed in SAADKO mice compared to WT mice (p>0.05). Results are presented as mean ± SEM (n=6).

3.1.4 SAADKO promotes loss of epithelial marker in DSS-induced acute colitis

Immunoblotting was used to assess the expression of epithelial (E-cadherin) and mesenchymal markers (vimentin and Snail) in WT and SAADKO mice, which play a role in epithelial to mesenchymal transition (EMT). EMT is a process by which epithelial cells lose their cell polarity and cell–cell adhesion, and gain migratory and invasive properties to become mesenchymal stem cells (Schneider *et al*., 2010). These cells are multipotent stromal cells that can differentiate into a variety of cell types. The results are displayed in Figure 3.1.9. A decreased trend of E-cadherin expression was observed in SAADKO mice compared to WT mice (100 ± 19.32 vs 61.18 ± 7.77, p=0.08). Furthermore, no significant change in Snail expression was observed (100 ± 15.67 vs 120.3 ± 18.84, p>0.05). Similarly, no changes in the expression of vimentin was observed in SAADKO compared to WT mice (100 ± 13.72 vs 102.2 ± 13.41, p>0.05).

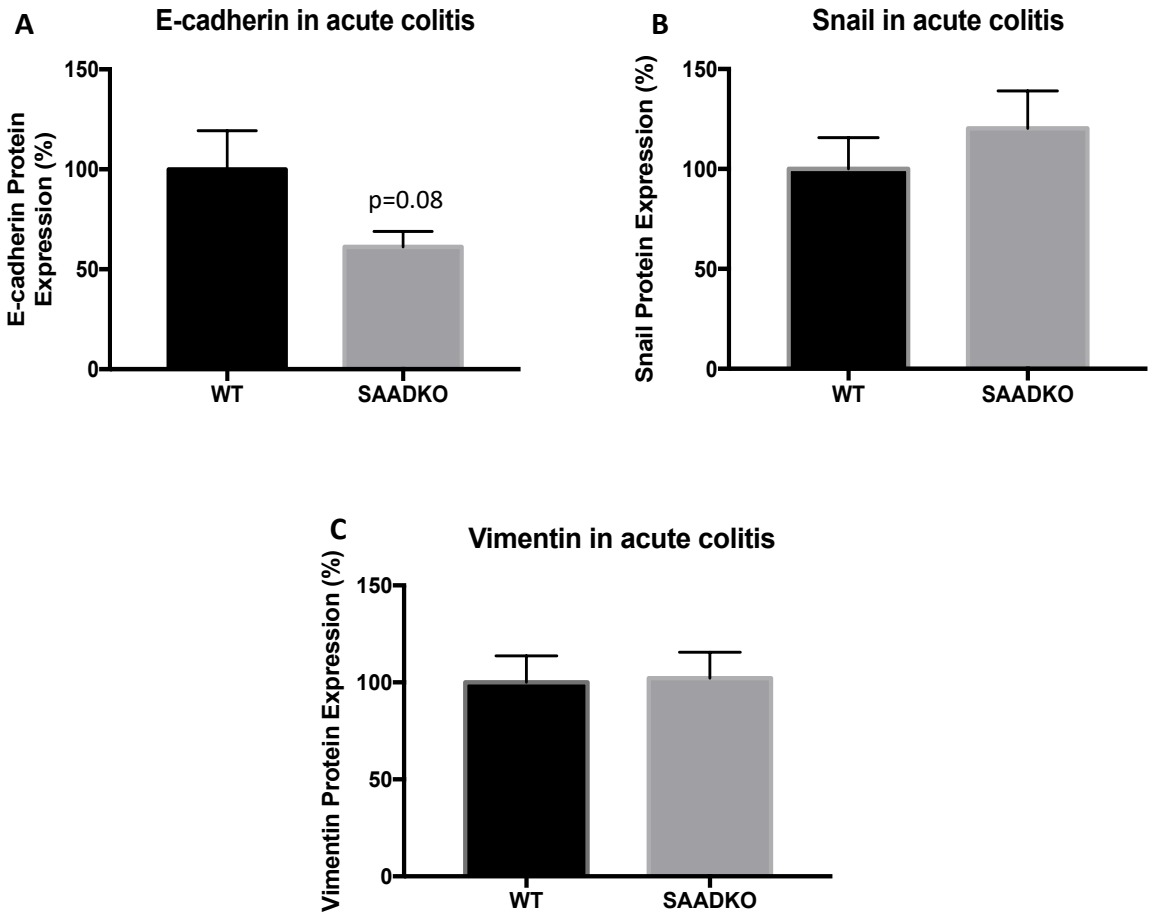

Figure 3.1.9: Western blot analysis to detect epithelial and mesenchymal markers in DSS-induced colitis. Proteins were separated by SDS-PAGE and transferred to a nitrocellulose membrane for analysis. Results are presented as mean ± SEM (n=12). Representative Western blot images can be found in Figure 3.1.10.

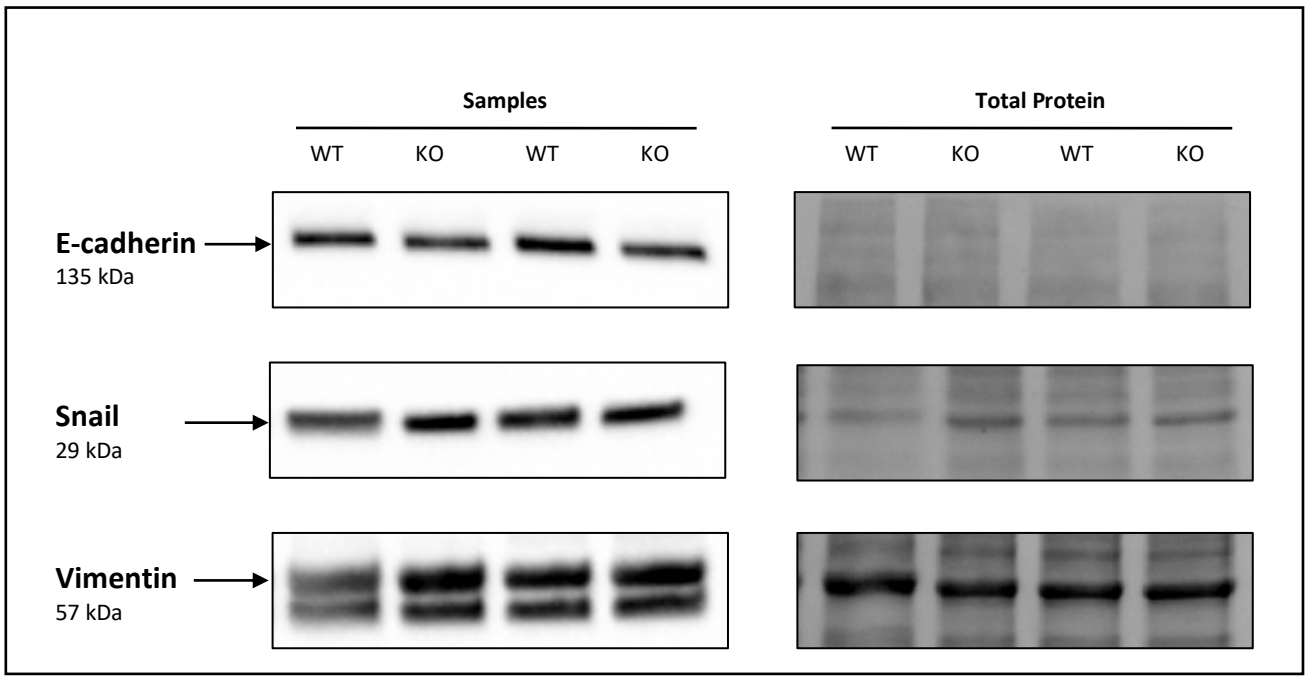

Figure 3.1.10: Representative images of Western blots for metastasis in DSS-induced acute colitis. Proteins were separated by SDS-PAGE and transferred to a nitrocellulose membrane for analysis. **Abbreviations**: **KO**: knockout; **WT**: Wild-type

3.1.5 Colon histology in acute colitis (AC)

3.1.5.1 SAADKO mice present with histomorphologic abnormalities

Haematoxylin and Eosin (H&E) staining was used to qualitatively assess histomorphologic changes in the distal colons (black arrow) of SAADKO mice (Figure 3.1.11 **B**) and WT mice (Figure 3.1.11 **A**). Microscopic analyses show that SAADKO mice present with increased histomorphologic abnormalities (Figure 3.1.11 **D**). Marked grades of crypt loss is highlighted (black arrow) in WT (**C**) and SAADKO mice (**D**). Epithelial erosion (red arrow) and cryptitis (blue arrow) is observed in SAADKO mice (**D**).

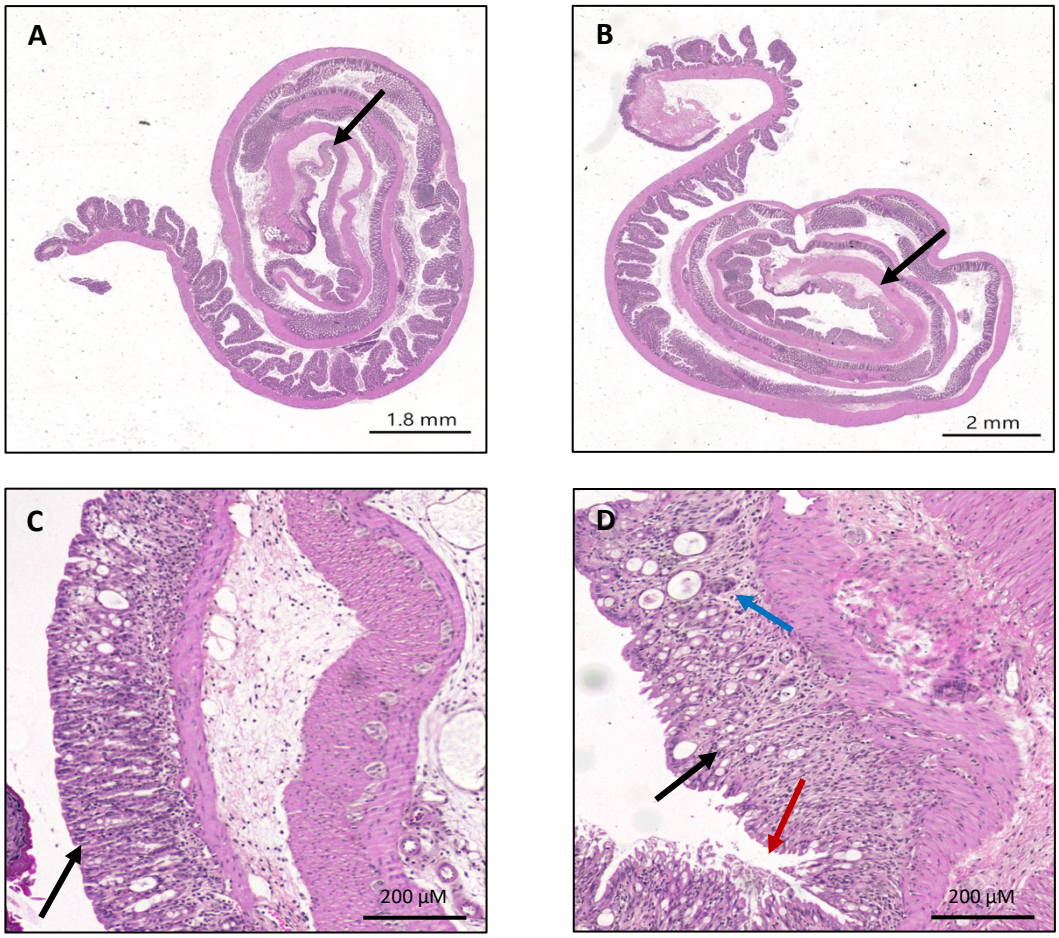

Figure 3.1.11: Colitis-associated morphologic abnormalities are increased in SAADKO mice. Representative images of H&E stains of the distal colon of WT (**A**) and SAADKO (**B**) mice.

3.1.5.2 SAADKO mice present with increased Ki67

Immunohistochemistry was used to qualitatively assess the expression of Ki67 in the distal colon of WT (Figure 3.1.12 **A**) and SAADKO (Figure 3.1.12 **B**) mice as indicated by the black arrow. Qualitatively, more Ki67 positive cells are observed in SAADKO mice (Figure 3.1.12 **D**) compared to WT mice (Figure 3.1.12 **C**).

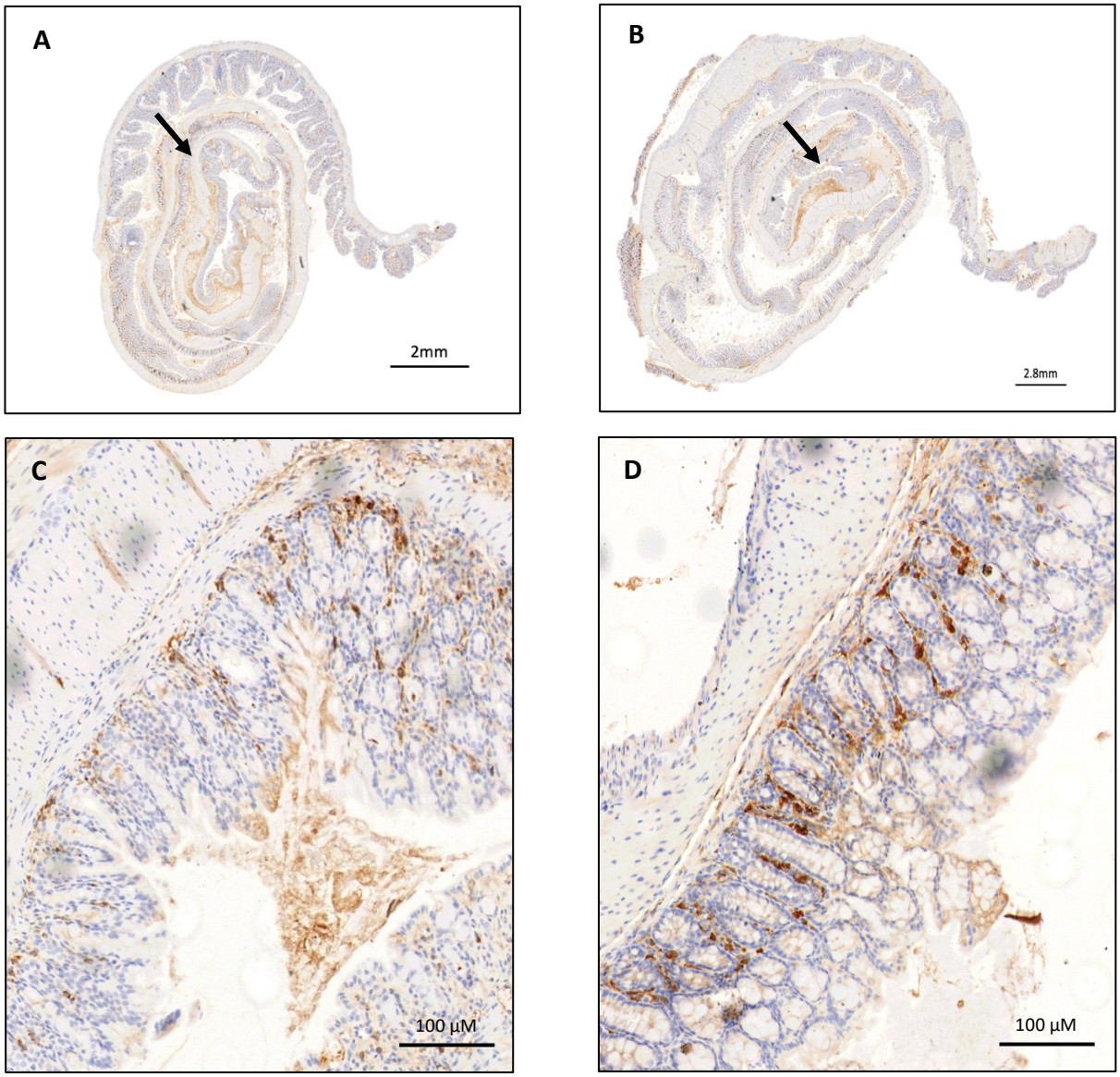

Figure 3.1.12: Ki67 is increased in SAADKO mice in DSS-induced colitis. Representative immunohistochemical images in the distal colon (black arrows) of WT (**A & C**) and SAADKO (**B & D**) mice stained with Ki67.

3.2 Introduction: The role of SAA in NLRP3 inflammasome activation in Azoxymethane (AOM)/Dextran sulfate (DSS)-induced Colitis-associated Cancer (CAC)

Significant evidence indicates that inflammation plays an important role in tumourigenesis by altering the tumour microenvironment (TME) through the overproduction of pro-inflammatory cytokines, the promotion of tumour proliferation, metastases, and evasion of programmed cell death (Mantovani *et al*., 2008). As mentioned previously, SAA is an acute phase protein, mainly found in hepatocytes. Although its role in the development and progression of tumourigenesis has been pointed out in recent literature, the exact role and functioning of SAA in this context remains to be elucidated (Uhlar & Whitehead, 1999). In several types of cancer, the NLRP3 inflammasome has been linked with the overproduction of pro-inflammatory cytokines, such as IL-1β, providing an inflammatory environment for cancer progression (Ning *et al*., 2015). However, the role of SAA in the activation of the NLRP3 inflammasome in colitis-associated cancer (CAC) remains unclear. For this part of the study, we utilized the AOM/DSS-induced model of CAC.

3.2.1 Confirmation of SAA1/2 knockout in colitis-associated cancer (CAC) in SAADKO mice

Immunoblotting and qPCR was used to determine whether SAA1/2 expression was successfully knocked out in SAADKO mice (Figure 3.2.1 and Figure 3.2.2). In plasma samples from SAADKO mice, the expression of SAA1 and SAA2 was decreased in the SAADKO group when compared to WT (100 ± 64.8 vs 9.3 ± 0.96, $p>0.05$) (Figure 3.1.1). To confirm these results, qPCR was performed by assessing *SAA1* and *SAA2* expression in these mice. Figure 3.2.2 shows that no expression of *SAA1* (1.17 ± 0.37 vs 0 ± 0, $p<0.05$) and *SAA2* (1.2 ± 0.45 vs 0 ± 0, $p<0.05$) were detected.

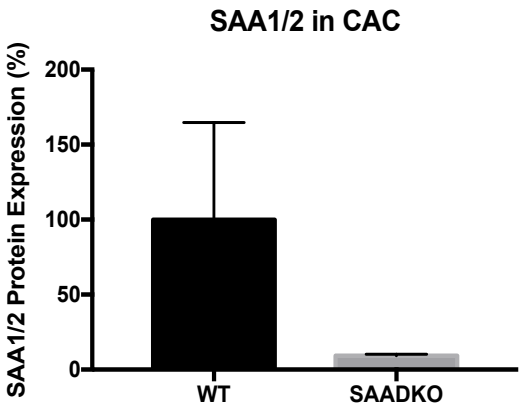

Figure 3.2.1: Western blot analysis to detect SAA1/2 in AOM/DSS-induced colitis-associated cancer (CAC). Proteins were separated by SDS-PAGE and transferred to a nitrocellulose membrane for analysis. Results are presented as mean ± SEM (n=6). Representative Western blot images can be found in Figure 3.2.7.

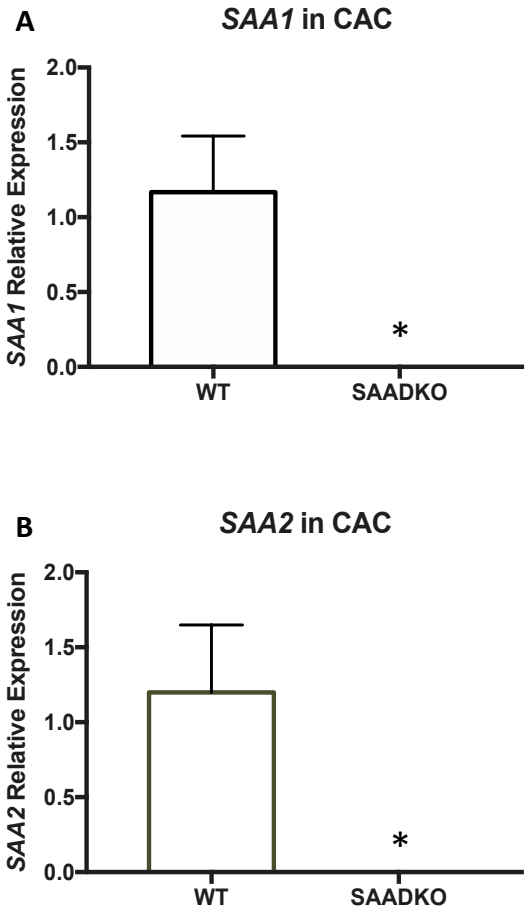

Figure 3.2.2: qPCR analysis to detect *SAA1/2* in AOM/DSS-induced colitis-associated cancer (CAC). The expression of *SAA1/2* was not detected in SAADKO mice. The vertical bars represent mean ± SEM (n=6). The asterisk (*) denotes a significant decrease in SAADKO mice compared to WT mice ($p<0.05$).

Furthermore, *SAA3*, which is also a functional and inducible protein in mice, was decreased in SAADKO compared to WT mice (1.12 ± 0.2 vs 0.13 ± 0.04, $p<0.01$) (Figure 3.2.3).

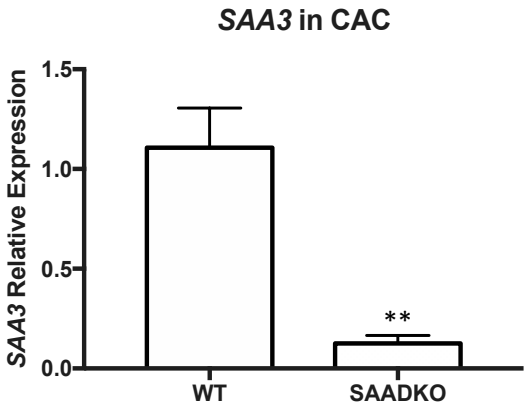

Figure 3.2.3: qPCR analysis to detect *SAA3* in AOM/DSS-induced colitis-associated cancer (CAC). The expression of SAA3 was decreased in SAADKO mice compared to WT mice ($p<0.01$). The vertical bars represent mean ± SEM (n=6).

3.2.2 SAA1/2 and inflammation in AOM/DSS-induced colitis-associated cancer (CAC)

3.2.2.1 SAADKO mice present with decreased levels of pro-inflammatory cytokines

CAC tissue was analyzed by immunoblotting for the inflammatory marker, IL-6 (Figure 3.2.4). Compared to WT mice, SAADKO mice had a decreased trend of IL-6 compared to WT mice (100 ± 30.39 vs 52.86 ± 7.08, p=0.09). qPCR was performed for *IL-1*β expression. Figure 3.2.5 shows that *IL-1*β was significantly decreased in SAADKO mice compared to WT mice (1.03 ± 0.08 vs 0.53 ± 0.11, p<0.01).

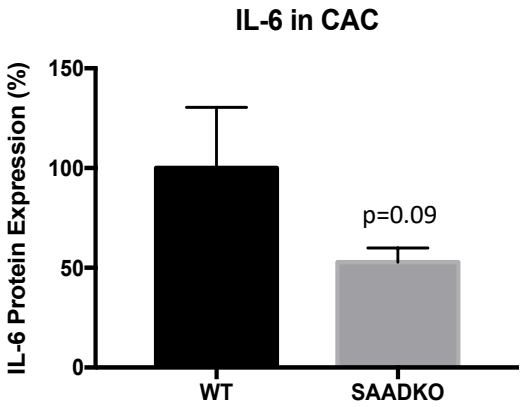

Figure 3.2.4: Western blot analysis to detect IL-6 in AOM/DSS-induced colitis-associated cancer (CAC). Proteins were separated by SDS-PAGE and transferred to a nitrocellulose membrane for analysis. Results are presented as mean ± SEM (n=6). Representative Western blot images can be found in Figure 3.2.10.

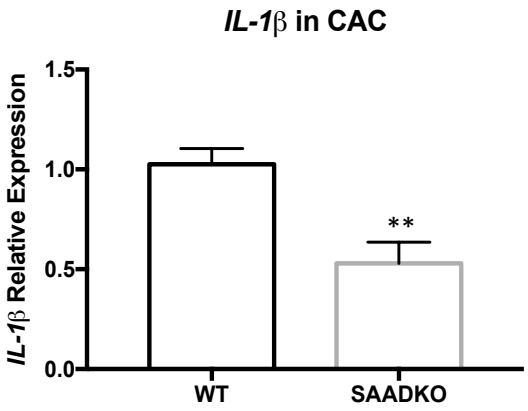

Figure 3.2.5: qPCR analysis to detect *IL-1*β in AOM/DSS-induced colitis-associated cancer (CAC). The asterisk (*) denotes a significant decrease in SAADKO mice compared to WT mice ($p<0.01$). Results are presented as mean ± SEM (n=6).

3.2.3 SAADKO suppresses NLRP3 activation in AOM/DSS-induced colitis-associated cancer (CAC)

Immunoblotting was used to characterize the biology of WT and SAADKO tumours in a CAC mouse model (Figure 3.2.6). MCM2 was decreased in SAADKO mice compared to WT mice (100 ± 9.35 vs 73.76 ± 10.55, $p=0.08$). In terms of the NLRP3 inflammasome complex, NLRP3 was significantly decreased in SAADKO mice compared to WT mice (100 ± 10.24 vs 66.95 ± 8.16, $p<0.05$). Corresponding with NLRP3, caspase-1 was decreased in SAADKO mice compared to WT mice (112.1 ± 20.45 vs 60.88 ± 11.78, $p=0.06$). however, no changes in NFkB expression levels were observed (124.7 ± 20.06 vs 118.4 ± 8.45, $p>0.05$).

Furthermore, no significant changes for total ERK1/2 (94.83 ± 17.11 vs 70.66 ± 10.73, $p>0.05$) were observed and no phosphorylated ERK1/2 bands were detected. The MAPK, p38, also showed no differences in SAADKO compared to WT mice (103 ± 13.96 vs 111.2 ± 11.24, $p>0.05$).

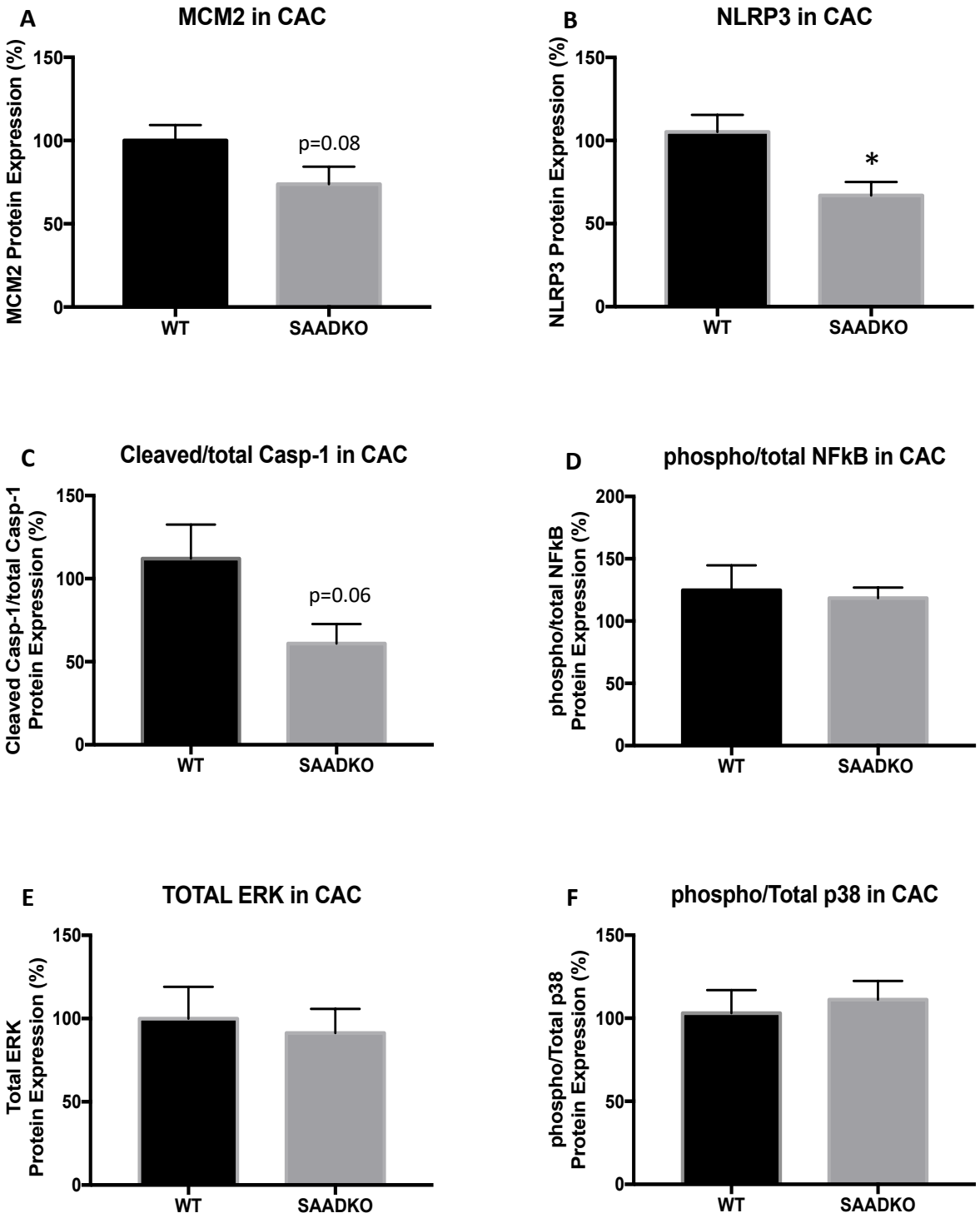

Figure 3.2.6*:* Western blot analysis to detect NLRP3 inflammasome components and signaling pathways in AOM/DSS-induced colitis-associated cancer (CAC). Proteins were separated by SDS-PAGE and transferred to a nitrocellulose membrane for analysis. Results are presented as mean ± SEM (n=12). The asterisk (*) denotes a significant decrease in NLRP3 in SAADKO mice compared to WT mice ($p<0.05$). Representative Western blot images can be found in Figure 3.2.7.

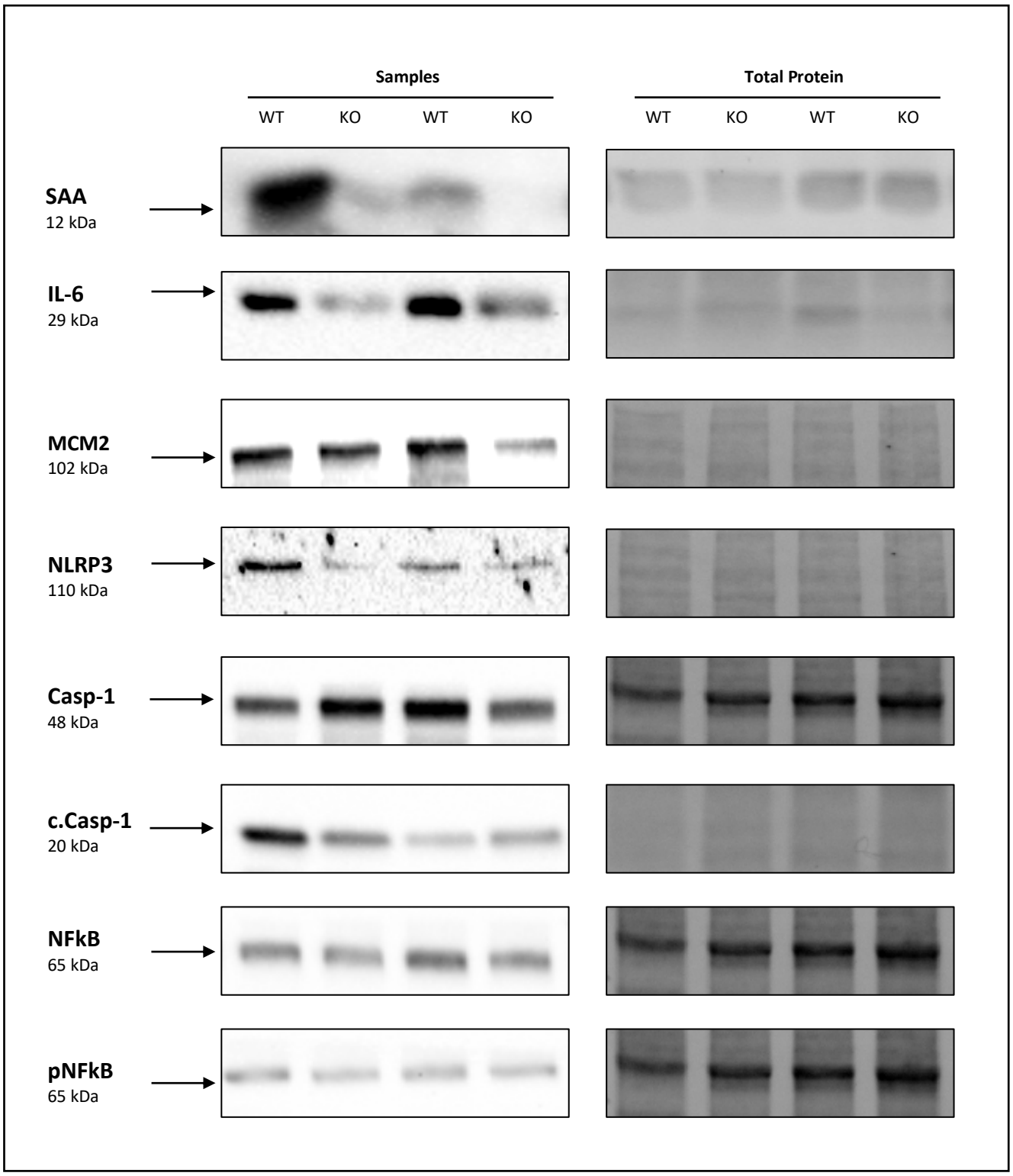

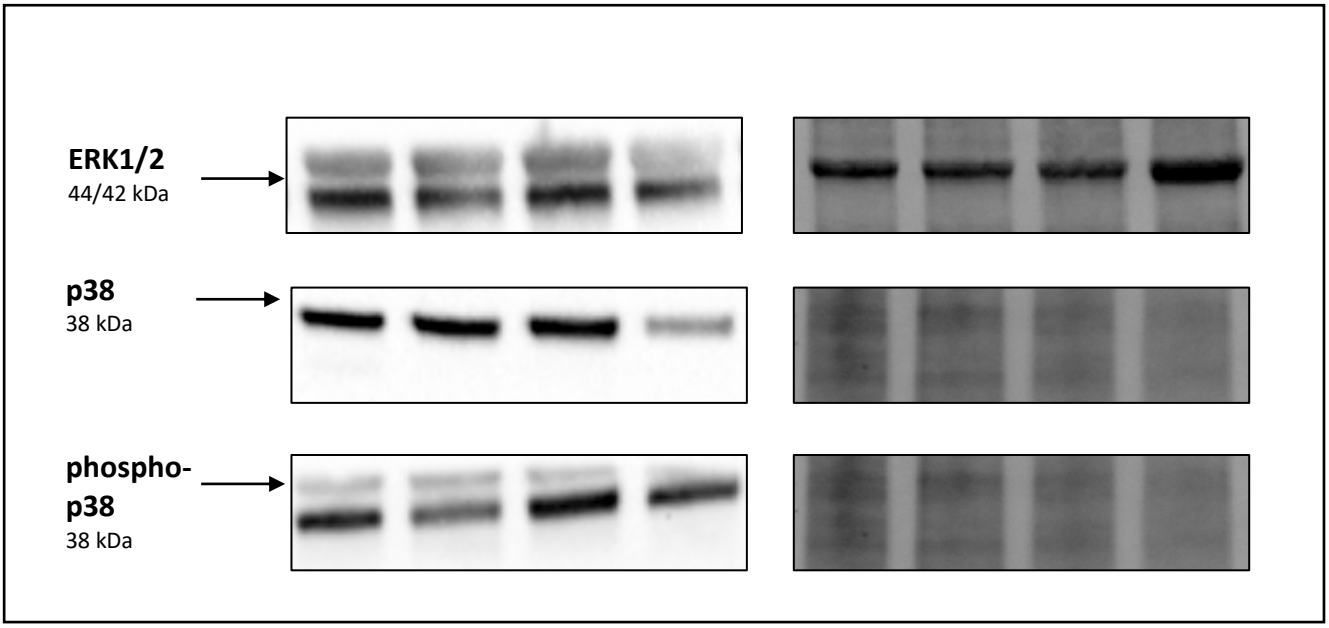

Figure 3.2.7: Representative images of Western blots for colitis-associated cancer (CAC). Proteins were separated by SDS-PAGE and transferred to a nitrocellulose membrane for analysis. **Abbreviations**: **KO**: knockout; **WT**: Wild-type

qPCR was also performed to determine the expression of *NLRP3* (Figure 3.2.8). No significant difference in *NLRP3* expression was detected in SAADKO mice compared to WT mice (1.04 ± 0.18 vs 0.85 ± 0.18; p>0.05).

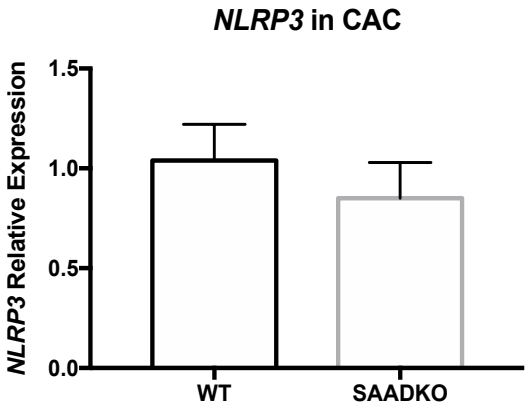

Figure 3.2.8: qPCR analysis to detect *NLRP3* in AOM/DSS-induced colitis-associated cancer (CAC). No significant changes were observed in SAADKO mice compared to WT mice (p>0.05). Results are presented as mean ± SEM (n=6).

3.2.4 SAADKO possibly suppresses EMT in AOM/DSS-induced colitis-associated cancer (CAC)

Immunoblotting was also performed for E-cadherin, vimentin and Snail because of SAA's association with metastasis in cancer. E-cadherin expression was not detected in these samples. A decreased tred of Snail was detected in SAADKO mice compared to WT mice (100 ± 21.22 vs 51.66 ± 13.03, p=0.07). Similarly, a decreased trend of vimentin was also detected in SAADKO mice compared to WT mice (100 ± 15.59 vs 58.27 ± 7.82, p=0.07). The results are displayed in Figures 3.2.9 and 3.2.10.

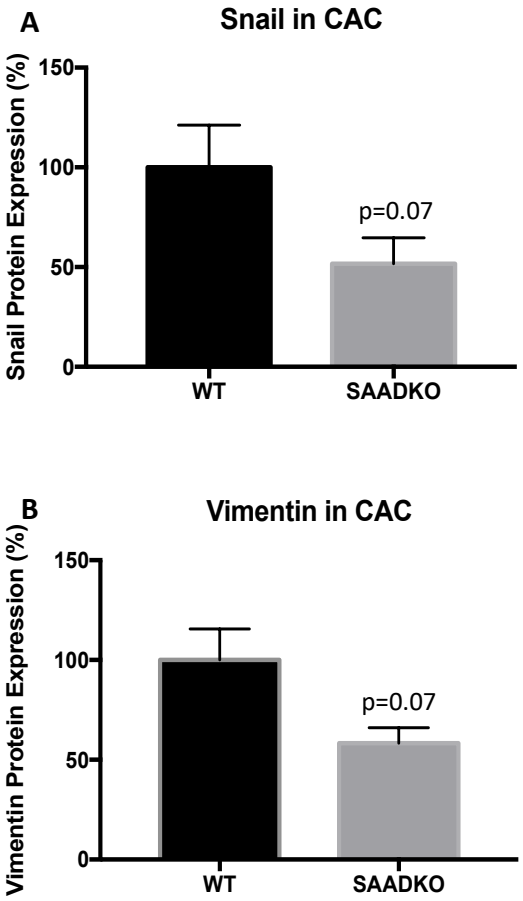

Figure 3.2.9*:* Western blot analysis to detect epithelial and mesenchymal markers in AOM/DSS-induced colitis-associated cancer (CAC). Proteins were separated by SDS-PAGE and transferred to a nitrocellulose membrane for analysis. Results are presented as mean ± SEM (n=9). Representative Western blot images can be found in Figure 3.2.10.

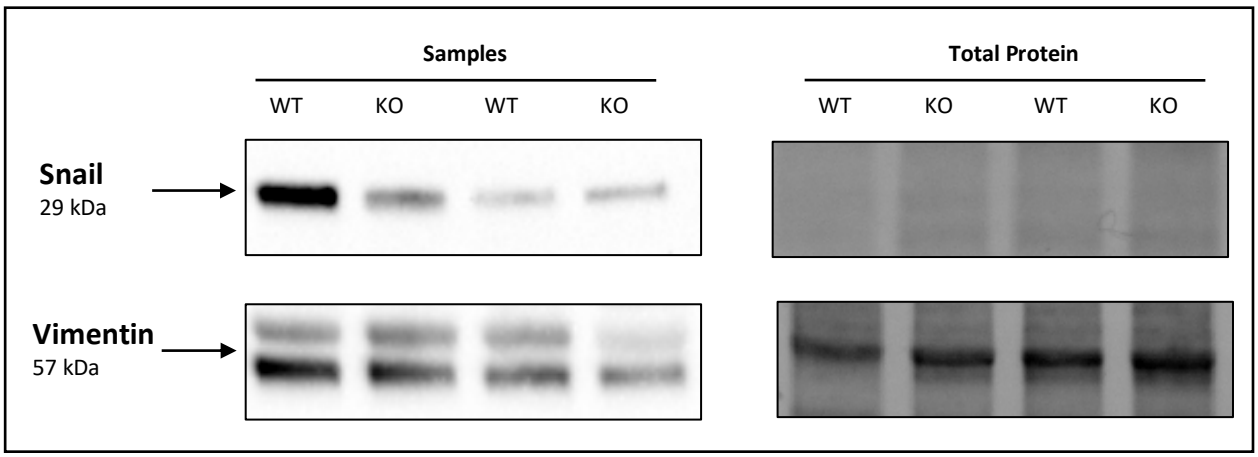

Figure 3.2.10: Representative images of Western blots for markers of metastasis in AOM/DSS-induced colitis-associated cancer (CAC). Proteins were separated by SDS-PAGE and transferred to a nitrocellulose membrane for analysis. **Abbreviations**: **KO**: knockout; **WT**: Wild-type

3.2.5 Tumour histology in colitis-associated cancer (CAC)

3.2.5.1 Tumours of SAADKO mice present with less histomorphologic abnormalities compared to WT mice

Haematoxylin and Eosin (H&E) staining was used to qualitatively assess histomorphologic changes in the distal colons (black arrow) of SAADKO mice (Figure 3.2.11 **B**) and WT mice (Figure 3.2.11 **A**). Microscopic analysis shows that SAADKO mice present with decreased histomorphologic abnormalities (Figure 3.2.11 **D**). Epithelial defects such as severe crypt loss are highlighted (black arrow) in WT (**C**) mice. Epithelial erosion (red arrow) is observed in WT (**C**) and SAADKO mice (**D**). Immune infiltrates in the submucosa are also observed in WT mice (blue arrow).

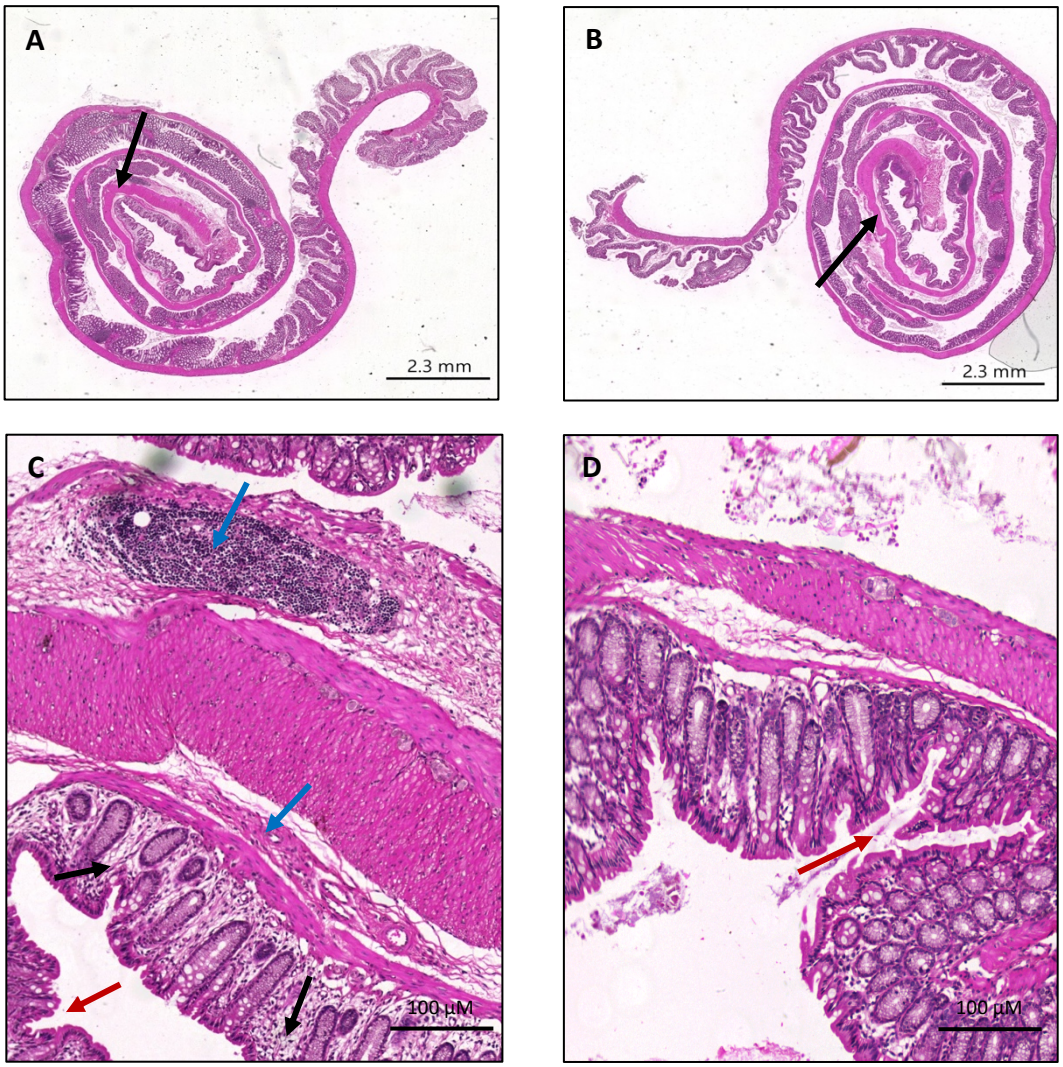

Figure 3.2.11: Colitis-associated cancer (CAC) morphologic abnormalities are decreased in SAADKO mice. Representative images of H&E stains of the distal colon of WT (**A**) and SAADKO (**B**) mice.

3.2.5.2 SAADKO mice present with decreased proliferation as indicated by Ki67 staining

Immunohistochemistry was used to assess the expression of Ki67 in the distal colon of WT (Figure 3.2.12 **A**) and SAADKO (Figure 3.1.12 **B**) mice as indicated by the black arrow. Qualitatively, less Ki67 positive cells are observed in SAADKO mice (Figure 3.1.12 **D**) compared to WT mice (Figure 3.1.12 **C**).

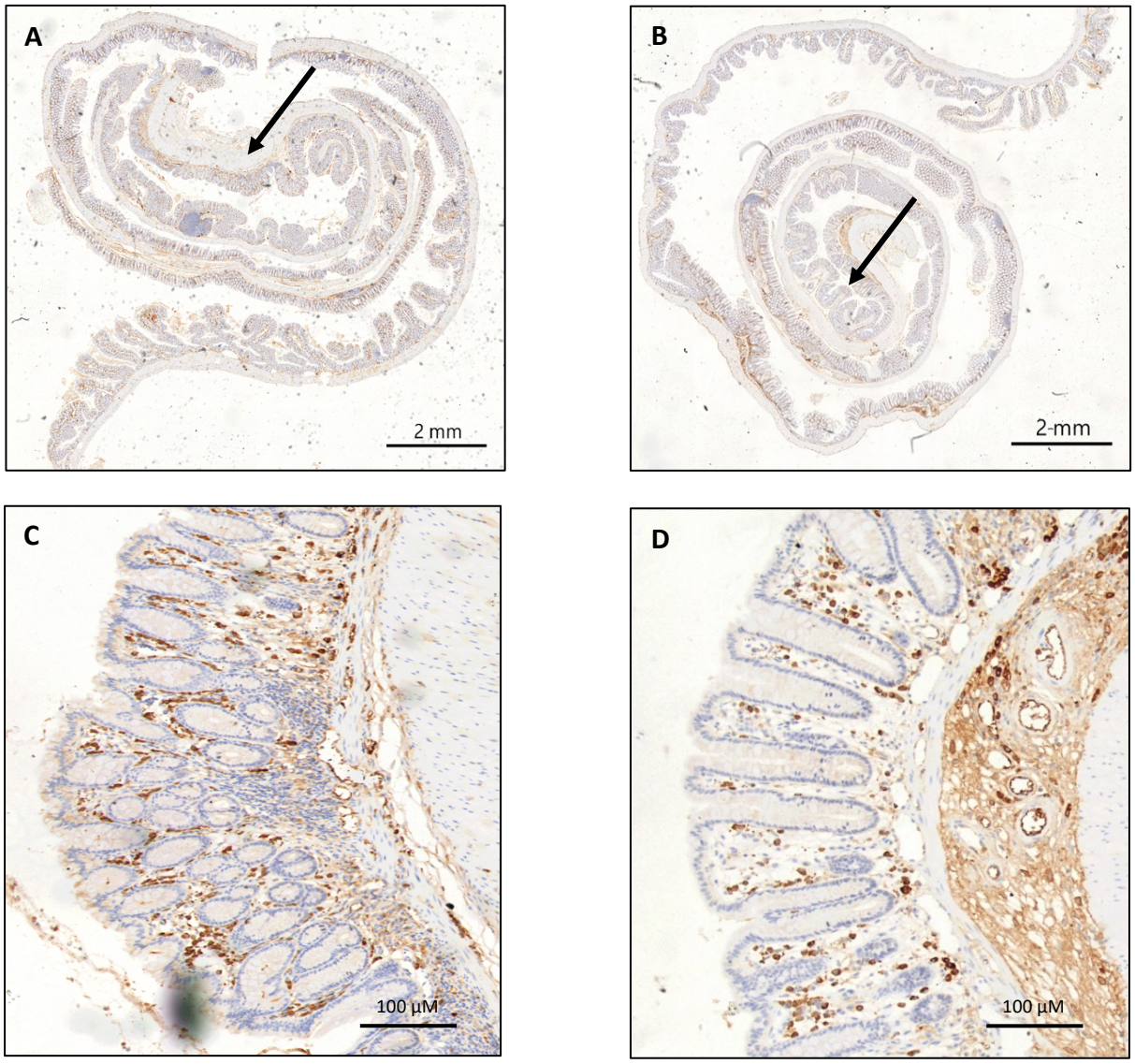

Figure 3.2.12: Ki67 is decreased in the colons of colitis-associated cancer (CAC) SAADKO mice. Representative immunohistochemical images in the distal colon (black arrows) of WT (**A & C**) and SAADKO (**B & D**) mice stained with Ki67.

3.2.5.3 SAADKO mice present with decreased NLRP3 staining

As NLRP3 activation was suppressed in SAADKO mice (Figure 3.2.6 **A**), IHC was used to qualitatively assess NLRP3 expression in the distal colon (black arrow) of WT (Figure 3.2.13 **A**) and SAADKO mice (Figure 3.2.12 **B**). SAADKO mice present with decreased staining of NLRP3 (Figure 3.2.13 **D**).

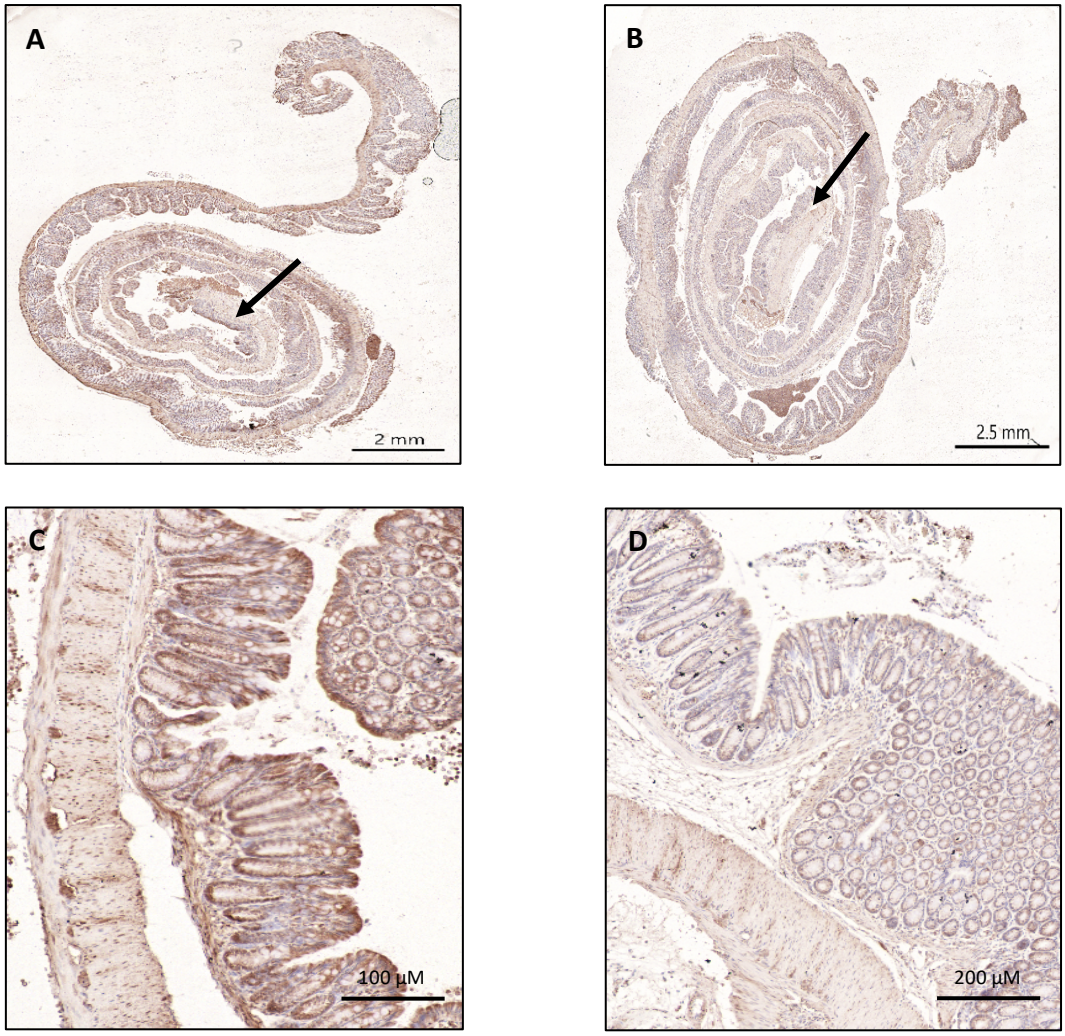

Figure 3.2.13: NLRP3 is decreased in the colons of colitis-associated cancer (CAC) SAADKO mice. Representative immunohistochemical images in the distal colon (black arrows) of WT (**A & C**) and SAADKO (**B & D**) mice stained with NLRP3.

3.3 SAADKO suppresses severity of Triple Negative Breast Cancer (TNBC)

The role of SAA1/2 and the NLRP3 inflammasome in TNBC was also investigated, similarly focusing on the canonical signaling pathway activated by the inflammasome as well as tumour proliferation following SAA1/2 ablation. Invasive breast cancer allografts were established in WT mice and mice lacking SAA1 and SAA2 (SAADKO). The tumour volume was monitored and modelled, the inflammatory profiles of the mice were assessed by means of a Milliplex assay at the experimental endpoints and the variation in tumour molecular biology and histology were assessed by Western blotting and microscopy. For this part of the study, we utilized the TNBC model to investigate the role of SAA in NLRP3 inflammasome signaling.

3.3.1 SAA1/2, tumour growth and host survival

Following initial tumour detection, tumour measurements were taken regularly, and the data was analyzed with a mixed model ANOVA. Significant differences in tumour growth were observed between WT and SAADKO mice over time ($p<0.05$) as seen in Figure 3.3.1 (**A**). A significant difference between WT and SAADKO mice on days 32 ($p<0.05$) and 35 ($p<0.05$) can be observed. Subsequent survival analysis conferred tumour growth data with the Cox-Mantel test where no differences between WT and SAADKO mice ($p>0.05$) were observed. Figure 3.3.1 (**B**) shows the Kaplan-Meier cumulative proportional survival of WT and SAADKO mice over time.

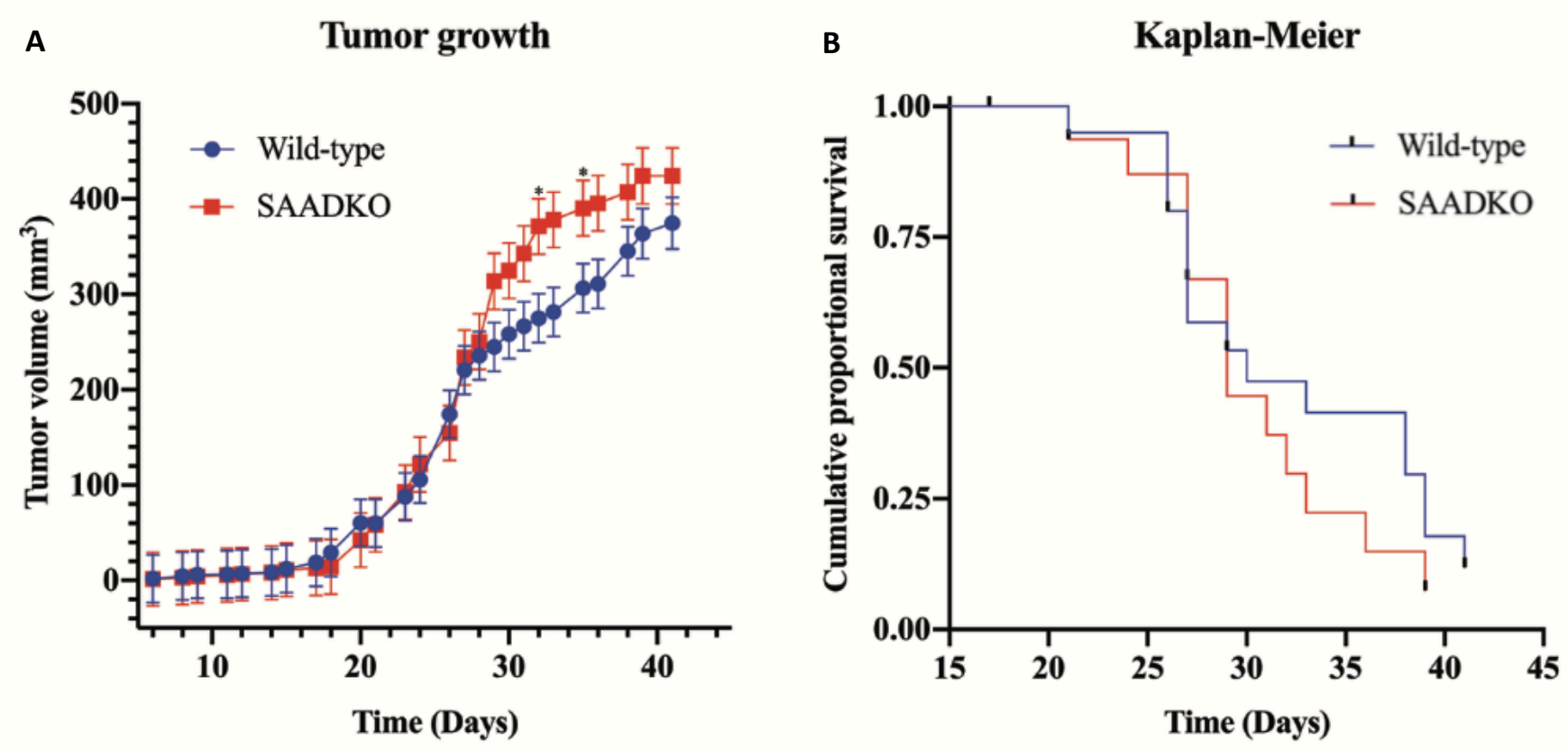

Figure 3.3.1: TNBC tumour growth in WT and SAADKO mice and their cumulative proportional survival over time. A- tumour growth over time for WT and SAADKO mice. Data represents mean ± SEM (n=20). The asterisk (*) indicates $p<0.05$. **B**- Kaplan-Meier plot of cumulative proportional survival over time (n=20).

3.3.2 Confirmation of SAA1/2 knockout in triple negative breast cancer (TNBC) SAADKO mice

Immunoblotting was used to determine whether SAA1/2 expression was successfully knocked out in C57BL/6 mice (Figure 3.3.2). In plasma samples from SAADKO mice, the expression of SAA1 and SAA2 was significantly decreased in the SAADKO group when compared to WT (100 ± 15.87 vs 2.9 ± 1.73, $p<0.01$).

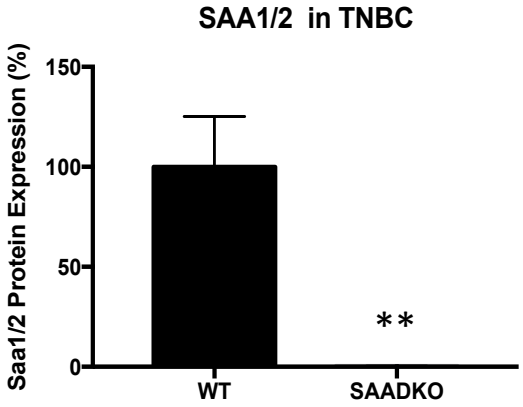

Figure 3.3.2: Western blot analysis to detect SAA1/2 in TNBC. Proteins were separated by SDS-PAGE and transferred to a nitrocellulose membrane for analysis. Results are presented as mean ± SEM (n=12). The asterisk (**) denotes a significant decrease in SAADKO mice compared to WT mice ($p<0.01$). Representative Western blot images can be found in Figure 3.3.5.

3.3.3 SAA1/2 and inflammation in triple negative breast cancer (TNBC) tumourigenesis

3.3.3.1 SAADKO mice present lower levels of pro-inflammatory cytokines

Blood plasma was analyzed for the inflammatory markers IL-1β, IL-6, IL-10, MCP-1 and TNF-α. Figure 3.3.3 shows the results. Compared to WT mice, SAADKO mice had significantly decreased levels of the pro-inflammatory cytokines, IL-6 (92.63 ± 20.46 vs 31.33 ± 6.46, $p<0.05$) and IL-10 (37.79 ± 9.26 vs 12.61 ± 1.90, $p<0.05$). Although not significant, IL-1β was also decreased in the SAADKO group (23.38± 9.15 vs 4.69 ± 0.78, $p=0.05$). The chemokine MCP-1 (371.6 ± 44.79 vs 706.6 ± 161.7, $p=0.09$) and the inflammatory cytokine, TNF-α (18.94 ± 3.88 vs 31.28 ± 4.96, $p=0.07$) was increased in SAADKO compared to WT mice.

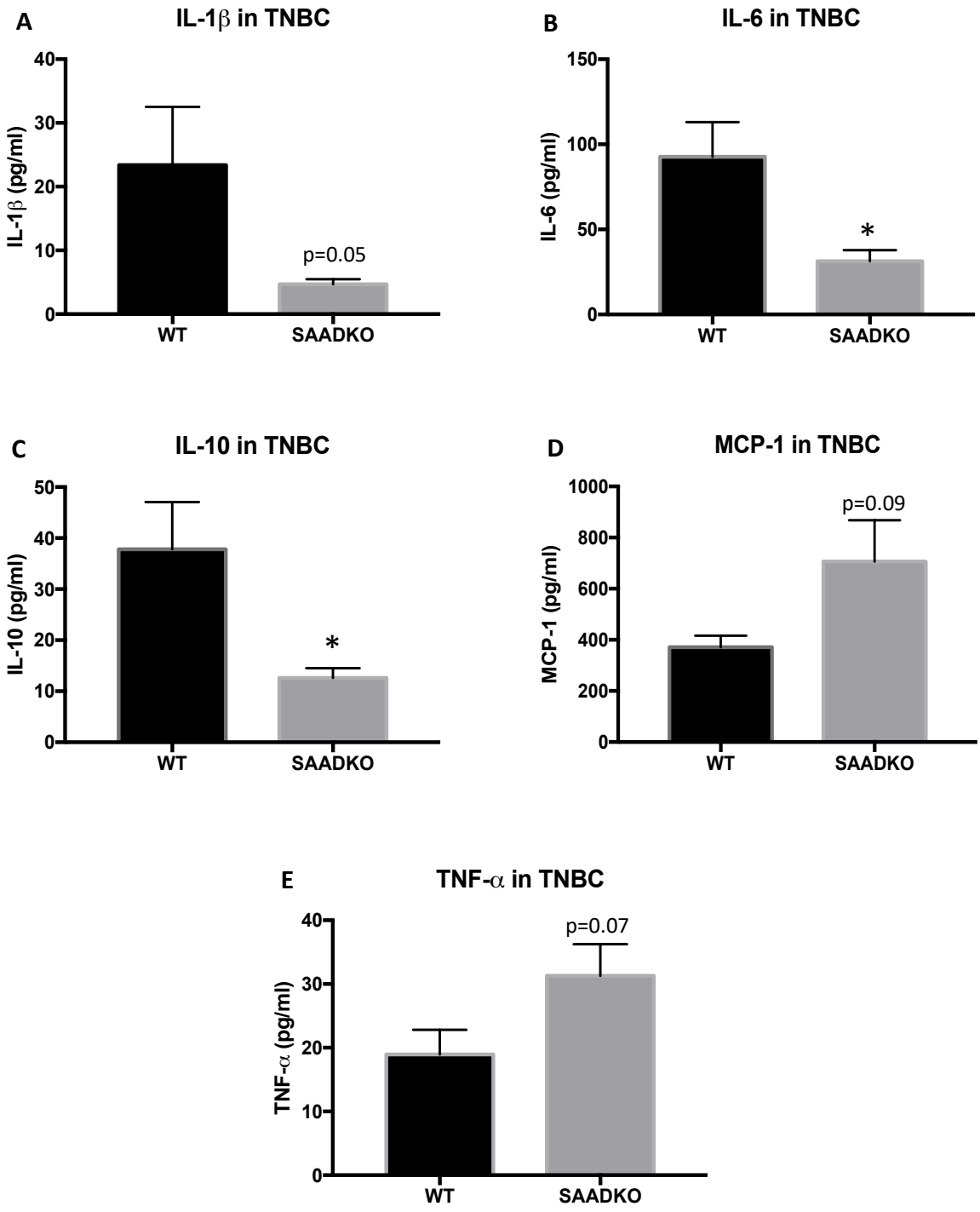

Figure 3.3.3: Inflammatory profile of WT and SAADKO mice in TNBC. A Milliplex assay was used to assess the inflammatory profile (IL-1β, IL-6, IL-10, MCP-1 and TNF-α) of the plasma of TNBC mice. Results are presented as mean ± SEM (n=12). The asterisk (*) denotes a significant decrease in SAADKO mice compared to WT mice ($p<0.05$).

3.3.4 SAADKO suppresses NLRP3 activation in triple negative breast cancer (TNBC)

Immunoblotting was used to characterize the tumour biology of WT and SAADKO mice with regards to NLRP3 inflammasome activation and signaling in TNBC samples (Figure 3.3.4). No significant changes were observed in MCM2, a regulator of cell proliferation (100 ± 8.58 vs 101 ± 8.7, $p>0.05$). In terms of the NLRP3 inflammasome complex, NLRP3 was significantly decreased in SAADKO mice compared to WT mice (100 ± 18.23 vs 49.02 ± 5.92, $p<0.05$). Supporting the decrease in NLRP3, caspase-1 was also significantly decreased in SAADKO mice compared to WT mice (93.99 ± 30.1 vs 16.02 ± 12.26, $p<0.05$). Furthermore, NFKB was significantly decreased in SAADKO mice compared to WT mice (138.1 ± 19.71 vs 83.25 ± 14.54, $p<0.05$).

No significant changes for ERK1/2 (114.9 ± 36.91 vs 75.42 ± 14.28, $p>0.05$) and p38 (100 ± 11.68 vs 118.1 ± 13.04, $p>0.05$) were observed between WT and SAADKO mice.

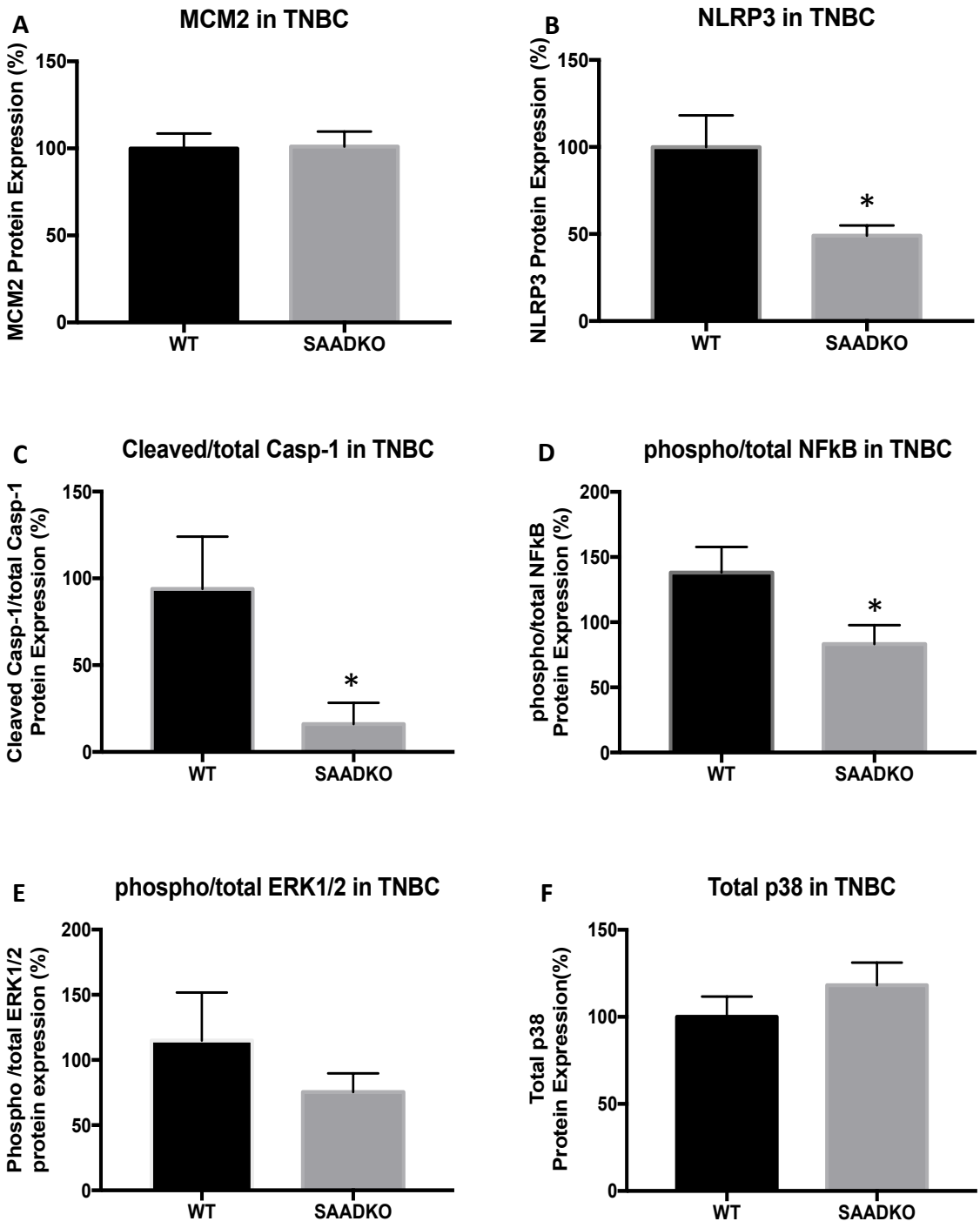

Figure 3.3.4: Western blot analysis to detect NLRP3 inflammasome components and signaling pathways in TNBC tumours. Proteins were separated by SDS-PAGE and transferred to a nitrocellulose membrane for analysis. Results are presented as mean ± SEM (n=12). The asterisk (*) denotes a significant decrease in NLRP3, caspase-1 and NFkB in SAADKO mice compared to WT mice ($p<0.05$). Representative Western blot images can be found in Figure 3.3.5.

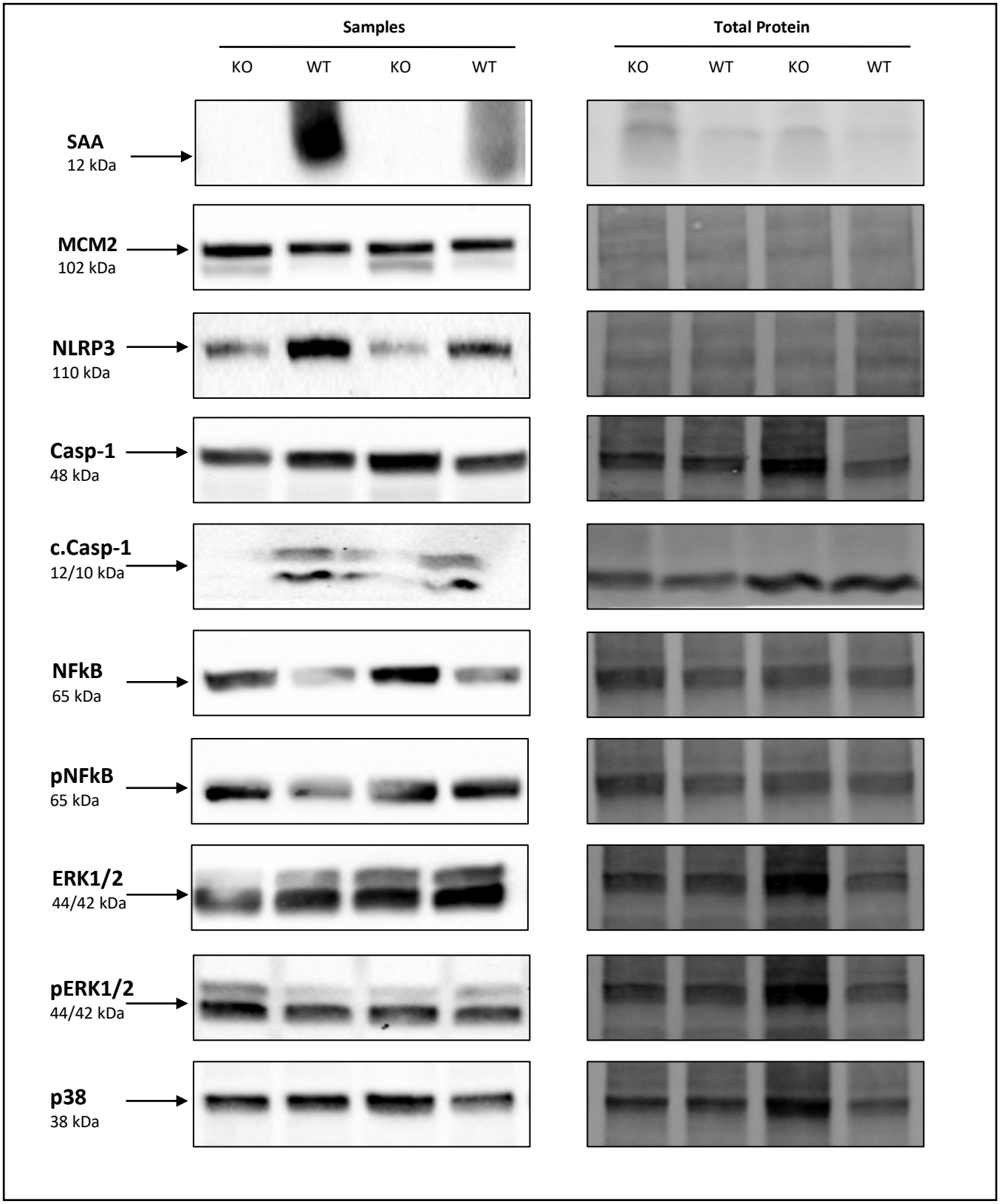

Figure 3.3.5: Representative images of Western blots for TNBC in SAADKO and WT mice. Proteins were separated by SDS-PAGE and transferred to a nitrocellulose membrane for analysis. **Abbreviations**: **KO**: knockout; **WT**: Wild-type

3.3.5 No significant changes in markers of metastasis in triple negative breast cancer (TNBC)

Immunoblotting was also performed for the metastasis markers E-cadherin, vimentin and Snail. E-cadherin expression was not detected in these samples. No significant changes in Snail expression were observed (100 ± 17.41 vs 79.78 ± 8.32, p>0.05). Although it did not reach significance, vimentin showed a decreased trend in SAADKO mice compared to WT mice (100 ± 15.59 vs 58.27 ± 7.82, p=0.09). Figure 3.3.6 shows the results.

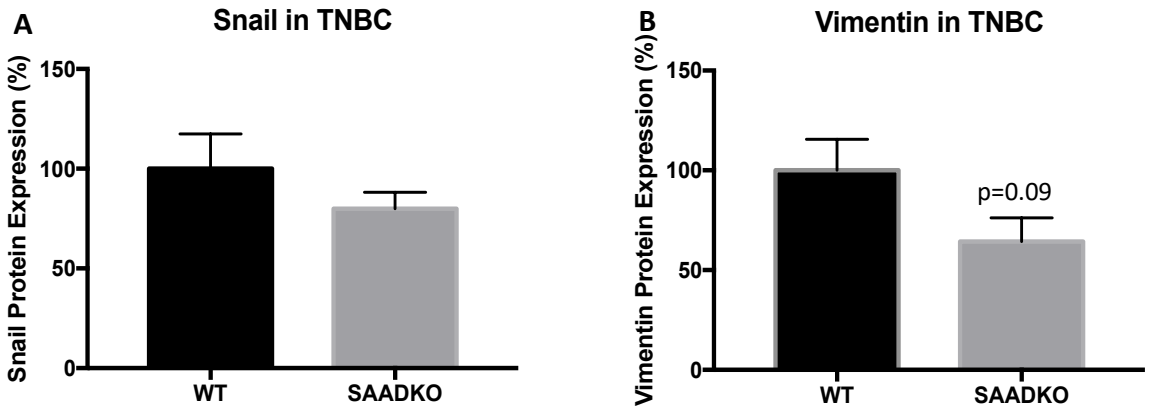

Figure 3.3.6: Western blot analysis to detect epithelial and mesenchymal markers in TNBC. Proteins were separated by SDS-PAGE and transferred to a nitrocellulose membrane for analysis. Results are presented as mean ± SEM (n=12). Representative Western blot images can be found in Figure 3.3.7.

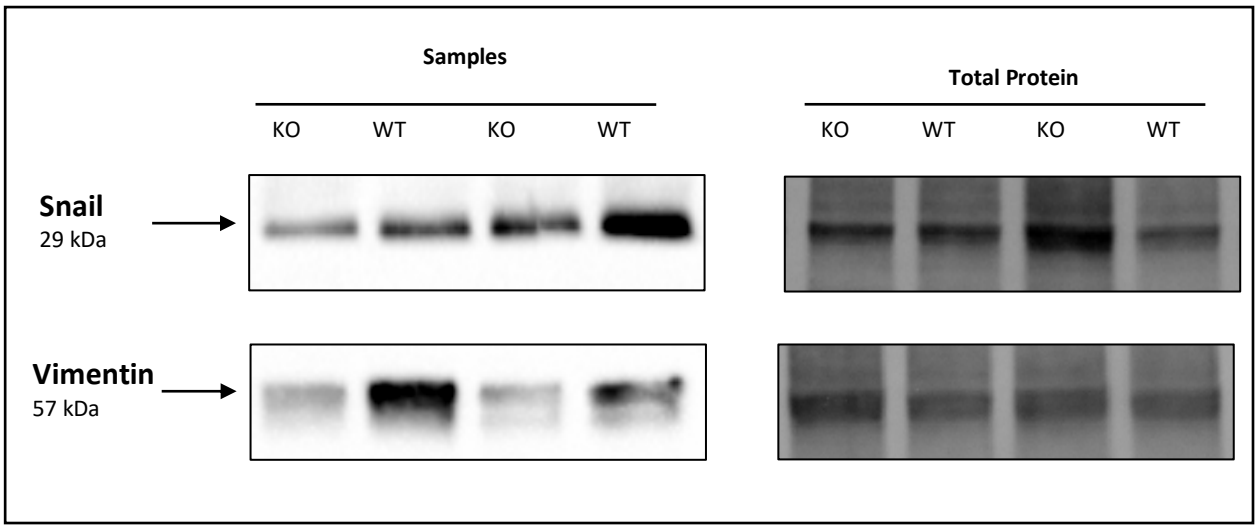

Figure 3.3.7: Representative images of Western blots for metastasis in TNBC. Proteins were separated by SDS-PAGE and transferred to a nitrocellulose membrane for analysis. **Abbreviations: KO**: knockout; **WT**: Wild-type

3.3.6 Tumour histology in triple negative breast cancer (TNBC)

3.3.6.1 SAADKO mice present with decreased histomorphologic abnormalities

Haematoxylin and Eosin (H&E) staining was used to qualitatively assess histomorphologic changes in the tumour tissue of WT (Figure 3.3.8) and SAADKO mice (Figure 3.3.9). Microscopic analysis shows that SAADKO mice present with decreased histomorphologic abnormalities. WT mice presented with large areas of necrotic tissue as well as decreased cellularity (**Figure 3.3.8 B & C**).

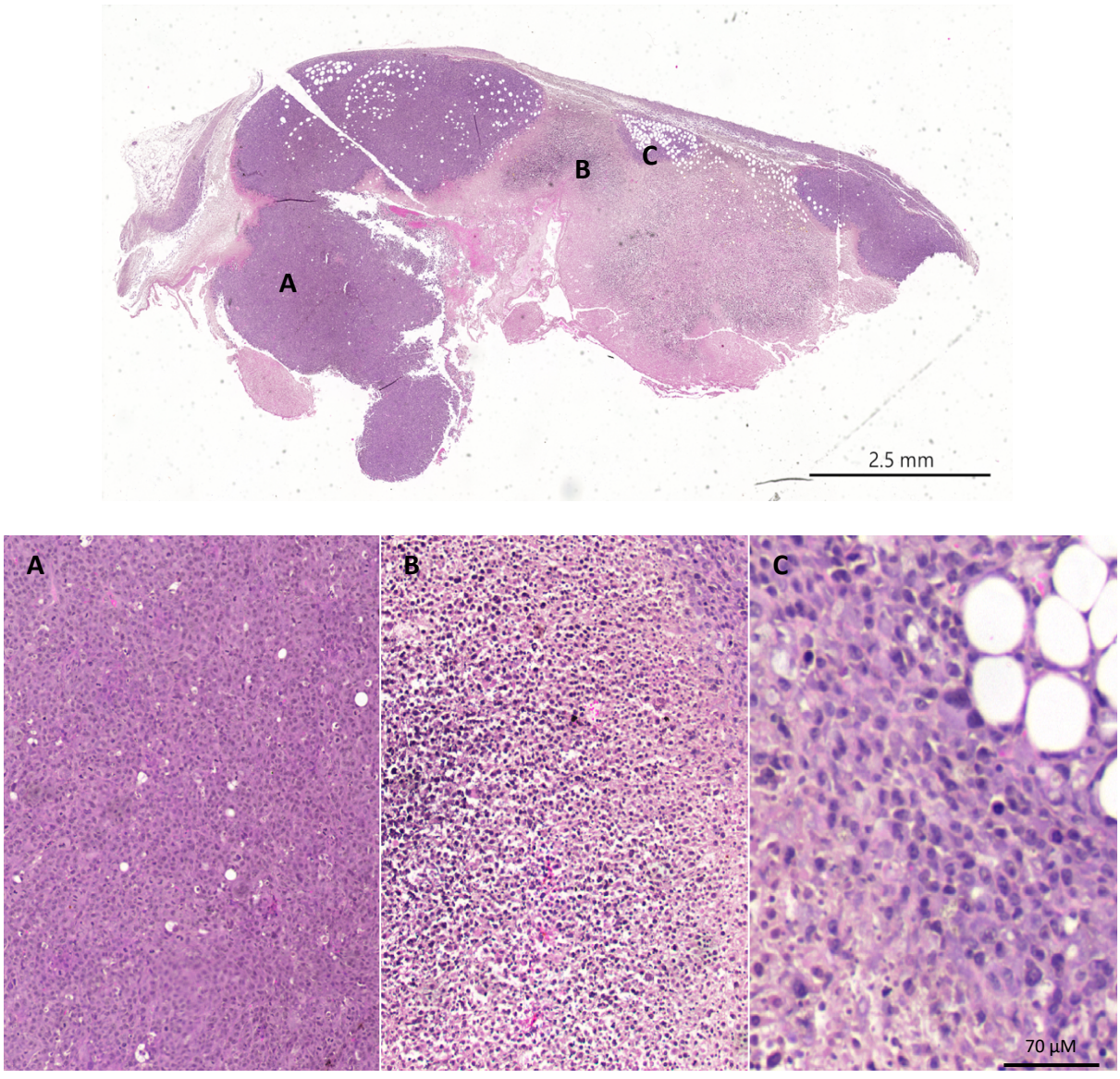

Figure 3.3.8: Representative H&E images for WT TNBC mice. A: Viable tumour tissue. **B**: Necrotic tissue. **C:** Decreased cellularity.

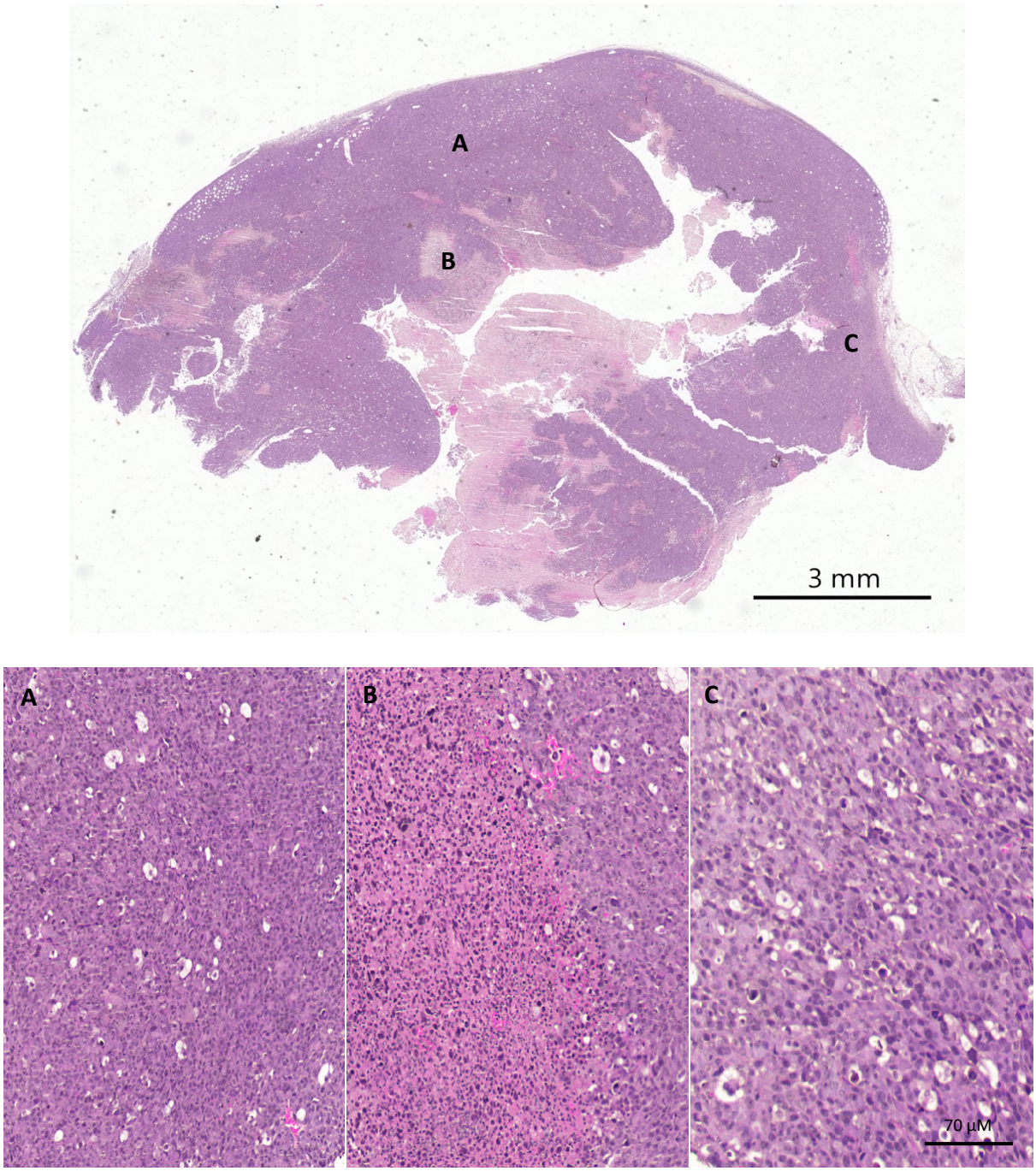

Figure 3.3.9: Representative H&E images for SAADKO TNBC mice. A: Viable tumour tissue. **B**: Necrotic tissue. **C:** Decreased cellularity.

3.3.6.2 Triple negative breast cancer (TNBC) SAADKO mice present with decreased NLRP3 staining

As NLRP3 activation was suppressed in SAADKO mice (Figure 3.3.4 **B**), IHC was used to confirm these results in WT (Figure 3.3.10 **A**) and SAADKO mice (Figure 3.3.10 **B**). Qualitatively, microscopic analysis shows that SAADKO mice present with decreased expression of NLRP3 (Figure 3.3.10 **D**).

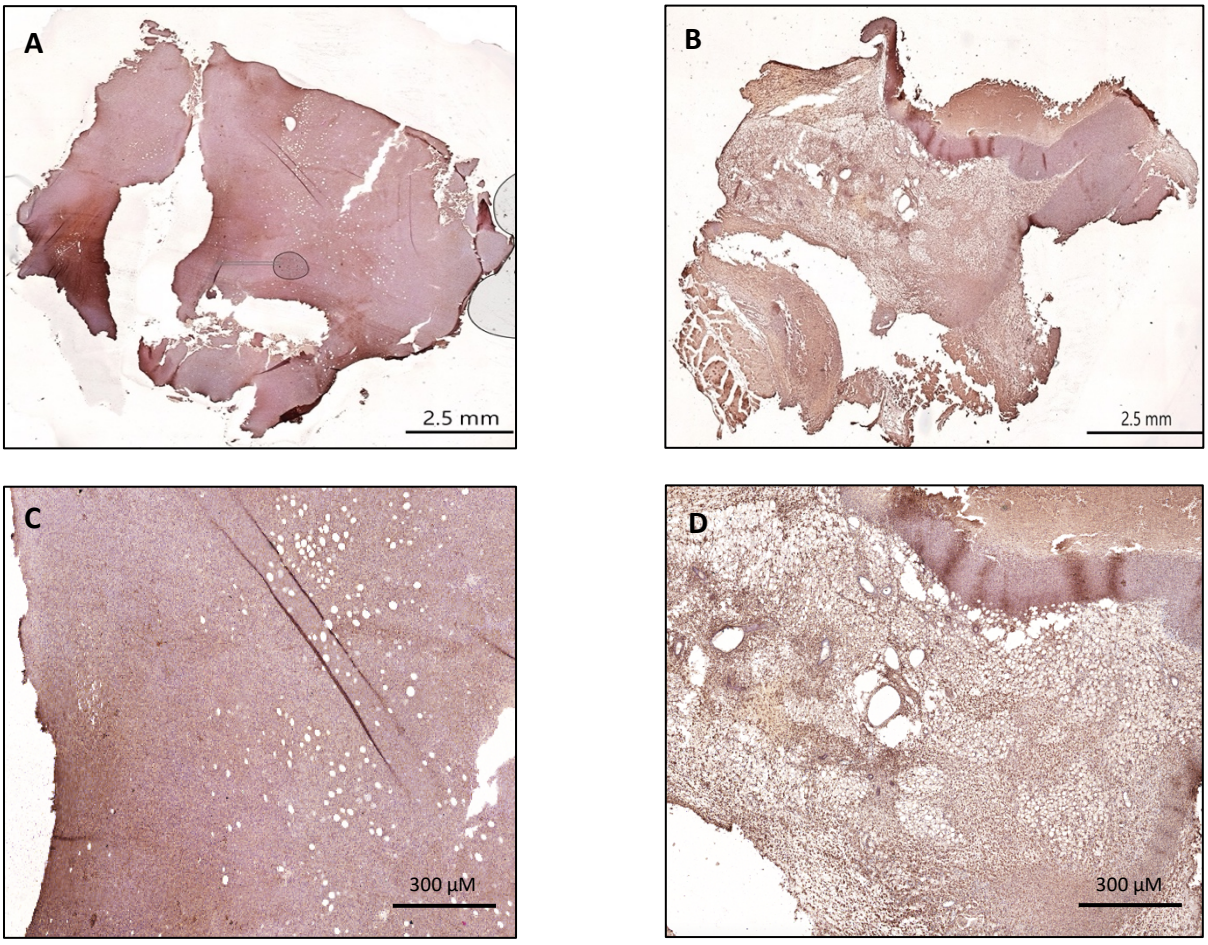

Figure 3.3.10: NLRP3 staining is decreased in triple negative breast tumours in SAADKO mice. Representative immunohistochemical images of WT (**A & C**) and SAADKO (**B & D**) mice stained with NLRP3.

Chapter 4

Discussion

4.1 SAA promotes an anti-inflammatory environment in acute colitis

4.1.1 Introduction

Inflammatory bowel disease (IBD) such as Crohn's disease and ulcerative colitis, is characterized by chronic and relapsing inflammation in the GI tract and studies have proposed that damage to the intestinal mucosa occurs as a result of a dysregulated innate immune response (Goyette *et al*., 2007). Therefore, understanding the mechanisms that control aberrant innate immune responses in the intestine is critical to elucidate the pathogenesis of IBD.

Various mouse models of experimental colitis have been developed to study the mechanisms of IBD. The dextran sodium sulfate (DSS) model has been extensively used to explore immune mechanisms of colitis. Oral administration of DSS directly damages colonic epithelium and triggers inflammation by destroying the compartmentalization of bacteria in the gut (Tanaka *et al*., 2003). This model exhibits similar clinical features of human IBDs such as weight loss, diarrhea, rectal bleeding and mortality. Furthermore, serum amyloid A (SAA), which is a major acute phase protein, plays an important role in the innate host response and increases by up to 1000-fold in response to inflammation (Uhlar & Whitehead, 1999). SAA has also been shown to act as a sensitive marker of disease severity in IBD. Taking the above-mentioned into consideration, NLRP3 inflammasomes and SAA can promote disease progression in IBD, however, the role of SAA in NLRP3 signaling remains to be elucidated. The aim of the first part of this study was therefore to determine whether SAA can promote NLRP3 signaling in an acute DSS-induced colitis model.

4.1.2 Deficiency in SAA1 and SAA2 limits SAA3 expression

Acute DSS-induced colitis was established in WT and SAADKO mice, allowing an investigation into the contribution of the acute phase SAA1/2 isoforms in this model. Immunoblotting and qPCR showed that SAA1 (**Figure 3.1.1**; $p<0.05$ and **Figure 3.1.2 A**; $p<0.01$), SAA2 (**Figure 3.1.1**; $p<0.05$ and **Figure 3.1.2 B**; $p<0.01$) and SAA3 (**Figure 3.1.3**; $p=0.06$) were decreased/ablated in SAADKO mice. Similarly, Davis and co-authors also reported a significant decrease in SAA3 expression when SAA1/2 was knocked out in mice (Davis *et al*., 2021).

4.1.3 SAADKO mice present with a pro-inflammatory profile in acute colitis (AC)

Acute phase SAA plays an important role in acute and chronic inflammation and is used in clinical laboratories as an indicator of inflammation, where it has also been reported that SAA correlates with the clinical presentation of ulcerative colitis (Wakai *et al*., 2020). We therefore set out to investigate whether SAA plays a role in cytokine secretion in acute colitis by determining whether SAA1/2 mediates cytokine alterations *in vivo*. The local concentrations of various cytokines in the distal colon of acute colitis mice were assessed. Interestingly, plasma profile analysis (**Figure 3.1.4**) showed that the pro-inflammatory cytokines, IL-1β and IL-6, was increased in SAADKO mice (**Figure 3.1.4 A & B**; $p=0.05$ and $p<0.01$). These findings suggest that the loss of SAA1/2 skews local cytokine production toward a pro-inflammatory profile. This finding is supported by the study of Witta *et al.* who reported that after DSS treatment in $SAA^{-/-}$ mice, disease activity was significantly increased compared to WT mice. An increase in plasma IL-6 levels were also observed in $SAA^{-/-}$ mice (Witta *et al*., 2006). Similarly to an extent, it was observed in another study that in $SAA3^{-/-}$ mice, IL-1β, IL-6 and TNF-α was significantly induced in colonic tissue (Zhang *et al*., 2018). No significant changes in TNF-α expression were observed in the present study (**Figure 3.1.4 E**). In contradiction to these findings, Davis and co-authors reported that IL-6 and TNF-α was significantly increased in $SAA1/2^{-/-}$ mice with acute colitis (Davis *et al*., 2021).

4.1.4 The pro-inflammatory profile of SAADKO mice is NLRP3-independent

The next aim was to establish whether this pro-inflammatory cytokine secretion in SAADKO mice is dependent on NLRP3 inflammasome signaling. Inflammasomes are groups of cytosolic protein complexes that recognize several danger signals and respond by producing IL-1β and IL-18 (Jo *et al*., 2016). Evidently, these pro-inflammatory cytokines are key players in the pathogenesis of IBD. Although inflammasomes comprise several subtypes, the NLRP3 inflammasome is best characterized. The multi-protein complex of the NLRP3 inflammasome consists of the sensor-NLRP3, the adaptor-apoptosis-associated speck-like protein containing a caspase recruitment domain (ASC) and the effector pro-caspase-1. Immunoblotting was therefore performed to determine if differences exist in inflammasome expression in SAADKO mice compared to WT mice. Immunoblotting showed that no significant changes in NLRP3 and caspase-1 (no cleaved caspase-1) in SAADKO mice compared to WT mice were observed (**Figure 3.1.6 B & C**), but interestingly, IL-1β and IL-6 expression were increased in SAADKO mice (**Figure 3.1.4 A & B**), which is generally associated with the activation of NLRP3. Contradicting these findings, Bauer *et al.* showed that DSS-induced colitis in mice is mediated by the NLRP3 inflammasome (Bauer *et al*., 2010). The authors showed that $NLRP3^{-}$

$^{-/-}$ mice developed a less severe colitis than WT mice and produced lower levels of pro-inflammatory cytokines in colonic tissue. Furthermore, by inhibiting caspase-1, mucosal protection comparable with NLRP3 deficiency was achieved. However, the role of the NLRP3 inflammasome in inflammation remains controversial. It was also shown that NLRP3 inflammasome deficiency resulted in increased intestinal inflammation where Zaki and co-authors reported that mice with NLRP3 deficiency exhibited more severe DSS-colitis than WT mice (Zaki *et al*., 2010).

Immunoblotting further indicated that p38 was significantly increased in SAADKO mice compared to WT mice (**Figure 3.1.6 F**; $p<0.001$). The p38 MAPK signaling pathway has been shown to play an important role in bowel inflammation and may be responsible for the immunopathogenesis of the over-active immune system. As such, it was shown that the activity of p38 increased in patients suffering from IBD. After the activation of p38, pro-inflammatory cytokines such as IL-1β and TNF-α were raised in both production and secretion; inversely IL-1β and TNF-α can activate p38 as well. The increased expression of p38 in SAADKO mice is supported by the increased expression of IL-1β, but no significant changes in TNF-α expression was observed in the present study (**Figure 3.1.4 E**). Hollenbach and co-authors also observed that when p38 was inhibited in DSS-induced acute colitis, mRNA levels of pro-inflammatory cytokines were significantly reduced. In addition to p38 signaling, the NFkB pathway was also strongly activated in acute colitis and was also significantly downregulated once p38 was inhibited (Hollenbach *et al*., 2004). However, no changes in NFkB expression were observed in SAADKO mice (**Figure 3.1.6 D**). Similarly, with regards to inflammatory profiles, Li *et al.* demonstrated that the mRNA expression levels of TNF-α and IL-6 are upregulated in WT mice when compared to p38$^{-/-}$ mice (Li *et al*., 2013). These findings are supported by the present study, where both an increase in p38 (**Figure 3.1.6 F**; $p<0.001$) and IL-6 (**Figure 3.1.4 B**; $p<0.001$) were observed in SAADKO mice, in comparison to WT mice.

More recently, the ability of p38 to induce the priming step of the inflammasome has emerged. It can therefore be speculated that the significant increase in p38 expression in SAADKO mice (**Figure 3.1.6 B**; $p<0.001$) can be associated with the increased NLRP3 expression observed. Fenini *et al.* showed that in primary human keratinocytes, p38 is required for inflammasome activation and IL-1β secretion (Fenini *et al*., 2018). Interestingly, Wang and authors showed that by inhibiting p38, activation of the NLRP3 inflammasome was suppressed, without NLRP3 expression blockade (Wang *et al*., 2018). We therefore speculate that in the present study, the increased expression of p38 in SAADKO mice resulted in the increased expression of

NLRP3 in these mice, but that the activation mechanisms (as seen by the lack of cleaved caspase-1 and non-significant NFkB activation) was suppressed. The pro-inflammatory profile of SAADKO mice is therefore attributed to MAPK signaling.

4.1.5 The loss of E-cadherin promotes an inflammatory environment in SAADKO mice

E-cadherin is a glycoprotein with a large extracellular domain, characterized by five cadherin-motif subdomains, a single-pass transmembrane segment and a short conserved cytoplasmic domain, which interacts with several proteins collectively termed catenins. Loss of E-cadherin function in the intestine has been linked to pathological processes (Schneider *et al*., 2010). E-cadherin is the principle adhesive component of the adherens junction, and it regulates paracellular permeability by facilitating the formation of tight junctions and organizing the entire epithelial junction complex. Therefore, E-cadherin is required for the proper functioning of the intestinal epithelial lining by providing mechanical integrity. A decreased trend of E-cadherin expression was observed in SAADKO mice (**Figure 3.1.6 A**; p=0.08). Studies have shown that E-cadherin expression is reduced in the inflamed epithelium of patients with Crohn's disease and ulcerative colitis (Schnoor, 2015). Another study showed that by activating E-cadherin with monoclonal antibodies, total colitis score and inflammation was reduced in mice (Bandyopadhyay *et al*., 2020). As such, the decreased expression of E-cadherin is supported by the increased expression of pro-inflammatory cytokines in SAADKO mice (**Figure 3.1.4**). However, the role of SAA and its relationship with E-cadherin is not well documented. One study showed that Caco-2 cells cultured in SAA1 increases E-cadherin expression in the SAA1-treated group when compared to the control (Hinrichs *et al*., 2018). The authors concluded that SAA1 promotes epithelial cell metastasis in these cells.

Additionally, studies have shown that IL-1β can induce changes in E-cadherin. In human trophoblasts, IL-1β treatment *in vitro* downregulated the expression of E-cadherin (Karmakar & Das, 2004). Similarly, in A549 lung cancer cells, IL-1β induced epithelial to mesenchymal transition (EMT) which was associated with decreased expression of E-cadherin (Li *et al*., 2020). Lastly, Dosh and co-authors showed that IL-1β was increased while IL-1R1 expression was decreased in IL-$1^{-/-}$ receptor negative mice (Dosh *et al*., 2019). Decreased expression of E-cadherin was also observed in these mice. The authors concluded that the presence of pro-inflammatory cytokines was associated with a leaky and dysfunctional epithelial barrier. It can therefore be speculated that in the present study, the increased expression of IL-1β in SAADKO mice induces the loss of E-cadherin, which promotes colitis.

With regards to mesenchymal markers, no changes in the expression of Snail and Vimentin were observed (**Figure 3.1.6 B & C**), but one study has showed that vimentin-KO mice develop significantly less gut inflammation than WT mice. In DSS-induced acute colitis, vimentin-KO mice have decreased bacterial extravasation, concluding that vimentin contributes to the pathogenesis of acute colitis *in vivo* (Mor-Vaknin *et al*., 2013).

4.1.6 SAADKO mice present with increased morphological abnormalities

H&E staining was used to identify morphological changes in WT and SAADKO mice with acute colitis. The results indicated that DSS-induced colitis was associated with histological abnormalities in both WT and SAADKO mice. Here we showed that although epithelial hyperplasia and crypt loss is observed in both WT and SAADKO mice, marked hyperplasia and crypt loss was observed in SAADKO mice (**Figure 3.1.11 D**). Immune infiltration was present in the submucosa of WT mice, but an absence/degradation of submucosa was observed in SAADKO mice. Furthermore, epithelial erosion, indicated by the loss of surface epithelium, and cryptitis was also observed in SAADKO mice. Similar to these findings, Metzger and authors reported that DSS-treated mice presented with muscularis externa thickening, crypt loss and immune cell infiltration into the mucosal compartment (Metzger *et al*., 2019).

Furthermore, relating to the marked morphological changes observed in SAADKO mice, Ki67 expression was also increased. Qualitatively, increased Ki67 signal is observed in SAADKO mice compared to WT mice (**Figure 3.1.12 D**). As such, immunohistochemical assessment of Ki67 has previously been used to assess the grading of ulcerative colitis (Wong *et al*., 2001). A study showed that in ulcerative colitis patients with low grade dysplasia, Ki67 staining of the lower half of the colonic crypt was significantly higher than that of the upper half of the crypt (Mikami *et al*., 2003). Needless to say, these results support our findings where we have indicated that the ablation of SAA1/2 in mice with acute colitis presents with advanced disease promoting properties.

4.1.7 Summary of results obtained in DSS-induced acute colitis model

Taking these findings into consideration, no significant evidence suggests that SAADKO promotes NLRP3 inflammasome signaling in acute colitis, as the immunoblots show no significant increases in NLRP3, caspase-1 and NFkB expression in SAADKO mice. However, IL-1β and IL-6 was significantly increased in this group, which is generally NLRP3-dependent. We therefore propose that the increased pro-inflammatory cytokine expression in SAADKO mice is associated with the significant upregulation of p38 MAPK. Based on the study by Wang

et al (2018), we showed that p38 suppressed NLRP3 signaling, but the expression of NLRP3 was not blocked in SAADKO mice. It can also be speculated that in the absence of SAA, with increased IL-1β secretion, E-cadherin is decreased, which can affect the mechanical integrity of the gut epithelial lining to promote inflammation and colitis. This is also associated with morphologic abnormalities such as epithelial erosion. We therefore conclude that SAA has anti-inflammatory and protective functions in IBDs, like ulcerative colitis (Figure 4.1).

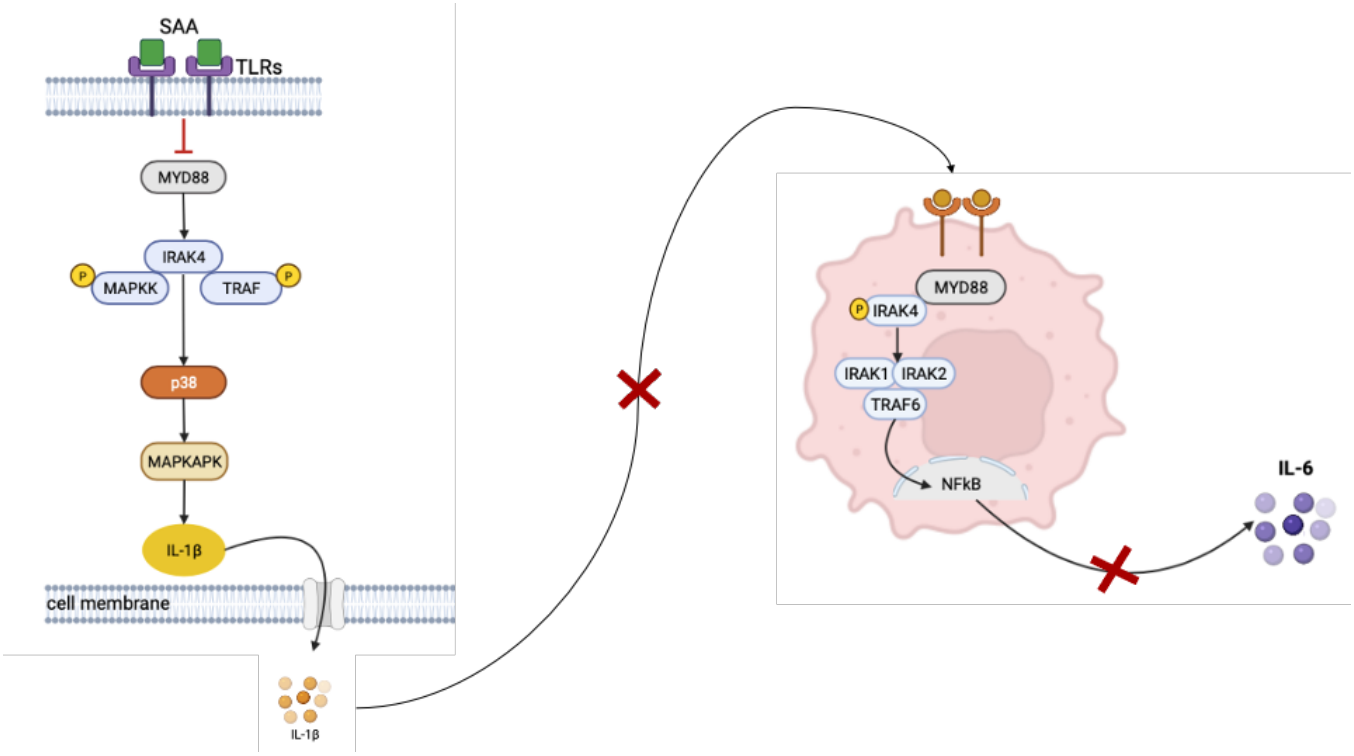

Figure 4.1: SAA promotes an anti-inflammatory profile in acute colitis. The binding of SAA to TLRs on epithelial cells in the colonic area inhibits MAPK p38 signaling, which prevents the secretion of IL-1β. This prevents IL-1β from binding to IL-1R on other cells, to inhibit the secretion of IL-6. **Abbreviations: MAPKAPK**: Mitogen-Activated Protein Kinase-Activated Protein Kinases; **P**: Phosphorylate; **SAA**: Serum amyloid A; **TLR**: Toll-like receptor

4.2 SAA promotes a pro-inflammatory environment in colitis-associated cancer (CAC)

4.2.1 Introduction

Colitis-associated cancer (CAC) is a type of colon cancer which is preceded by clinically detectable IBD, such as Crohn's disease or ulcerative colitis, as discussed in section 4.1. Ulcerative colitis increases cumulative risk of CAC by up to 20% (Rubin *et al*., 2012). In mouse models, a single injection of the carcinogen, AOM, gives rise to multiple colonic tumours, when coupled with the induction of chronic colitis. These clinical observations highlight the inflammatory-driven profile of CAC and make mouse models of CAC extremely valuable to understand the general mechanisms which connect inflammation and cancer. As described earlier, the role of SAA in inflammation is also being investigated and studies have shown that SAA plasma levels are upregulated in several malignancies including, lung, breast, and colon cancer (Urieli-Shoval, 1998). Although the underlying mechanisms which link inflammation and carcinogenesis are not clear, the molecular platforms of the inflammasomes have been implicated. It has been suggested that the NLRP3 inflammasome is associated with the development of colitis-associated colorectal cancer, but the role of SAA in inflammasome signaling in CAC remains to be elucidated.

4.2.2 Deficiency in SAA1 and SAA2 limits SAA3 expression

AOM/DSS-induced CAC was established in WT and SAADKO mice, allowing an investigation into the contribution of the acute phase SAA1/2 isoforms in this model. Immunoblotting and qPCR showed that SAA1 (**Figure 3.2.1**; $p>0.05$ and **Figure 3.2.2 A**; $p<0.05$), SAA2 (**Figure 3.2.1**; $p<0.05$ and **Figure 3.2.2 B**; $p<0.05$) and SAA3 (**Figure 3.2.3**; $p<0.001$) was significantly decreased/ablated in SAADKO mice. Although studies on CAC and SAA1/2 knockout in mice are limited, Davis *et al.* also showed that SAA3 is significantly decreased in SAADKO mice in an AOM/DSS-induced CAC model (Davis *et al*., 2021).

4.2.3 SAADKO mice present with an anti-inflammatory profile

It has been suggested that pro-inflammatory cytokines regulate pre-neoplastic growth during CAC tumourigenesis and that chronic inflammation in IBD progresses to CAC with constant overproduction of pro-inflammatory cytokines includinh IL-1β, IL-6 and TNF-α (Ishiguru, 1999). We therefore set out to determine whether SAA1/2 mediates cytokine alterations *in vivo* in a CAC mouse model. Immunoblotting showed that a decreased trend of IL-6 was observed in the colon tumour lysate in SAADKO mice compared to WT mice (**Figure 3.2.4**; $p=0.09$). Subsequently, qPCR was performed to assess the expression of IL-1β, which was significantly decreased in SAADKO mice, compared to WT mice (**Figure 3.2.5**; $p<0.01$). These findings

suggest that the ablation of SAA1/2 with CAC yields an anti-inflammatory response. SAA1/2 could therefore elicit tumour promoting properties in this model. This has also been the case with other studies. Han and authors showed that IL-6 is upregulated in DSS/AOM-induced CAC mice and following IL-6 inhibition, tumour size and number was significantly reduced (Han *et al*., 2016). Furthermore, a study has showed that the treatment of WT mice with recombinant IL-6 during early or late stages of CAC, resulted in significant increase in tumour size when compared to IL-$6^{-/-}$ mice. It has also been shown that IL-6 is upregulated in patients with CRC, which correlated with increased tumour size and metastasis (Chung & Chang, 2003). When comparing IL-1β expression to other studies, Wang and authors observed that CAC-bearing mice had more IL-1β protein than their naïve littermates and concluded that the intestinal inflammatory milieu elicits high IL-1β expression in infiltrating neutrophils and that this is critical for CAC development (Wang *et al*., 2014). The next aim was therefore to determine whether the increased expression of these pro-inflammatory cytokine correlates with inflammasome signaling.

4.2.4 The anti-inflammatory profile in SAADKO mice correlates with suppressed NLRP3 inflammasome signaling

MCM2 is a cancer proliferation biomarker that functions as a permitting factor in the initiation of DNA replication (Cheung *et al*., 2017). The immunoblotting results showed that a decreased trend of MCM2 was observed in SAADKO mice, compared to WT mice (**Figure 3.2.6 A**; p=0.09). It can therefore be speculated that knockout of SAA suppresses tumour proliferation. These results have also been previously reported where Davis *et al.* found that MCM2 was associated with proliferative properties in WT AOM/DSS-induced CAC mice, when compared to SAADKO mice (Davis *et al*., 2021). However, the role between MCM2 and SAA is not well documented.

As mentioned earlier, the NLRP3 inflammasome has been implicated in the progression and development of CAC, but its role in cancer remains controversial. In this study, NLRP3 expression was significantly decreased in SAADKO mice compared to WT mice and a decreased trend of caspase-1 was observed (**Figure 3.2.6 B & C**; $p<0.05$ and $p=0.06$). To the best of our knowledge, this study is the first to report the novel role of SAA in NLRP3 inflammasome signaling in CAC. This decreased expression of inflammasome components in SAADKO mice is supported by the decreased expression of pro-inflammatory cytokines, as seen in **Figures 3.2.4 and 3.2.5**. It has also been shown that NFkB transcription is critical for the activation of NLRP3, however, no significant changes in the expression of NFkB was observed (**Figure 3.2.6 D**). In contrast to our results, a protective role of NLRP3 in CAC was

reported. Allen and authors showed that components of the inflammasome are protective during acute and recurring colitis and CAC in the AOM/DSS-induced CAC model. Mice lacking caspase-1 and apoptosis-associated speck-like protein containing a CARD (ASC) had increased disease, morbidity, histopathology and polyp formation. This increased tumour burden was correlated with attenuated levels of IL-1β and IL-18 at the tumour site (Allen *et al*., 2010). Similarly, Hirota and authors also described a protective role of NLRP3 in CAC, $NLRP3^{-/-}$ mice were more susceptible to colitis compared to WT mice and this was also associated with decreased IL-1β (Hirota *et al*., 2011). As mentioned, CAC is often a risk factor for developing colon cancer and in contrast to the protective role of NLRP3 in CAC, it has been observed that NLRP3 expression is upregulated in colon adenocarcinoma tissues in cancer patients (Shi *et al*., 2021). High levels of NLRP3 correlated with malignant tumours, the occurrence of metastasis and vascular invasion. Other studies therefore reported a protective role of NLRP3 in CAC, but a tumour-promoting role in CRC, therefore, further investigation is required.

As mentioned above, the present study is the first to report the relationship between SAA and NLRP3 inflammasome signaling in CAC. SAADKO mice presented with suppressed NLRP3 and caspase-1 expression compared to WT mice (**Figure 3.2.6 B & C**), supporting our hypothesis that SAA functions as an endogenous DAMP in the TME to promote tumourigenesis by potentially binding to PRRs, such as TLRs. To support these findings, Cheng *et al.* reported that SAA stimulates TLR2 activation in cervical cancer cells (HeLa cells) and this was associated with the degradation of Iκβ and an increase in NFκB activity (Cheng *et al*., 2008). Furthermore, relatively low concentrations of SAA induced robust phosphorylation of ERK1/2 and p38 in the Hela cells, but no significant changes in the expression of these MAPKs were observed in the present study (**Figure 3.2.6 E & F**). SAA can also bind to TLR4 (Sandri *et al*., 2008) and it was found that after AOM/DSS administration, the number of colonic tumours in villin-TLR4 mice (a transgenic mouse model carrying a constitutively active TLR4 in the intestinal epithelium) was significantly higher than WT mice. Furthermore, inhibition of TLR4 markedly suppressed the development of colonic tumors in the WT mice (Fukata *et al*., 2007). These findings highlighted the ability of SAA to bind to TLRs to promote inflammasome signaling in CAC.

Additionally, an *in vitro* model was also performed to assess the role of SAA in inflammasome signaling in colon cancer, where the aim was to assess the extent of inflammasome activation in the presence of TLR inhibitors (Supplementary information). However, no NLRP3 expression was detected. Although studies to describe the role of SAA in inflammasome signaling are limited, it has been reported that SAA binds to TLRs in inflammatory conditions

to activate the NLRP3 inflammasome. In mice, macrophages from TLR4-deficient strains did not produce significant amounts of nitric oxide (NO) upon SAA stimulation when compared to WT mice and the authors concluded that SAA acts as an endogenous TLR4 ligand (Sandri *et al*., 2008). Furthermore, contributing to the involvement of TLR4 in cancer progression, high expression of TLR4 mediated signaling has been associated with a high risk of liver metastasis and poor prognosis in CRC patients.

4.2.5 SAADKO possibly suppresses EMT in AOM/DSS-induced colitis-associated cancer (CAC)

As mentioned, EMT is a process by which epithelial cells lose their cell polarity and cell–cell adhesion and gain migratory and invasive properties to become mesenchymal stem cells. These cells can then differentiate into several cell types. Consequently, EMT is associated with advanced tumour progression, metastasis, and invasion. Immunoblotting for mesenchymal markers, Snail and vimentin, showed a decreased trend in the expression of these EMT markers in SAADKO mice compared to WT mice (**Figure 3.2.9 A & B**; p=0.07 and p=0.07). SAADKO mice therefore presented with less aggressive and metastatic properties. These findings suggest the SAA promotes metastasis in CAC. Similar to these findings, it was also found that SAA promoted the upregulation of mesenchymal markers, vimentin and Snail and suppressed the epithelial marker, E-cadherin, in ovarian cancer (Li *et al*., 2020). In the present study however, no E-cadherin expression was detected.

As mentioned previously, the NLRP3 inflammasome plays an important role in the process of colitis and colitis-associated colon cancer, but the role of NLRP3 and EMT promotion in CAC is limited. In an *in vivo* mouse study, Yuan and authors observed that in an AOM/DSS-induced CAC model, myofibroblasts from MyD88 knockout mice presented with decreased α-SMA (a mesenchymal markers which generally contributes to tumour cell migration and invasion by suppressing E-cadherin) (Yuan *et al*., 2021). It is therefore plausible that in CAC, NLRP3 activation promotes EMT. In the present study, the decreased expression of NLRP3 in SAADKO mice (**Figure 3.2.6 B**) correlates with the decreased expression of IL-1β (**Figure 3.2.5**) and attenuated levels of both Snail and vimentin (**Figure 3.2.9 A & B**) in SAADKO mice compared to WT mice. However, to the best of our knowledge, no other studies exist to support or contradict these findings in CAC.

It has been shown that NLRP3 was significantly upregulated in human CRC tissues which were associated with tumour size, invasion, and lymph node metastasis as well as increased vimentin and decreased E-cadherin expression. Furthermore, knockdown of NLRP3 in CRC

cells inhibited their migration and growth and reversed EMT *in vitro* (Shao *et al*., 2020). Similarly, Marandi and authors showed that the upregulation of NLRP3 inflammasome components (NLRP3, ASC and caspase-1) together with the increased production of IL-1β promoted EMT in CRC patients (Marandi *et al*., 2021). This phenomenon was associated with an increase in vimentin expression and a reduction in E-cadherin protein levels. During their study, IL-1β directly correlated with NLRP3 and MMP-9 expression. The authors concluded that the upregulation of NLRP3 and IL-1β was associated with EMT during CRC progression *in vivo.*

Taking these findings into consideration, we show that in the present study, metastasis is suppressed in SAADKO mice, when compared to WT mice in CAC. This finding was associated with the decreased expression of IL-1β and NLRP3 in SAADKO mice. We therefore propose that SAA-NLRP3 dependent IL-1β secretion promotes EMT in CAC.

4.2.6 SAADKO mice present with decreased morphological abnormalities

Qualitative analysis of H&E staining shows that both WT and SAADKO mice presented with epithelial erosion (**Figure 3.2.11**). However, WT mice presented with increased characteristics associated with morphological abnormalities (**Figure 3.2.11 C**). This includes epithelial defects such as crypt loss, as well as thickening of the muscularis externa and immune infiltrates into the submucosa. Similarly, to these findings, Davis and authors showed that in WT mice, epithelial defects and loss of architecture in the mucosa were observed, as well as immune infiltrates in the mucosa when compared to SAADKO mice (Davis *et al*., 2021). Collectively, SAA induced more severe morphological abnormalities in CAC mice.

Furthermore, the proliferative marker, Ki67, is a human nuclear antigen which plays an important role in cell division, in both normal and malignant tissue (Mannel, 2016). Since one of the hallmarks of cancer is uncontrolled cell proliferation, the Ki67 proliferative index is increasingly used to assess cancer growth. Qualitatively, our results show that Ki67 signal was decreased in SAADKO mice compared to WT mice (**Figure 3.1.12**). These findings correlate with the decreased trend of MCM2 in SAADKO mice (**Figure 3.2.6**). Similar to our findings, Davis and authors also showed that in AOM/DSS-induced CAC, Ki67 is decreased in SAADKO mice (Davis *et al*., 2021). Lastly, the suppressed expression of NLRP3 as indicated by immunoblotting (**Figure 3.2.6 B**), is supported by the decreased immunohistochemical signal of NLRP3 in SAADKO mice (**Figure 3.2.13 D**).

4.2.7 Summary of AOM/DSS-induced colitis-associated cancer (CAC)

Taking these findings into consideration, SAADKO promotes an anti-inflammatory profile in CAC dependent on the NLRP3 inflammasome, as this was associated with the decreased expression of NLRP3. Furthermore, it can be speculated that SAADKO mice presented with decreased mesenchymal markers associated with EMT and was therefore less aggressive and metastatic. SAADKO mice also presented with decreased proliferative properties, as indicated by the decreased expression of Ki67. However, in contrast to our findings, previous studies have mainly reported a protective role of NLRP3 in CAC. It is therefore plausible that the activation of the NLRP3 inflammasome by SAA promotes tumourigenesis, in contrast to other PAMPs and DAMPs in this model. To the best of our knowledge, it can be concluded that this model highlights the novel role of SAA in NLRP3 inflammasome signaling in CAC, where SAA functions as an endogenous DAMP in the TME to promote tumour growth and progression (Figure 4.2).

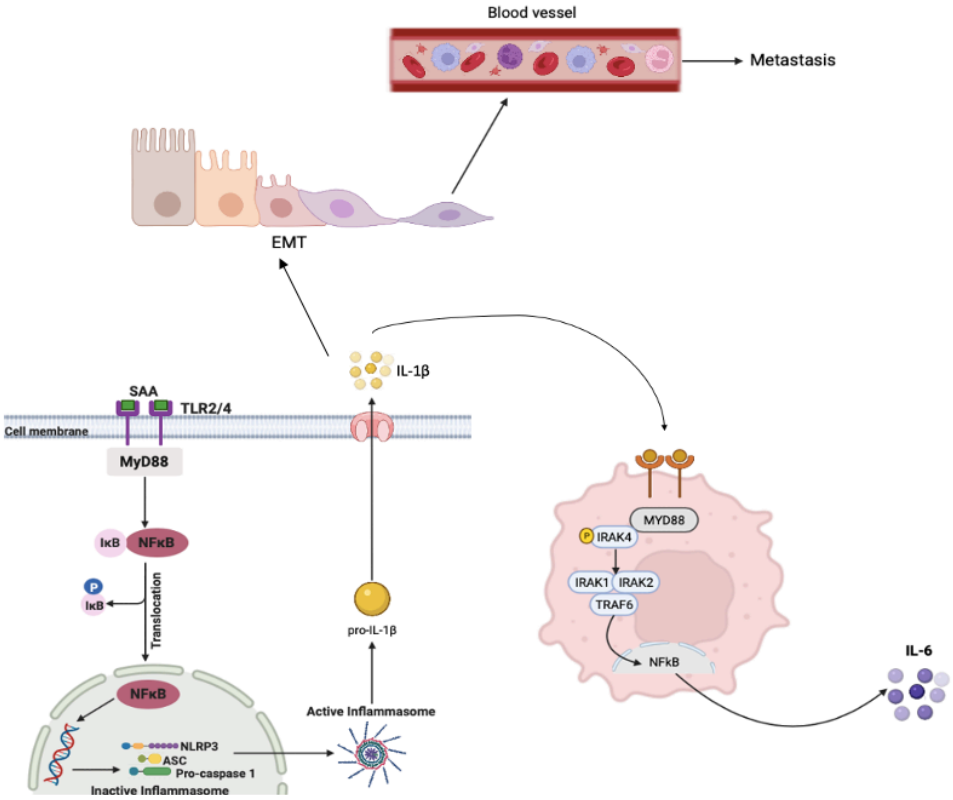

Figure 4.2: SAA-NLRP3-signaling promotes cancer progression in CAC. SAA binding to TLRs on cancer cells activates the NLRP3 inflammasome to secrete IL-1β. The binding of IL-1β to IL-1R on other cell types promotes the secretion of IL-6. IL-1β also promotes EMT which could result in tumour metastasis. **Abbreviations**: **EMT**: Epithelial-mesenchymal transition; **P**: Phosphorylate; **SAA**: Serum amyloid A; **TLR**: Toll-like receptor

4.3 SAA promotes a pro-inflammatory environment in triple negative breast cancer (TNBC)

4.3.1 Introduction

Chronic inflammation contributes to the malignant transformation of several cancers and is also an important component of breast cancer. However, the role of chronic inflammation in the initiation and development of breast cancer is still unclear. Many nude immune-compromised mouse models make use of human cancer cells to study the development of breast cancer. To assess the involvement of the immune system, we made use of a model where syngeneic TNBC cells (E0771 cells) were injected subcutaneously in mice with intact immune systems, which resulted is spontaneous tumour development in the mammary fat pad. Although the underlying mechanisms that link inflammation and carcinogenesis are not clear, the molecular platforms of the inflammasome have also been implicated in breast cancer. It has been demonstrated that NLRP3 inflammasome components and IL-1β is upregulated in the breast TME (Guo *et al*., 2016). Several other factors also contribute to the development and progression of breast cancer, where it has been shown that SAA is upregulated in the breast TME (Yang *et al*., 2016). However, the tumour promoting properties of SAA in NLRP3 inflammasome signaling in breast cancer remains to be elucidated.

4.3.2 Deficiency of SAA1 and SAA2 in triple negative breast cancer (TNBC) mice

TNBC was established in WT and SAADKO mice, allowing an investigation into the contribution of the acute phase SAA1/2 isoforms in this model. Immunoblotting showed that SAA1/2 (**Figure 3.3.2**; $p<0.01$) was significantly decreased in SAADKO mice.

4.2.3 SAADKO mice present with an anti-inflammatory profile

Inflammation has been proposed as an important player in tumour initiation, promotion, angiogenesis, and metastasis, in which cytokines are prominent role players. The Milliplex results show that IL-1β and IL-6 are decreased in plasma of SAADKO mice compared to WT mice (**Figure 3.3.3 A & B**; $p=0.05$ and $p<0.001$). Interestingly and contradicting these results, TNF-α showed an increased trend in SAADKO mice (**Figure 3.3.3 E**; $p=0.07$). IL-10, which is generally considered as an anti-inflammatory cytokine, was also decreased in SAADKO mice (**Figure 3.3.3 C**; $p<0.05$). Guo and authors measured IL-1β levels in tumour tissues from WT mice and from normal mammary glands and found an elevated concentration of IL-1β in the TME of WT mice (Guo *et al*., 2016). Furthermore, tumour tissues from caspase-1-deficient mice had reduced levels of IL-1β compared to wild-type mice. It has also been confirmed that

IL-1β promotes a high level of SAA1/2 in TNBC cells (Ignacio *et al*., 2018). This supports the decreased expression of IL-1β when SAA1/2 is ablated (**Figure 3.3.3 A**). Furthermore, Oh and co-authors showed that IL-6 secretion is dependent on IL-1β expression in MCF-7 breast cancer cells (Oh *et al*., 2016). High IL-6 levels in breast cancer patients are also associated with poor outcome and the upregulation of malignant features (Sanguinetti *et al*., 2015).

In ER- breast cancer cell lines (HER+ or TNBC), TNF-α seems to have a dual role regarding primary tumour development. It promotes apoptosis in some cases (Pileczki *et al*., 2013), but stimulates survival and proliferation through multiple pro-tumorigenic molecular pathways in other cases (Qiao *et al*., 2016). Here the results show that in the presence of SAA, TNF-α promotes an anti-inflammatory response (**Figure 3.3.3 E**). Contradicting these findings, it has been shown that SAA promotes TNF-α secretion in inflammatory conditions, such as rheumatoid arthritis (Migita *et al*., 2009). Similarly in another study, SAA induced rapid secretion of TNF-α in human neutrophils (Hatanaka *et al*., 2004).

Similar to TNF-α, IL-10 also exerts dual proliferative and inhibitory effects on breast tumour cells, once again highlighting the complex roles of these cytokines in breast cancer initiation and progression. The results show that IL-10 expression was significantly decreased in SAADKO mice compared to WT mice (**Figure 3.3.3 C**; $p<0.05$). It has been shown that IL-10 inhibits the release of pro-inflammatory cytokines such as TNF-α, IL-1β and IL-6 (Hamidullah *et al*., 2012), however that was not the case in our study. In line with the present study, De Santo and authors showed that SAA1 induced IL-10 secretion from neutrophils in melanoma patients (De Santo *et al*., 2010). However, not much is known about the relationship between SAA and IL-10 in breast cancer and further investigation is required.

4.3.4 The anti-inflammatory profile in SAADKO mice correlates with suppressed NLRP3 inflammasome signaling

Not much evidence is currently available to support the role of NLRP3 activation in breast cancer, to the best of our knowledge, this is the first study that shows that SAADKO suppresses NLRP3 signaling in TNBC. This indicates that SAA functions as an endogenous DAMP in the TME to promote tumourigenesis by potentially binding to PRRs, such as TLRs. Subsequently, immunoblotting showed that inflammasome components NLRP3, caspase-1 and NFkB was significantly decreased in SAADKO mice compared to WT mice (**Figure 3.3.3 B & C**; $p<0.05$). Similarly, Wang and authors showed that when NLRP3 is knocked down in MDA-MB-231 cells, caspase-1 expression and IL-1β secretion was downregulated (Wang *et al*., 2021). Yet, little is known about the role of SAA in NLRP3 inflammasome activation in

cancer. In neutrophils however, Migita and authors observed that NLRP3 expression was increased at 4 hours with SAA stimulation. Furthermore, by inhibiting SAA-induced JNK phosphorylation, p38 and ERK1/2 was marginally affected. On the other hand, SAA-stimulation induced phosphorylation of p65 (NFkB) in these neutrophils (Migita *et al*., 2014). Based on their findings, the authors concluded that SAA induces NLRP3-mediated IL-1β secretion in neutrophils.

To date, it has been reported that SAA has multiple receptors, including the FPR2, and TLR2 and TLR4 (Ignacio *et al*., 2018). With regards to SAA and the inflammasome, it has been shown that SAA triggers the inflammasome cascade by signaling through TLR2 and TL4 to promote IL-1β secretion in phagocytic cells in the liver (Lee *et al*., 2021). TLR4 was also found to be the highest expressed TLR in MDA-MB-231 cells (TNBC) and knockdown of TLR4 resulted in the dramatic reduction of breast cancer cell viability and the inhibition of IL-6 (Yang *et al*., 2006). Additionally, in a mouse breast cancer model, mice treated with LPS have increased TLR4 expression compared to control mice and this was associated with increased tumour size and metastasis (Yang *et al*., 2014). To date, it has been reported that TLR4 is the only TLR thus far that can signal via MyD88-dependent and MyD88-independent pathways. Based on studies using MyD88-deficient macrophages, the MyD88-dependent signaling pathway was shown to be responsible for pro-inflammatory cytokine expression (Lu *et al*., 2008). This phenomenon is supported by the decreased expression of NFkB (**Figure 3.3.4 D**; $p<0.05$) as well as pro-inflammatory cytokines, IL-1β and IL-6 (**Figure 3.3.3 A & B**; $p=0.05$ and $p<0.05$) in the present study. We therefore speculate that SAA binds to TLRs to promote pro-inflammatory secretion via canonical NLRP3 signaling in the TME of TNBC.

4.3.5 SAADKO possibly suppresses epithelial-mesenchymal transition (EMT) in triple negative breast cancer (TNBC)

To date, the EMT phenomenon has been the favoured mechanism of distant metastases for epithelial cancers, including breast cancer. We therefore aimed to determine the role of EMT in this model. Immunoblotting for EMT markers show a decreased trend in vimentin expression in SAADKO mice, compared to WT mice (**Figure 3.3.6 B**; $p=0.09$). Integrated changes in several cell signaling events in TNBC leads to an EMT phenotypic shift and provide cells with more migratory and invasive properties that eventually results in metastatic colonization at a secondary site. It has been reported that when vimentin expression is reduced in MDA-MB-231 cells, the migration and adhesion ability of these cells is attenuated (McInroy and Maatta, 2007). However, the exact mechanisms are unknown and studies regarding the role of SAA, inflammasome signaling and EMT are limited.

More recently, Wang and colleagues showed that canonical NLRP3 activation in MDA-MB-231 cells and the secretion of IL-1β promoted EMT (Wang *et al*., 2021). Knockdown of NLRP3 in these cells downregulated the expression of secreted IL-1β and suppressed EMT in MDA-MB-231 cells. The authors showed that the addition of recombinant IL-1β in NLRP3 knockout cells, decreased E-cadherin expression and increased the expression of vimentin. However, no E-cadherin expression was detected in the present study. Furthermore, it has been shown that IL-6 decreases E-cadherin in MCF-7 cells *in vitro*, followed by the induction of both Snail and vimentin (Sullivan *et al*., 2009). However, no significant change in Snail expression was observed in the present study (**Figure 3.3.6 A**). It is therefore plausible that the decreased expression of NLRP3 (**Figure 3.3.4 B**), IL-1β and IL-6 (**Figure 3.3.3 A & B**) in SAADKO mice correlates with the decreased expression of vimentin in the present study. Further supporting the role of IL-1β in EMT, Guo *et al.* observed that reduced tumour growth and metastasis is observed in caspase-1 deficient mice and therefore hypothesized that blocking inflammasome activity or IL-1R signaling may inhibit tumor growth (Guo *et al*., 2016). Mice injected with IL-1Ra had significantly inhibited tumour growth compared to control mice in a breast cancer model and tumour-bearing mice treated with IL-1Ra had a reduced number of tumour nodules in the lungs.

However, the role of SAA in EMT in breast cancer is not well understood. In an *in vitro* model, MDA-MB-231 cells cultured in conditioned media with SAA1 or SAA3 had significantly enhanced invasiveness compared to controls (Hansen *et al*., 2015). In a breast cancer mouse model, ectopic expression of SAA1 or SAA3 in tumour cells promoted widespread metastasis. These findings indicate a metastatic effect of SAA in TNBC. It is therefore plausible that in the present study, SAA-NLRP3 dependent IL-1β secretion promotes EMT in TNBC.

4.3.6 SAADKO mice present with decreased morphological abnormalities

Overall, SAADKO mice present with distinct morphological qualities compared to WT mice. Here we show that qualitatively, SAADKO mice present with fewer morphological abnormalities than WT mice (**Figure 3.3.9**). Firstly, a necrotic front between viable and necrotic tissue was seen in WT mice (**Figure 3.3.8**) and to a lesser extent in SAADKO mice. Areas of decreased cellular viability was observed in both WT and SAADKO mice (**Figure 3.3.8 C and 3.3.9 C**). These results support the idea that the ablation of SAA1/2 in TNBC presents with a protective function. In association with these results, high-grade invasive ductal carcinoma with a large central acellular zone is frequently reported in TNBCs. In one study, 58.7% of patients with TNBC presented with necrotic tissue (Ryu *et al*., 2011).

Furthermore, the larger necrotic tissue regions observed in WT mice (**Figure 3.3.8 B**) presented with increased staining of NLRP3 (**Figure 3.1.10 C**) when compared to SAADKO mice (**Figure 3.3.10 D**). This finding can be attributed to the fact that necrotic tissue constantly secretes DAMPs/PAMPs, which is associated with inflammasome activation. Li and colleagues have shown that necrotic but not apoptotic cells secrete mature IL-1β which was mediated by the ASC inflammasome (Li *et al*., 2009).

4.3.7 Summary of results in our model of triple negative breast cancer (TNBC)

Taking these findings into consideration, SAADKO promoted an anti-inflammatory profile in TNBC, which was associated with the decreased expression of NLRP3, NFkB as well as caspase-1. Both ERK and p38 displayed no significant changes, indicating that NLRP3 inflammasome was activated via the canonical pathway. Furthermore, it can be speculated that SAADKO mice presented with decreased mesenchymal markers associated with EMT and was therefore less aggressive and metastatic. To the best of our knowledge, it can be concluded that this model highlights the novel role of SAA in NLRP3 inflammasome signaling in TNBC, where SAA functions as an endogenous DAMP in the TME to promote tumour growth and progression (Figure 4.3).

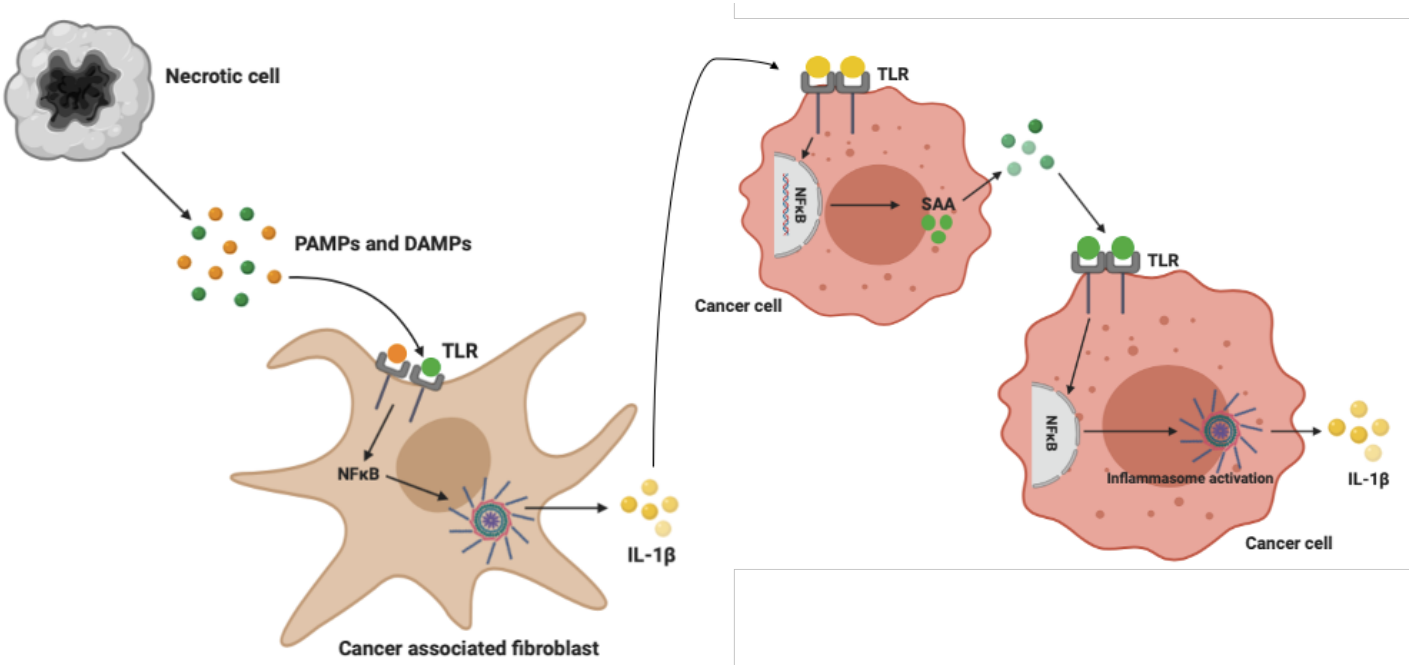

Figure 4.3: Positive feedback mechanism for IL-1β and SAA secretion in the tumour microenvironment (TME) (Fourie *et al*., 2021)**. Abbreviations: DAMP**: Damage associated molecular pattern; **PAMP**: Pattern associated molecular pattern; **TLR**: Toll-like receptor

4.4. Summary

In this study we have shown that during highly inflammatory conditions, such as acute colitis (AC), SAA had a protective role by promoting an anti-inflammatory profile. When SAA1/2 was ablated, p38 MAPK was responsible for the production of pro-inflammatory cytokines like IL-1β and IL-6 and not the NLRP3 inflammasome as originally hypothesized. The pro-inflammatory profile of SAADKO mice was also associated with reduced E-cadherin, which could ultimately promote the severity of colitis. However, in cancer models, the opposite effects were seen in both CAC and TNBC. In both studies, it is plausible that SAA promoted a pro-inflammatory profile, which could have detrimental effects for cancer patients. When SAA1/2 is ablated, NLRP3 signaling was suppressed and this was accompanied by the decreased expression of pro-inflammatory cytokines. Furthermore, SAA ablation was associated with decreased EMT in these models. This study highlights the novel role of SAA functioning as a DAMP in the TME, which promoted NLRP3 signaling and the subsequent release of pro-inflammatory cytokines in CAC as well as in TNBC. We have therefore clearly demonstrated that the tumour-induced systemic environment acts as a critical regulator of cancer progression and metastasis.

Chapter 5

Conclusion

It is clear that inflammation affects all stages of tumour development and IL-1β, a pro-inflammatory cytokine, plays an important role in inflammation-induced tumourigenesis (Voronov *et al*., 2003). The NLRP3 inflammasome is an intracellular signaling complex that functions as a regulator of innate immune activity by modulating the production of pro-inflammatory cytokines, such as IL-1β. SAA, an acute phase protein, can bind to pattern recognition receptors like TLRs on several cell types within the TME to stimulate the production of IL-1β, thereby creating a favourable inflammatory environment that supports tumour growth. SAA is capable of triggering the generation of pro-inflammatory cytokines as well as activating the NLRP3 inflammasome, two mechanisms known to promote tumour development and metastasis. However, in this study, we demonstrated that SAA-NLRP3 signaling differs between an inflammatory condition such as acute colitis (AC) and models of colitis-associated cancer (CAC) and triple negative breast cancer (TNBC). With colitis, SAA functions independently of the NLRP3 inflammasome to suppress the secretion of pro-inflammatory cytokines and has a protective effect by promoting an anti-inflammatory environment. In contrast, in both colitis-associated cancer (CAC) and triple negative breast cancer (TNBC), it is demonstrated that SAA promotes a pro-inflammatory environment through NLRP3 signaling. This increased secretion of cytokines also promotes epithelial-mesenchymal transition (EMT). Therefore, in tumourigenesis, SAA functions as an endogenous damage associated molecular pattern (DAMP) in the TME to promote cancer progression. In conclusion, simultaneously targeting serum amyloid A and NLRP3 components through inhibiting receptors or by preventing downstream signaling mechanisms from occurring, could be beneficial for cancer treatments.

Chapter 6

Summary and Future work

In this 3-part in *vivo* study, the role of SAA in inflammasome signaling was investigated. It was hypothesized that SAA functions as a DAMP in the tumour microenvironment to promote cancer growth and progression. Interestingly, we have demonstrated that SAA functioned independently of the NLRP3 inflammasome in our model of acute colitis and induced an anti-inflammatory environment. In our tumourigenesis models however, SAA-NLRP3 signaling induced a pro-inflammatory environment and promoted EMT. Overall, all aims and objectives were achieved for the *in vivo* models, except for quantifying the Ki-67 proliferation index in TNBC mouse tumours, which will be addressed in the future.

In section 3.1, the role of SAA in NLRP3 inflammasome signaling in an acute DSS-induced colitis model was investigated. Here, colitis was established in WT and SAADKO mice by administering 2.5% DSS in autoclaved water for five days. Subsequently, mice were euthanized and colon tissue and blood was collected. The blood was processed to plasma to determine the expression of SAA and several other cytokines. Colon tissue was assessed by using Western blots and histopathology and RNA was collected for qPCR. The data showed that all three isoforms of SAA (SAA1, SAA2 and SAA3) were decreased in SAADKO mice. Interestingly, SAA functioned independently of the NLRP3 inflammasome to promote a pro-inflammatory profile in SAADKO mice which was instead attributed to MAPK signaling. Furthermore, SAA-dependent IL-1β secretion promoted the loss of E-cadherin which can have detrimental effects such as a leaky epithelial barrier in ulcerative colitis patients. Since SAA3 has been associated with the increased expression of pro-inflammatory cytokines such as IL-1β, IL-6 and TNF-α, it would be beneficial to establish an *in vivo* model where all three isoforms of SAA are knocked-out.

In section 3.2 the role of SAA in NLRP3 inflammasome signaling in AOM/DSS-induced CAC was investigated. Here, mice received an intraperitoneal injection of AOM and after one week, DSS treatment was administered in autoclaved drinking water at a concentration of 2.5% for a total of 5 days, followed by a recovery period of 16 days. DSS treatment was administered for a total of 3 cycles. Subsequently, mice were euthanized and colon tumours and blood was collected. The blood was processed to plasma to determine the expression of SAA and several other cytokines. Colon tissue was assessed by using Western blots and histopathology and RNA was collected for qPCR. The data showed that all three isoforms of SAA (SAA1, SAA2 and SAA3) was decreased in SAADKO mice. Performing Western blots to determine whether

SAA is present in colon tumours would have been beneficial, but further optimizing of our antibody is required. Contradictory to other NLRP3-CAC models, SAADKO suppressed inflammasome signaling which was also associated with the decreased expression of pro-inflammatory cytokines. However, a previous Multiplex assay to assess cytokine expression in plasma yielded an insufficient response and another repeat would have been beneficial, which would have allowed us to assess a broader range of inflammatory markers. IL-18 is also associated with CAC progression, and analysing the expression of this cytokine could be beneficial to determine its role in our model. It was also shown that SAADKO mice presented with decreased expression of mesenchymal markers, indicating that SAA promotes invasion and metastasis in CAC. Since our CAC results contradicted results from other studies in literature, analysing human tissue samples could provide clarity in this regard. As mentioned above, it would also be beneficial to establish an *in vivo* model where all three isoforms of SAA are knocked-out as SAA3 also plays a role during inflammation in mice.

In section 3.3 the role of SAA in NLRP3 inflammasome signaling in triple negative breast cancer (TNBC) was investigated. Here, TNBC tumours (by subcutaneously injecting EO771 cells) were established in WT and SAADKO mice. Subsequently, mice were euthanized after reaching the experimental endpoint and tumours and blood were collected. Blood was processed to plasma to assess SAA and inflammatory cytokine expression and tumours were subjected to Western blots and histopathology. The data showed that similar to our CAC model, SAADKO suppressed NLRP3 signaling which was associated with the decreased expression of pro-inflammatory cytokines and mesenchymal markers. Performing Western blots to determine whether SAA is present in breast tumours would also have been beneficial to ensure that SAA was not upregulated in mice undergoing stress.

Lastly, supplementary information showed that an attempt to assess the role of SAA in inflammasome signaling in both colon and breast cancer cells was investigated. However, Western blot data shows that no NLRP3 expression was detected in these cell lines. Several concentrations and treatment durations of the primer, LPS, were optimized as well as the activator, ATP. To ensure that our reagents or the antibody was not the cause of this problem, we tested LPS and ATP priming and activation in THP-1 cells (monocytes) and NLRP3 as well as caspase-1 expression were detected. It could therefore be beneficial to use other primers, like *Nigecerin*. The aim of this model was to assess the role of NLRP3 by overexpressing SAA in these cells. Since the role of the inflammasome remains controversial in cancer, optimizing this protocol would have confirmed whether the *in vivo* results accurately represent the function of SAA and NLRP3 inflammasomes in tumourigenesis as hypothesized. See supplementary data after the reference section.

Reference list

Allen IC., TeKippe E., Woodford R-M., Uronis JM., et al, 2010. The NLRP3 inflammasome functions as a negative regulator of tumorigenesis during colitis-associated cancer. *Journal of Experimental Medicine*; 207(5): 1045-1056.

Ancsin JB & Kisilevsky R, 1999. The heparin/heparan sulfate-binding site on apo-serum amyloid A. Implications for the therapeutic intervention of amyloidosis. *Journal of Biological Chemistry*;274: 7172 – 7181.

Asquith M & Powrie F, 2010. An innately dangerous balancing act: intestinal homeostasis, inflammation, and colitis-associated cancer. *Experimental Medicine*; 207(8): 1573-7.

Ather JL., Ckless K., Martin R., Foley KL., Suratt BT., et al, 2011. Serum amyloid A activates the NLRP3 inflammasome and promotes Th17 allergic asthma in mice. *Journal of Immunology*: 87(1):64-73.

Badolato R., Wang JM., Murphy WJ., Lloyd AR., Michiel DF., Bausserman LL., Kelvin DJ & Oppenheim JJ, 1994. Serum amyloid A is chemoattractant: induction of migration, adhesion, and tissue infiltration of monocytes and polymorphonuclear leukocytes. *Journal of Experimental Medicine*; 180(1):203-9.

Bae JY., Lee S-W., Shin Y-H., Lee J-H., Jahng JW & Park K, 2017. P2X7 receptor and NLRP3 inflammasome activation in head and neck cancer. *Oncotarget*; 8(30):48972.

Bandyopadhyay C., Schecterson L & Gumbiner B, 2020. P150 enhancing epithelial barrier function with novel E-cadherin activating monoclonal antibodies reduces inflammatory bowel disease progression in mouse models. *Inflammatory bowel diseases*; 26: 29-30.

Bardou V., Arpino G., Elledge RM., Osborne CK & Clark GM, 2003. Progesterone receptor status significantly improves outcome prediction over estrogen receptor status alone for adjuvant endocrine therapy in two large breast cancer databases. *Journal of Clinical Oncology*; 21(10): 1973-9.

Bauer KR., Brown M., Cress RD., Parise CA & Caggiano V, 2007. Descriptive analysis of estrogen receptor (ER)-negative, progesterone receptor (PR)-negative, and HER2-negative invasive breast cancer, the so-called triple-negative phenotype. *Cancer*; 109(9):1721-1728.

Bauer C., Duewell P., Mayer C., et al, 2010. Colitis induced in mice with dextran sulfate sodium (DSS) is mediated by the NLRP3 inflammasome. *Gut*; 59(9):1192-9.

Bhatelia K., Singh K & Singh R., 2014. TLRs: linking inflammation and breast cancer. *Cell Signal*; 26(11):2350-7.

Boraschi D., Italiani P., Weil S & Martin MU, 2018. The family of the interleukin-1 receptors. *Immunology Reviews*; 281: 197–232.

Brough D., Tyrrell PJ & Allan SM, 2011. Regulation of interleukin-1 in acute brain injury. *Trends in Pharmacological Sciences*; 32:617–622.

Broz P & Dixit VM, 2016. Inflammasomes: mechanism of assembly, regulation and signalling. *Nature Reviews Immunology*; 16(7):407-20.

Cario E, 2010. Toll-like as receptors in inflammatory bowel diseases: a decade later. *Inflammatory Bowel Diseases*; 16(9):1583-97.

Chan AH & Schroder K, 2020. Inflammasome signaling and regulation of interleukin-1 family cytokines. *Cell*; 118(3):285-96.

Chaturvedi A & Pierce SK, 2009. How location governs toll-like receptor signaling. *Traffic*; 210:621-8.

Cheng N., He R., Tian J., Ye PP & Ye RD, 2008. Cutting edge: TLR2 is a functional receptor for acute-phase serum amyloid A. *Journal of Immunology*; 81(1):22-6.

Cheng K., Wang X, Zhang S & Yin H, 2012. Discovery of small molecule inhibitors of the TLR1-TLR2 complex. *European Journal of Organic Chemistry*; 51(49): 12246–12249.

Cheung C., Hsu C-L., Chen K-P., Chong S-T., et al, 2017. MCM2-regulated functional networks in lung cancer by multi-dimensional proteomic approach. *Scientific Reports*; 7: 13302.

Chung, YC & Chang YF, 2003. Serum interleukin-6 levels reflect the disease status of colorectal cancer. *Journal of Surgical Oncology*; 83(4):222-6.

Cui X., Schiff R., Arpino G., Osborne CK & Lee AV, 2005. Biology of progesterone receptor loss in breast cancer and its implications for endocrine therapy. *Journal of Clinical Oncology*; 23(30):7721-35.

Daniel AR., Hagan CR & Lange CA, 2011. Progesterone receptor action: defining a role in breast cancer. *Expert Review of Endocrinology and Metabolism*; 6(3): 359-369.

D'anneo A., Carlisi D., Lauricella M., Puleio R., Martinez R., Di Bella S., et al, 2013. Parthenolide generates reactive oxygen species and autophagy in MDA-MB-231 cells. A soluble parthenolide analogue inhibits tumour growth and metastasis in a xenograft model of breast cancer. *Cell Death*; 4: e891.

Davis T., Conradie D., Shridas P., De Beer FC., Engelbrecht AM & De Villiers WJS, 2021. Serum Amyloid A Promotes Inflammation-Associated Damage and Tumorigenesis in a Mouse Model of Colitis-Associated Cancer. *Cellular and Molecular Gastroenterology and Hepatology*; 12(4):1329-1341.

de Beer MC., Webb NR., Wroblewski JM., Noffsinger VP., Rateri DL., Ji A., van der Westhuyzen DR & de Beer FC, 2010. Impact of serum amyloid A on high density lipoprotein composition and levels. *Journal of Lipid Research*; 51:3117–3125.

De Buck M., Gouwy M., Wang JM., Van Snick J., Opdenakker G., Struyf S & Van Damme J, 2016. Structure and Expression of Different Serum Amyloid A (SAA) Variants and Their Concentration-Dependent Functions During Host Insults. *Current Medicinal Chemistry*; 23(17):1725-55.

Deisseroth A., Ko CW., Nie L., et al, 2015. FDA Approval: Siltuximab for the Treatment of Patients with Multicentric Castleman Disease. *Clinical Cancer Research*; 21:950–954.

Dent R., Hanna WM., Tradeau M., Rawlinson E., Sun P., & Narod SA, 2009. Triple-negative breast cancer: clinical features and patterns of recurrence. *Breast Cancer Research and Treatment*; 115:423-428.

Desantis CE., Ma J., Gaudet MM., et al, 2019. Breast cancer statistics, 2019. *ACS Journals*; 69(6): 438-451.

De Santo C., Arscott R., Booth S., Karydis S., et al, 2010. Invariant NKT cells modulate the suppressive activity of Serum Amyloid A-differentiated IL-10-secreting neutrophils. *Nature Immunology*; 11(11): 1039-1046.

Dinarello CA, 2009. Immunological and inflammatory functions of the interleukin- 1 family. *Annual Reviews Immunology*; 27:519–50.

Dinarello CA, 2011. interleukin-1 in the pathogenesis and treatment of inflammatory diseases. *Blood*;117(14):3720-32.

Dinarello CA, 2018. Overview of the IL-1 family in innate inflammation and acquired immunity. *Immunology Reviews*; 281(1): 8-27.

Ding J., Wang K., Liu W., She Y., Sun Q et al, 2016. Pore-forming activity and structural autoinhibition of the gasdermin family. *Nature*; 535(7610):111–116.

Doglioni G., Parik S & Fendt SM, 2019. Interactions in the (Pre)metastatic Niche support metastasis formation. *Frontiers in Oncology*; 9:219.

Dosh RH., Jordan-Mahy N., Sammon C & Le Maitre C, 2019. Interleukin 1 is a key driver of inflammatory bowel disease-demonstration in a murine IL-1Ra knockout model. *Oncotarget*; 10 (37):3559-3575.

Drexler SK., Bonsignore L., Masin M., Tardivel A., et al, 2012.Tissue-specific opposing functions of the inflammasome adaptor ASC in the regulation of epithelial skin carcinogenesis. *Proceedings of the National Academy of Sciences of the United States of America*; 109:18384–18389.

Drukteinis JS., Mooney BP., Flowers CI & Gatenby RA, 2013. Beyond mammography: new frontiers in breast cancer screening. *American Journal of Medicine*; 126(6):472-9.

Eaden JA., Abrams KR., Mayberry JF, 2001. The risk of colorectal cancer in ulcerative colitis: a meta-analysis. *Gut*; 48:526-535.

Ershaid N., Sharon Y., Doron H., Raz Y., et al, 2019. NLRP3 inflammasome in fibroblasts links tissue damage with inflammation in breast cancer progression and metastasis. *Nature Communications*; 10:4375.

Fan Y., Vong CT & Ye RD, 2019. Serum amyloid A and Immunomodulation. *Amyloid Diseases*, IntechOpen: 10.5772/intechopen.81617.

Fang H., Ang B., Xu X., Huang X., Wu Y., Sun Y., Wang W. Li N., Cao X & Wang T, 2014. TLR4 is essential for dendritic cell activation and anti-tumor T-cell response enhancement by DAMPs released from chemically stressed cancer cells. *Cellular and Molecular Immunology*; 11(2):150–159.

Fenini G., Grossi S., Gehrke S., Beer HD., et al, 2018. The p38 mitogen-activated protein kinase critically regulates human keratinocyte inflammasome activation. *Journal of Investigative Dermatology*; 138: 1380-90.

Fourie C., Davis T., Shridas P., De Villiers WJS & Engelbrecht A-M. Serum Amyloid A and Inflammasome activation: A link to cancer progression? *Cytokine and Growth Factor Reviews*; 59:62-70.

Francescone R., Hou V & Grivennikov SI, 2015. Cytokines, IBD, and colitis-associated cancer. *Inflammatory Bowel Disease*; 21:409–418.

Fukata M., Chen A., Vamadan AS., Cohen J., et al, 2007. Toll-like receptor-4 promotes the development of colitis-associated colorectal tumours. *Gastroenterology*; 133:1869-81.

Furlaneto CJ & Campa A, 2000. A novel function of serum amyloid A: a potent stimulus for the release of tumor necrosis factor-', inter- leukin-1', and interleukin-8 by human blood neutrophil. *Biochemical and Biophysical Research Communications*; 268:405–8.

Gabay C & Kushner I, 1999. Acute-phase proteins and other systemic responses to inflammation. *The New England Journal of Medicine*; 340:448–454.

Garlanda C., Dinarello CA & Mantovani A, 2013. The interleukin-1 Family: Back to the Future. *Immunity Reviews*; 39(6):1003-18.

Gonzalez-Reyes S., Marin L., Gonzalez L., Gonzalez LO., et al, 2010. Study of TLR3, TLR4 and TLR9 in breast carcinomas and their association with metastasis. *BMC Cancer*; 10: 665.

Greten FR., Eckmann L., Greten TF., Park JM., Li ZW., Egan LJ., Kagnoff MF & Karin M, 2004. IKKbeta links inflammation and tumorigenesis in a mouse model of colitis-associated cancer. *Cell*; 118:285–296.

Goyette P., Labbe C., Trinh TT., Xavier RJ & Rioux JD, 2007. Molecular pathogenesis of inflammatory bowel disease: genotypes, phenotypes, and personalized medicine. *Annual Medicine*; 39:177–99.

Grabowskia M., Murgueitiob MS., Bermudezb M., Wolberb G & Weindla G, 2019. The novel small-molecule antagonist MMG-11 preferentially inhibits TLR2/ 1 signaling. *Biochemical Pharmacology*; 171:113687.

Guo B., Fu S., Zhang J., Liu B & Li Z, 2016. Targeting inflammasome/IL-1 pathways for cancer immunotherapy. *Science Reports*:36107.

Halle A., Hornung V., Petzold GC., Stewart CR., Monks BG., Reinheckel T., Fitzgerald KA., Latz E., Moore KJ & Golenbock DT, 2008. The NALP3 inflammasome is involved in the innate immune response to amyloid-beta. *Nature Immunology*; 9(8):857-65.

Hamidullah., Changkija B & Konwar R, 2012. Role of interleukin-10 in breast cancer. *Breast Cancer Research and Treatment*; 133: 11-21.

Hanahan D & Weinberg RA, 2000. The Hallmarks of Cancer. *Cell*; 100(1): 57-70.

Hanahan D & Weinberg RA, 2011. Hallmarks of Cancer: the next generation. *Cell*; 144(5):646-74.

Hansen M., Forst B., Cremer, N., Quagliata L., et al, 2015. A link between inflammation and metastasis: serum amyloid A1 and A3 induce metastasis and are targets of metastasis inducing S100A4. *Oncogene*; 34(4):424-435.

Hatanaka E., Furlaneto CJ., Ribeiro FP., Souza GM & Campa A, 2004. Serum amyloid A-induced MRNA expression and release of tumor necrosis factor-alpha (TNF-α) in human neutrophils. *Immunology Letters*; 91(1): 33-7.

He R., Shepard LW., Chen J., Pan ZK. & Ye RD, 2006. Serum amyloid A is an endogenous ligand that differentially induces IL-12 and IL-23. *Journal of Immunology*; 177:4072 – 4079.

Hernandez C., Huebener P & Schwabe RF, 2016. Damage-associated molecular patterns in cancer: A double- edged sword. *Oncogene*;35(46):5931–5941.

Hinrichs BH., Matthews JD., Siuda D., O'Leary MN., Wolfarth-Bejan A & Neish AS, 2018. Serum Amyloid A1 Is an Epithelial Prorestitutive Factor. *The American Journal of Pathology*; 188(4):937-949.

Hirota SA., Ng J., Lueng A., Khajah M., et al, 2011. NLRP3 inflammasome plays a key role in the regulation of intestinal homeostasis. *Inflammatory bowel Disease*; 17(6):1359-72.

Holen I., Lefley DV., Francis SE., Rennicks S., Bradbury S., Coleman RE., et al, 2016. IL-1 drives breast cancer growth and bone metastasis in vivo. *Oncotarget*; 7(46):75571–84.

Hollenbach E., Neumann M., Vieth M., et al, 2004. Inhibition of p38 MAP kinase- and RICK/NF-κB-signaling suppresses inflammatory bowel disease. *FASEB Journal*; 18(13):1550-2.

Hoshino A., Kim HS., Bojmar L., Gyan KE., et al, 2020. Extracellular vesicle and particle biomarkers define multiple human cancers. *Cell*; 182:1-18.

Huang B., Zhao J., Li H., et al, 2005. "Toll-like receptors on tumor cells facilitate evasion of immune surveillance". *Cancer Research*; 65(12);5009–5014.

Ignacio A., Morales CI., Olsen N, Camara S & Almeida RR, 2016. Innate Sensing of the Gut Microbiota: Modulation of Inflammatory and Autoimmune Diseases. *Frontiers in Immunology*; 7:54.

Ishiguro Y, 1999. Mucosal proinflammatory cytokine production correlates with endoscopic activity of ulcerative colitis. *Journal of Gastroenterology*; 34:66-74.

Ishiguro Y, 2016. Mucosal proinflammatory cytokine production correlates with endoscopic activity of ulcerative colitis. *Cellular and Molecular Biology*; 13(2):148-159.

Jo E., Kim K., Shin JK., & Sasakawa C, 2016. Molecular mechanisms regulating NLRP3 inflammasome activation. *Cellular and Molecular Immunology*; 13:148–159.

Jo E-K., Kim JK., Shin D-M & Sasakawa C, 2020. Molecular mechanisms regulating NLRP3 inflammasome activation. Experimental Medicine; 217(1): e20190314.

Johnston CN., Smith YE., Cao Y., et al, 2015. Functional and molecular characterization of E0771. LMB tumors, a new C57BL/6-mouse-derived model of spontaneously metastatic mammary cancer. *Disease Models & Mechanisms*; 8(3):237-51.

Kalluri R & Weinberg RA, 2009. The basics of epithelial–mesenchymal transition. *Journal of Clinical Investigation*; 1420-8.

Kang JS., Bae SY., Kim HR., Kim YS., et al, 2009. Interleukin-18 increases metastasis and immune escape of stomach cancer via the downregulation of CD70 and maintenance of CD44. *Carcinogenesis*; 30(12):1987-1996.

Karan D, 2018. Inflammasomes: Emerging Central Players in Cancer Immunology and Immunotherapy. *Frontiers in Immunology*; 9:3028.

Karmakar S & Das C, 2004. Modulation of ezrin and E-cadherin expression by IL-1beta and TGF-beta1 in human trophoblasts. *Reproductive Immunology*; 64(1-2):9-29.

Karki R., Man SM & Kanneganti T-D, 2015. Inflammasomes and Cancer. *Mucosal Immunology*; 8(6):1275-84.

Katsnelson MA., Rucker G., Russo HM & Dubyak GR, 2015. K+ Efflux Agonists Induce NLRP3 Inflammasome Activation Independently of Ca2+ Signaling. *Journal of Immunology*:1402658.

Kawaguchi M., Takahashi M., Hata T., Kashima Y., Usui F., et al, 2011. Inflammasome activation of cardiac fibroblasts is essential for myocardial ischemia/reperfusion injury. *Circulation*; 123(6):594-604.

Kawai T & Akira S, 2006. TLR signalling. *Cell Death and Differentiation*; 13:816–825.

Kennecke H., Yerushalmi R., Woods R., et al, 2010. Metastatic behavior of breast cancer subtypes. *Journal of Clinical Oncology*; 28:3271-3277.

Kuemmerle-Deschner JB & Haug I, 2013. Canakinumab in patients with cryopyrin-associated periodic syndrome: an update for clinicians. Therapeutic advances in musculoskeletal disease; 5(6):315–329.

Kushner I, 1982. The phenomenon of the acute phase response. *Annals of the New York academy of Sciences*; 389:39–48.

Kwok BH., Koh B., Ndubuisi MI., Elofsson M & Crews CM, 2001. The anti-inflammatory natural product parthenolide from the medicinal herb Feverfew directly binds to and inhibits Ikappa-B kinase. *Chemistry and Biology*; 8(8):759–66.

Lambert WA., Pattabiraman DR & Weinberg RA, 2017. Emerging biological principles of metastasis. *Cell*; 168:670-691.

Lee HY., Kim MK., Park KS., Bae YH., Yun J., Park JI., Kwak JY & Bae YS, 2005. Serum amyloid A stimulates matrix-metalloprotein- ase-9 upregulation via formyl peptide receptor like-1-mediated signaling in human monocytic cells. *Biochemical and Biophysical Research Communications*; 330:989–998.

Lee MS & Kim YJ, 2007. Signaling pathways downstream of pattern-recognition receptors and their cross talk. *Annual Reviews Biochemistry*; 76:447–480.

Lee SM., Rudd R., Woll PJ., Ottensmeier C., Gilligan D., Price A., et al, 2009. Randomized double-blind placebo-controlled trial of thalidomide in combination with gemcitabine and Carboplatin in advanced non-small-cell lung cancer. *Journal of Clinical Oncology*; 27(31):5248–54.

Lee HE., Lee JY., Yang G., Kang HC., Cho Y., Lee HS & Le JY, 2019. Inhibition of NLRP3 inflammasome in tumor microenvironment leads to suppression of metastatic potential of cancer cells. *Scientific Reports*: 9:12277.

Li M., Matsunaga N., Hazeki K., Nakamura K., Takashima K., Seya T., Hazeki O., Kitazaki T & Iizawa Y, 2006. A novel cyclohexene derivative, ethyl (6R)-6- [N-(2- Chloro-4-fluorophenyl) sulfamoyl] cyclohex-1-ene-1-carboxylate (TAK-242), selectivly inhibits toll-like receptor 4-mediated cytokine production through suppression of intracellular signaling. *Molecular Pharmacology*; 69(4):1288–1295.

Li H., Ambade H & Re F, 2009. Cutting Edge: Necrosis Activates the NLRP3 Inflammasome. *Journal of Immunology*; 183(3):1528-1532.

Li Z., Hou Y., Zhao M., Li T., et al, 2020. Serum amyloid a, a potential biomarker both in serum and tissue, correlates with ovarian cancer progression. *Journal of Ovarian Research*; 13:67.

Li R., Ong SL., Tran LM., Jing Z., et al, 2020. Chronic IL-1β-induced inflammation regulates epithelial-to-mesenchymal transition memory phenotypes via epigenetic modifications in non-small cell lung cancer. *Scientific Reports*; 10:377.

Lu YC., Yeh WC & Ohashi PS, 2008. LPS/TLR4 signal transduction pathway. *Cytokine*; 42:145-51.

Maglione PJ., Simchoni N., Cunningham-Rundles C., Ann NY, 2015. Toll-like receptor signaling in primary immune deficiencies. *Proceedings of the National Academy of Sciences of the United States of America*; 1356:1-21.

Malle, E & De Beer FC, 1996. Human serum amyloid A (SAA) protein: a prominent acute-phase reactant for clinical practice. *European Journal of Clinical Investigation*; 26:427 – 435.

Mallea E., Sodin-Semrlb S & Kovacevica A, 2009. Serum amyloid A: An acute-phase protein involved in tumour pathogenesis. *Cellular and Molecular life sciences*; 66(1):9-26.

Mannel A, 2016. The role of Ki-67 in breast cancer. *South African Journal of Surgery*; 54(2):10-13.

Marandi Y., Hasemzade S., Tayebibia H., Karimi J., Zamani A & Khodadadi I, 2021. NLRP3-inflammasome activation is associated with epithelial-mesenchymal transition and progression of colorectal cancer. *Iranian Journal of basic Medicine*; 24(4):483–492.

McInroy L & Maata A, 2007. Down-regulation of vimentin expression inhibits carcinoma cell migration and adhesion. *Biochemical and Biophysical Research and Communications*; 360(1):109-114.

Melgar S., Karlsson A & Michaëlsson E, 2005. Acute colitis induced by dextran sulfate sodium progresses to chronicity in C57BL/6 but not in BALB/c mice: correlation between symptoms

and inflammation. *American Journal of Physiology-Gastrointestinal and Liver*; 288: G1328–38.

Merrel MA., Ilvesaro JM., Lehtonen N., et al, 2006. Toll-like receptor 9 agonists promote cellular invasion by increasing matrix metalloproteinase activity. *Molecular Cancer Research*; 4(7);437-447.

Metzger CE., Narayanan SA., Elizondo JP., Carter AM., et al, 2019. DSS-induced colitis produces inflammation-induced bone loss while irisin treatment mitigates the inflammatory state in both gut and bone. *Scientific Reports*; 9: 15144.

Michaeli A., Finci-Yeheskel Z., Dishon S., Linke RP., Levin M & Urieli-Shoval S, 2008. Serum amyloid A enhances plasminogen activation: Implication for a role in colon cancer. *Biochemical and Biophysical Research Communications*; 368(2):368–373.

Migita K., Kawabe Y., Tominaga M., Origuchi T., Aoyagi T & Eguchi K, 1998. Serum amyloid A protein induces production of matrix metalloproteinases by human synovial fibroblasts. *Laboratory Investigation*; 78:535–539.

Migita K., Izumi Y., Jiuchi Y., Kozuru H., et al, 2014. Serum Amyloid A Induces NLRP-3-mediated IL-1β Secretion in Neutrophils. *PLoS One*; 9(5): e96703.

Mikami T., Yoshida T., Akino F & Motoori T, 2003. Apoptosis Regulation Differs Between Ulcerative Colitis–Associated and Sporadic Colonic Tumours. Association With Survivin and bcl-2. *American Journal of Clinical Pathology*; 119(5):723-30.

Moosavi M., Parsamanesh N., Bahrami A., Atkin SL & Sahebkar A, 2018. Role of the NLRP3 Inflammasome in Cancer. *Molecular Cancer Review*s; 17(1):158.

Mor-Vaknin N., Legendre M., Yu Y., Serezani C., et al, 2013. Murine colitis is mediated by vimentin. *Scientific Reports*; 3:1045.

Mullan RH., Bresnihan B., Golden-Mason L., Markham T., O'Hara R., FitzGerald O., Veale DJ & Fearon U, 2006. Acute-phase serum amyloid A stimulation of angiogenesis, leukocyte recruitment, and matrix degradation in rheumatoid arthritis through an NF-κB–dependent signal transduction pathway. *Arthritis & Rheumathology*; 54:105–114.

Neal MD., Jia H., Eyer B., Good M., Guerriero CJ., et al, 2013. Discovery and Validation of a New Class of Small Molecule Toll-like Receptor 4 (TLR4) Inhibitors. *PLoS One*; 8(6): e65779.

Ning C., Li Y-Y., Wang Y., Han G-C et al, 2002. Complement activation promotes colitis-associated carcinogenesis through activating intestinal IL-1β/IL-17A axis. *Biochemical Pharmacology*; 64(1):1-8.

Oh K., Lee O-Y., Park Y., Seo MW & Lee D-S, 2016. IL-1β induces IL-6 production and increases invasiveness and estrogen-independent growth in a TG2-dependent manner in human breast cancer cells. *BMC Cancer*; 16(1):724.

O'Hanlon DM., Lynch J., Cormican M & Given HF, 2002. The acute phase response in breast carcinoma. *Anticancer Research*; 22:1289 – 1293.

O'Reilly S., Cant R., Ciechomska M., Finnegan J., Oakley F., Hambleton S & van Laar JM, 2014. Serum Amyloid A (SAA) induces IL-6 in dermal fibroblasts via TLR2, IRAK4 and NF-kappaB. *Immunology*; 143(3):331–340.

Ovcaricek T., Frkovic SG., Matos E., Mozina B., & Borstnar S, 2011. Triple negative breast cancer - prognostic factors and survival. *Radiology and Oncology*; 45(1):46-52.

Pandey S., Singh S., et al, 2015. Pattern Recognition Receptors in Cancer Progression and Metastasis. *Cancer Growth Metastasis*; 8:25-24.

Parian A & Lazarev M, 2015. Who and how to screen for cancer in at-risk inflammatory bowel disease patients. *Expert Reviews of Gastroenterology & Hepatology*; 9(6):731-46.

Pileczki V., Braicu C., Gherman CD & Berindan-Neagoe I, 2013. TNF-α gene knockout in triple negative breast Cancer cell line induces apoptosis. *International Journal of Molecular Science*; 14(1):411–420.

Preciado-Patt L., Cahalon L., Hershkovitz R., Lider O., Pras M & Fridkin M, 1998. Serum amyloid A complexed with extracellular matrix induces the secretion of tumor necrosis factor-a by human T-lymphocytes. *Letters in Peptide Science*; 5:349 – 355.

Qiao Y., Jonsson P., Sinha I., Zhao C & Dahlman-Wright K, 2016. AP-1 is a key regulator of proinflammatory cytokine TNFalpha-mediated triple-negative breast cancer progression. *Journal of Biological Chemistry*; 291:18309.

Rakoff-Nahoum S & Medzhitov R, 2009. Toll-like receptors and cancer. *Nature Reviews Cancer*; 9(1):57-63.

Reis-Filho JS., Weigelt B., Fumagalli D & Sotiriou C, 2010. Molecular profiling: moving away from tumor philately. *Science Translational Medicine*; 2:47.

Ridker PM., MacFadyen JG., Thuren T., Everett BM., Libby P & Glynn RJ, 2017. Effect of interleukin-1beta inhibition with canakinumab on incident lung cancer in patients with atherosclerosis: exploratory results from a randomised, double-blind, placebo-controlled trial. *Lancet (London, England)*; 390(10105):1833–1842.

Ross JS., Slodkowska EA., Symmans WF., Pusztai L., Ravdin PM & Hortobagyi GN, 2009. The HER-2 receptor and breast cancer: ten years of targeted anti-HER-2 therapy and personalized medicine. *Oncologist*; 14(4):320-68.

Rossi J., Lu Z., Jourdan M & Klein B, 2015. Interleukin-6 as a therapeutic target. *Clinical Cancer Research*; 21:1248–1257.

Rubin DC., Shaker A & Levin MS, 2012. Murine Colitis is Mediated by Vimentin. *Frontiers in Immunology*; 3:107.

Ryu DW., Jung MJ., Choi WS & Lee CH, 2011. Clinical significance of morphologic characteristics in triple negative breast cancer. *Journal of the Korean Surgical Society*; 80(5):301-306.

Sanguinetti A., Santini D., Bonafe M., Taffurelli M & Avenia N, 2015. Interleukin-6 and pro inflammatory status in the breast tumor microenvironment. *World Journal of Surgical Oncology*; 13: 129.

Salcedo R., Worschech A., Cardone M., Jones Y., et al, 2010. MyD88-mediated signaling prevents development of adenocarcinomas of the colon: role of interleukin 18. *Journal of Experimental Medicine*; 207(8):1625-36.

Sandri S., Rodriguez D., Gomes E., Monteiro HP., Russo M & Campa A, 2008. Is serum amyloid A an endogenous TLR4 agonist? *Journal of Leukocyte Biology*; 83(5):1174-80.

Sato Y., Goto Y., Narita N & Hoon DS, 2009. Cancer Cells Expressing Toll-like Receptors and the Tumor Microenvironment. *Cancer Microenvironment*; 1:205-14.

Schneider MR., Dahlhoff M., Horst D., Hirschi B., et al, 2010. A Key Role for E-cadherin in Intestinal Homeostasis and Paneth Cell Maturation. *PloS ONE*; 5(12): e14325.

Schnoor M, 2015. E-cadherin Is Important for the Maintenance of Intestinal Epithelial Homeostasis Under Basal and Inflammatory Conditions. *Digestive Diseases and Sciences*; 60: 816–818.

Shridas P., De Beer MC & Webb NR., 2018. High-density lipoprotein inhibits serum amyloid A-mediated reactive oxygen species generation and NLRP3 inflammasome activation. *The Journal of Biological Chemistry*; 293(34):13257-13269.

Siegel RL., Miller KD., Fedewa S., Ahnen DJ., et al, 2017. Colorectal cancer statistics, 2017. *CA: A Journal for Clinicians*; 67:177-193.

Siegel RL., Miller KD., Fuchs HE & Jemal A, 2021. Cancer Statistics. *A Cancer Journal for clinicians*; 71:7-33.

Siegmund B, 2010. Interleukin-1beta converting enzyme (caspase-1) in intestinal inflammation. *Biochemical Pharmacology*; 207(8):1625-36.

Sims GP., Rowe DC., Rietdijk ST., Herbst R & Coyle AJ, 2010. Hmgb1 and Rage in Inflammation and Cancer. *Annual Reviews Immunology*; 28:367–388.

Shao X., Lei Z & Zhou C, 2020. NLRP3 Promotes Colorectal Cancer Cell Proliferation and Metastasis via Regulating Epithelial Mesenchymal Transformation. Anti-Cancer Agents in Medicinal Chemistry; 20(7): 820-827.

Slamon DJ, 2001. Use of Chemotherapy plus a Monoclonal Antibody against HER2 for Metastatic Breast Cancer That Overexpresses HER2. *New England Journal of Medicine*;344: 783-792.

Sohma I., Fujiwara Y., Sugita Y., Yoshioka A., Shirakawa M., Moon JH., et al, 2011. Parthenolide, an NF-kappa-B inhibitor, suppresses tumor growth and enhances response to chemotherapy in gastric cancer. *Cancer Genomics and Proteomics*; 8(1):39–47.

Song HK & Hwang DY, 2017. Use of C57BL/6N mice on the variety of immunological research. *Laboratory Animal Research*; 33:119–23.

Soria G., Ofri-Shahak M., Haas I., Yaal-Hahoshen N., et al, 2011. Inflammatory mediators in breast cancer: coordinated expression of TNFα & IL-1β with CCL2 & CCL5 and effects on epithelial-to-mesenchymal transition. *BMC Cancer*; 12(11):130.

Sullivan NJ., Sasser AK., Axel AE., Vesuna F., et al, 2009. Interleukin-6 induces an epithelial–mesenchymal transition phenotype in human breast cancer cells. *Oncogene*; 28(33):2940-7.

Sung H., Ahn J., Yoon Y., Rhim T., et al, 2010. Identification and Validation of SAA as a Potential Lung Cancer Biomarker and its Involvement in Metastatic Pathogenesis of Lung Cancer. *Journal of Proteome Research*; 10(3):1383-1395.

Sutterwala FS., Ogura Y., Szczepanik M., Lara-Tejero M., Lichtenberger GS., Grant EP., et al, 2006. Critical role for NALP3/CIAS1/Cryopyrin in innate and adaptive immunity through its regulation of caspase-1. *Immunity*; 24:317–27.

Takagi H., Kani T., Okazawa A., Kishi Y., Sato T., Takaishi H., et al, 2003. Contrasting action of IL-12 and IL-18 in the development of dextran sodium sulfate colitis in mice. *Scandinavian Journal of Gastroenterology*; 38:837–44.

Tanaka T., Kohno H., Suzuki R, Yamada Y., Sugie S & Mori H, 2003. A novel inflammation-related mouse colon carcinogenesis model induced by azoxymethane and dextran sodium sulfate. *Cancer Science*; 94(11):965-73.

Tang H., Pang S., Wang M., Xiao X., et al, 2010. TLR4 activation is required for IL-17-induced multiple tissue inflammation and wasting in mice. *Journal of Immunology*; 185(4):2563-9.

Thaker AI., Shaker A., Rao MS & Ciorba MA, 2012. Modeling colitis-associated cancer with azoxymethane (AOM) and dextran sulfate sodium (DSS). *Journal of visualized experiments*; 67:4100.

Ting JP., Lovering RC., Alnemri ES., Bertin J., et al, 2008. The NLR gene family: a standard nomenclature. *Immunity*; 28:285–287.

Tschopp J & Schroder K, 2010. NLRP3 inflammasome activation: The convergence of multiple signaling pathways on ROS production? *Nature*: 10:210.

Tsikitis VL., Larson DW., Huebner M., Lohse CM & Thompson PA, 2014. Predictors of recurrence free survival for patients with stage II and III colon cancer. *BMC Cancer*; 14: 336.

Uhlar CM., Burgess CJ., Sharp PM & Whitehead AS, 1994. Evolution of the serum amyloid A (SAA) protein superfamily. *Genomics*; 19(2):228-35.

Uhlar CM & Whitehead AS, 1999. Serum amyloid A, the major vertebrate acute-phase reactant. *European Journal of Biochemistry*; 265(2):501-23.

Urieli-Shoval S., Cohen P., Eisenberg S & Matzner Y, 1998. Widespread expression of serum amyloid A in histologically normal human tissues. Predominant localization to the epithelium. *Journal of Histochemistry and Cytochemistry*; 46:1377-1384.

Veeranki S, 2013. Role of inflammasomes and their regulators in prostate cancer initiation, progression and metastasis. *Cellular and Molecular Biology Letters*; 18(3):355.

Vlasova MA & Moshkovskii SA, 2006. Molecular interactions of acute phase serum amyloid A: possible involvement in carcinogenesis. *Biochemistry*; 71:1051–1059.

Wang Y., Wang K., Han G-C., Wang R-X., et al, 2014. Neutrophil infiltration favors colitis-associated tumorigenesis by activating the interleukin-1 (IL-1)/IL-6 axis. *Mucosal Immunology*; 7:1106-1115.

Wang Y., Kong H., Zeng X., Liu W., Wang Z., Yan X., Hong Y & Xie W, 2016. Activation of NLRP3 inflammasome enhances the proliferation and migration of A549 lung cancer cells. *Oncology Reports*; 35(4):2053-2064.

Wang C., Hockerman S., Jacobsen EJ & Alippe Y, 2018. Selective inhibition of the p38alpha MAPK-MK2 axis inhibits inflammatory cues including inflammasome priming signals. *Journal of Experimental Medicine;* 215:1315–25.

Wang C., Yang T., Xiao J., et al, 2021. NLRP3 inflammasome activation triggers gasdermin D-independent inflammation. *Science Immunology*; 22;6(64):eabj3859.

Wei Q., Mu K., Li T., Zhang Y., Yang Z., Jia X., et al, 2014. Deregulation of the NLRP3 inflammasome in hepatic parenchymal cells during liver cancer progression. *Laboratory Investigation*; 94(1):52.

Weigelt B., Baehner FL & Reis-Filho JS, 2010.The contribution of gene expression profiling to breast cancer classification, prognostication, and prediction: a retrospective of the last decade. *Journal of Pathology*; 220:263–280.

Wu Y., Sarkissyan M & Vadgama JV, 2016. Epithelial-Mesenchymal Transition and Breast Cancer. *Journal of Clinical Medicine*; 5(2):13.

Wu TC., Xu K., Martinek J., Young RR., Banchereau R., George J., et al, 2018. IL1 Receptor antagonist controls transcriptional signature of inflammation in patients with metastatic breast cancer. *Cancer Research*; 78:5243–58.

Xu S., Li X., Liu Y., Xia Y., Chang R & Zhang C, 2019. Inflammasome inhibitors: promising therapeutic approaches against cancer. *Journal of Haematology and Oncology*; 12:64.

Yang H., Wang B., Wang T., Xu L., He C., Wen H., Yan J., Su H & Zhu X, 2014. Toll-like receptor 4 prompts human breast cancer cells invasiveness via lipopolysaccharide stimulation and is overexpressed in patients with lymph node metastasis. *PLoS One*; 9(10): e109980.

Yang H., Zhou H., Feng P., et al, 2010. Reduced expression of Toll-like receptor 4 inhibits human breast cancer cells proliferation and inflammatory cytokines secretion. *Journal of Experimental and Clinical Cancer Research*; 29:92.

Yang M., Liu F., Higuchi K., Sawashita J., Fu X., Zhang L., Zhang L., Fu L., Tong Z & Higuchi K, 2016. Serum amyloid A expression in the breast cancer tissue is associated with poor prognosis. *Oncotarget*; 7(24):35843-35852.

Yazdi AS & Drexler SK, 2013. Regulation of interleukin 1α secretion by inflammasomes. *Annals of the Rheumatic Diseases*;72 Suppl 2: ii96-9.

Yu N., Liu S., Yi X., Zhang S & Ding Y, 2015. Serum amyloid A induces interleukin-1β secretion from keratinocytes via the NACHT, LRR and PYD domains-containing protein 3 inflammasome. *Clinical and Experimental Immunology*; 179(2):344–353.

Yuan Q., Gu J., Zhang J., Liu S., et al, 2021. MyD88 in myofibroblasts enhances colitis-associated tumorigenesis via promoting macrophage M2 polarization. *Cell Reports*; 2;34(5):108724.

Zahid A., Li B., Kombe AJ., Jin T & Tao J, 2019. Pharmacological Inhibitors of the NLRP3 Inflammasome. *Frontal Immunology Reviews*: 10:2538.

Zaki MH., Boyd KL., Vogel P., Kastan MB., Lamkanfi M & Kanneganti T-D, 2010. The NLRP3 inflammasome protects against loss of epithelial integrity and mortality during experimental colitis. *Immunity*; 32(3):379–91.

Zandi Z., Kashani B., Poursani EM., Bashash D., Kabuli M., Momeny M & Mousavi-Pa SH, 2019. TLR4 blockade using TAK-242 suppresses ovarian and breast cancer cells invasion through the inhibition of extracellular matrix degradation and epithelial-mesenchymal transition. *European Journal of Pharmacology*; 853:256-263.

Zhang G., Liu J., Wu L., Fan Y., et al, 2018. Elevated Expression of Serum Amyloid A 3 Protects Colon Epithelium Against Acute Injury Through TLR2-Dependent Induction of Neutrophil IL-22 Expression in a Mouse Model of Colitis. *Frontiers in Immunology*; 9:1503.

Zhou M., McFarland-Mancini MM., Funk HM., Husseinzadeh N., Mounajjed T & Drew AF, 2009. Toll-like Receptor Expression in Normal Ovary and Ovarian Tumors. *Cancer Immunology*; 58(9):1375-85.

Supplementary information

2. In vitro cancer model: does SAA play a role in NLRP3 inflammasome activation?

2.1 Introduction

It is well established that inflammation and persistent infection contributes to several human malignancies where inflammation promotes cancer initiation, development and invasion. An immune response can be induced by inflammation through many cell types including macrophages and neutrophils. As mentioned earlier (in Chapter 1), inflammasomes, such as the NLRP3 inflammasome which is best characterized, are the multi-protein platforms in the innate immune system that induces pro-caspase-1 activation and pro-inflammatory cytokine maturation, such as IL-1β. Over-expression of IL-1β can influence several autoimmune diseases and may result in carcinogenesis. Evidence suggests that NLRP3 inflammasome polymorphisms are related to different malignancies such as breast cancer and CAC. The precise clinical function of NLRP3 in the role of the initiation and promotion of several neoplasms also highlights the therapeutic potential of inflammasomes, and as prognostic markers.

The "two-hit hypothesis" has been proposed for NLRP3 activation. The first hit, "**priming**" can be initiated by LPS *in vitro*. The second hit, referred to as "**activation**" assists the oligomerization of the inactive inflammasome complex (NLRP3, ASC and caspase-1), and can be induced by many factors, including ATP. To determine whether SAA acts as an endogenous DAMP in the TME to promote tumourigenesis, we first had to determine whether the components of the NLRP3 inflammasome can be activated in breast (MDA-MB-231 and MCF-7) and colon (Caco-2, HCT116 and HT29) cancer cell lines. This was confirmed with Western blots, however, no evidence suggesting that the inflammasome components were activated in these cells were observed. Our reagents (ATP and LPS) were tested on THP-1 cells. Therefore, our aim to determine whether SAA functions as an endogenous DAMP that activates the NLRP3 inflammasome in an *in vitro* setting remains to be elucidated.

2.3 Inflammasome activation in THP-1 cells

As optimization to test our reagents, THP-1 cells (monocytes) were treated with LPS (1μg/ml for 4 hours) and ATP (3 mM for 45 minutes). These concentrations were previously used in literature (Shridas *et al*., 2018). Immunoblotting was performed to assess inflammasome components. As seen in the figure below (Figure 1.1), NLRP3 expression was increased in the treated group versus the control group. Cleaved caspase-1 was also detected in these cells.

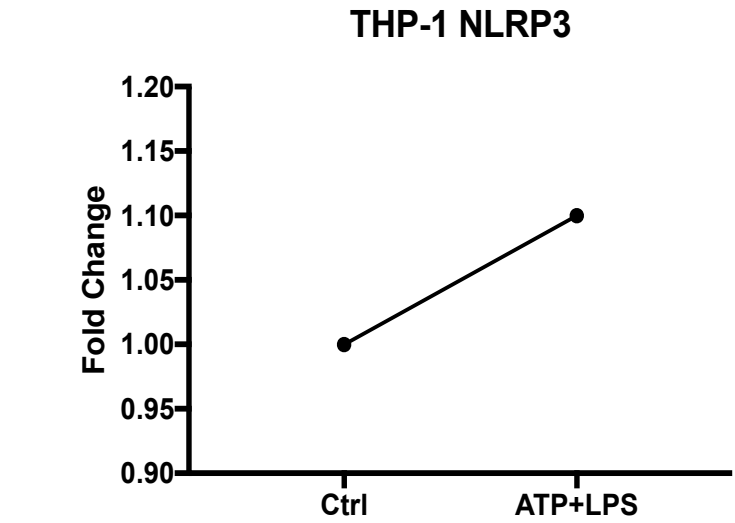

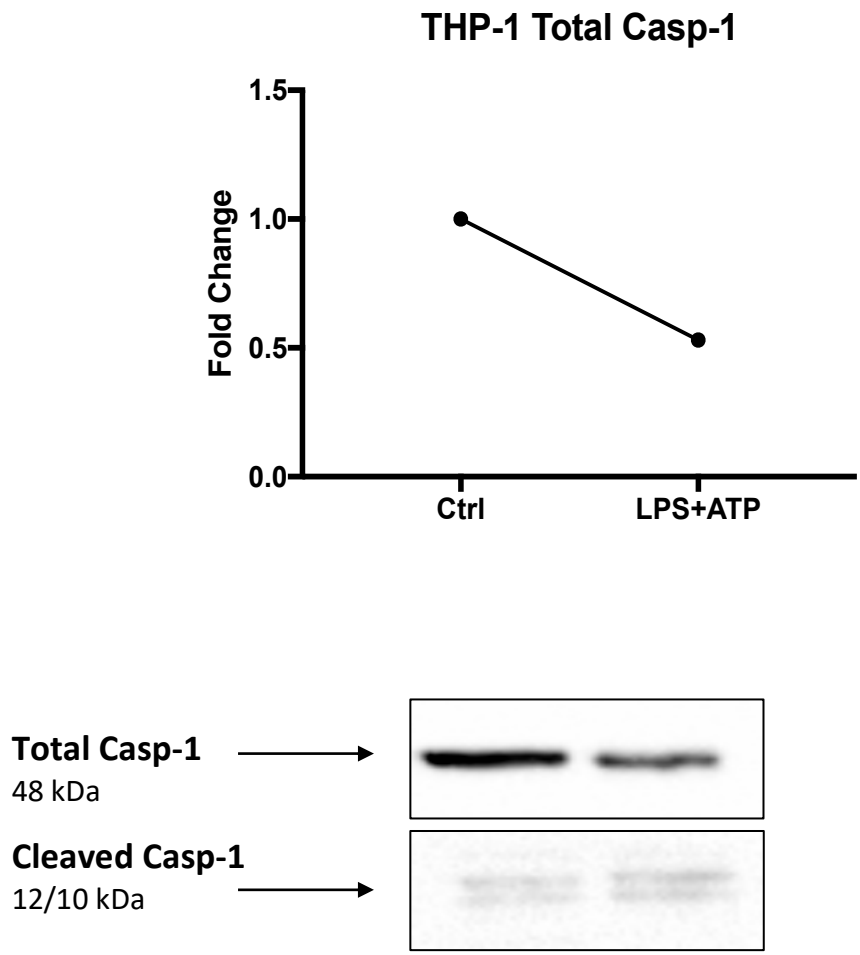

Figure 1.1*:* Western blot analysis to detect NLRP3 inflammasome components in THP-1 cells. Proteins were separated by SDS-PAGE and transferred to a nitrocellulose membrane for analysis. Results are presented as mean ± SEM (n=1).

2.4 LPS and ATP treatment in cancer cells

All five cancer cell lines were treated with 1 μg/ml LPS for 4 hours and during the last hour, ATP was added (3 mM) for 45 minutes (L+A). As seen in the figure below, caspase-1 expression was barely detected in these cell lines. Furthermore, No NLRP3 expression was observed.

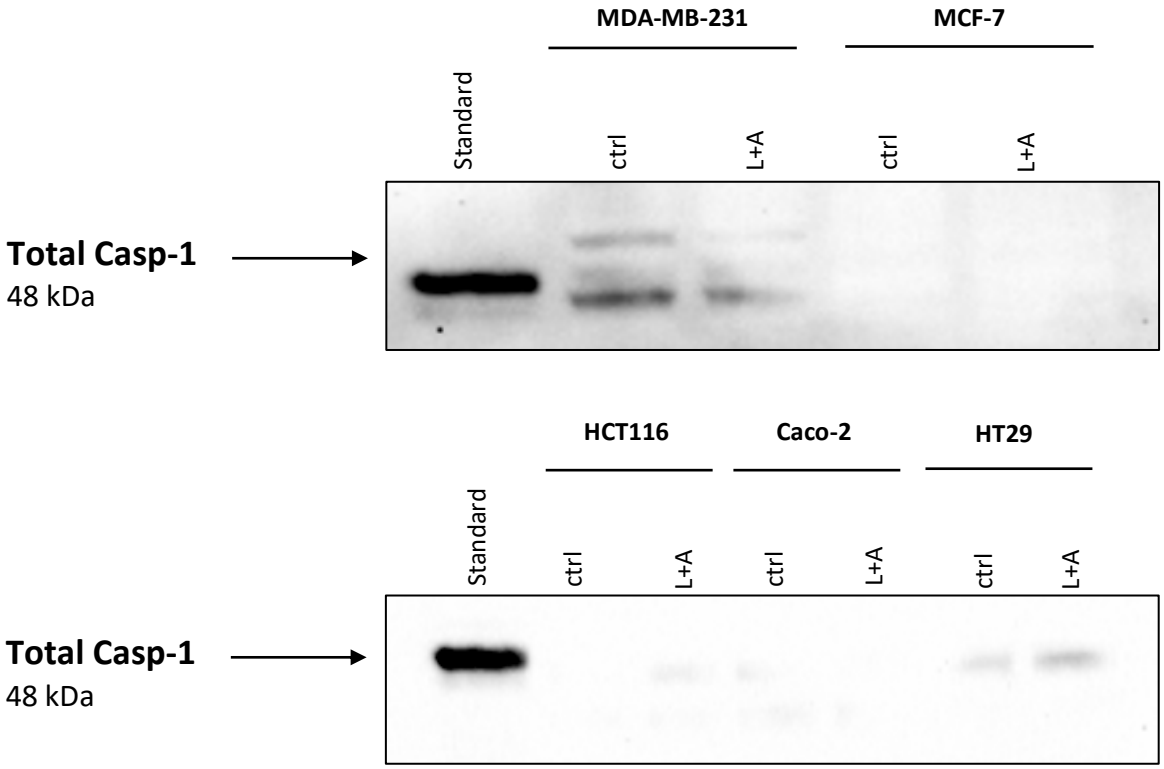

Figure 1.2: Western blot analysis to detect NLRP3 inflammasome components in cancer cells. All five cancer cell lines were treated with 1 μg/ml LPS for 4 hours and during the last hour, ATP was added (3 mM) for 45 minutes (L+A). Proteins were separated by SDS-PAGE and transferred to a nitrocellulose membrane for analysis.

Based on the results above (Figure 1.2), the treated groups were subjected to longer LPS treatment durations as well as increased concentrations and longer treatment periods with ATP. Similar to the above-mentioned results, no NLRP3 expression was observed. No cleaved caspase-1 bands were detected in these samples. Results are only shown for MDA-MB-231 and MCF-7 cells (breast cancer).

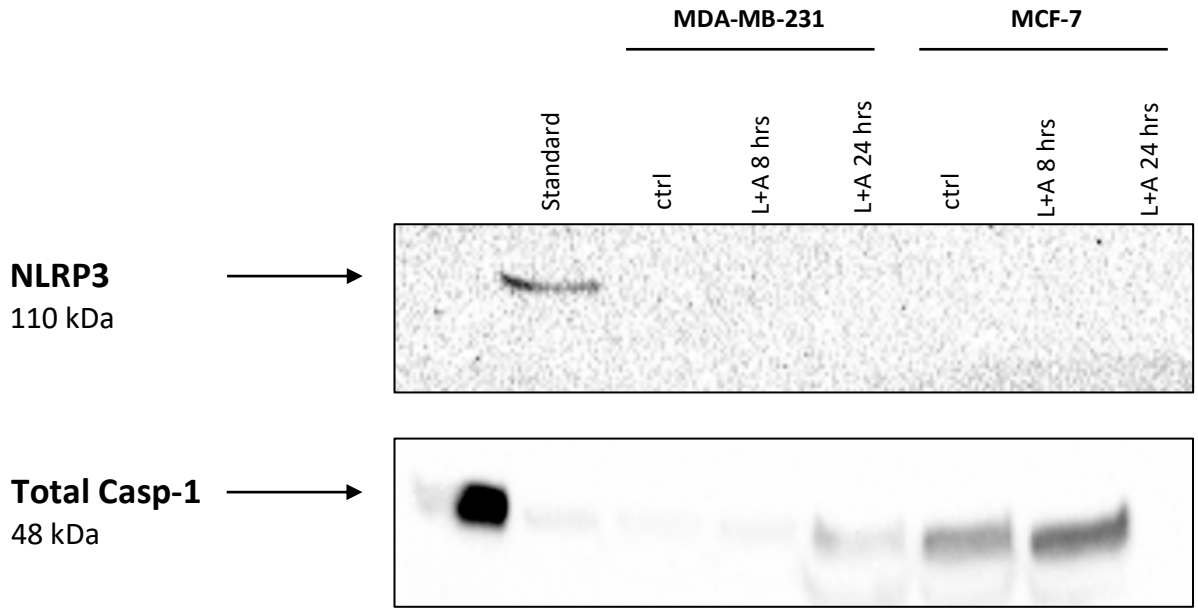

Figure 1.2: Western blot analysis to detect NLRP3 inflammasome components in cancer cells. All five cancer cell lines were treated with 1 μg/ml LPS for 8 and 24 hours and during the last hour, ATP was added (5 mM) (L+A). Proteins were separated by SDS-PAGE and transferred to a nitrocellulose membrane for analysis.

Following the 8 hours LPS treatment duration, cancer cells were treated with 1 μg/ml LPS for 24 and 48 hours, respectively, and 5 mM ATP for 2 hours. No NLRP3 expression is observed in breast cancer cells. Caspase-1 results are shown for colon cancer cells.

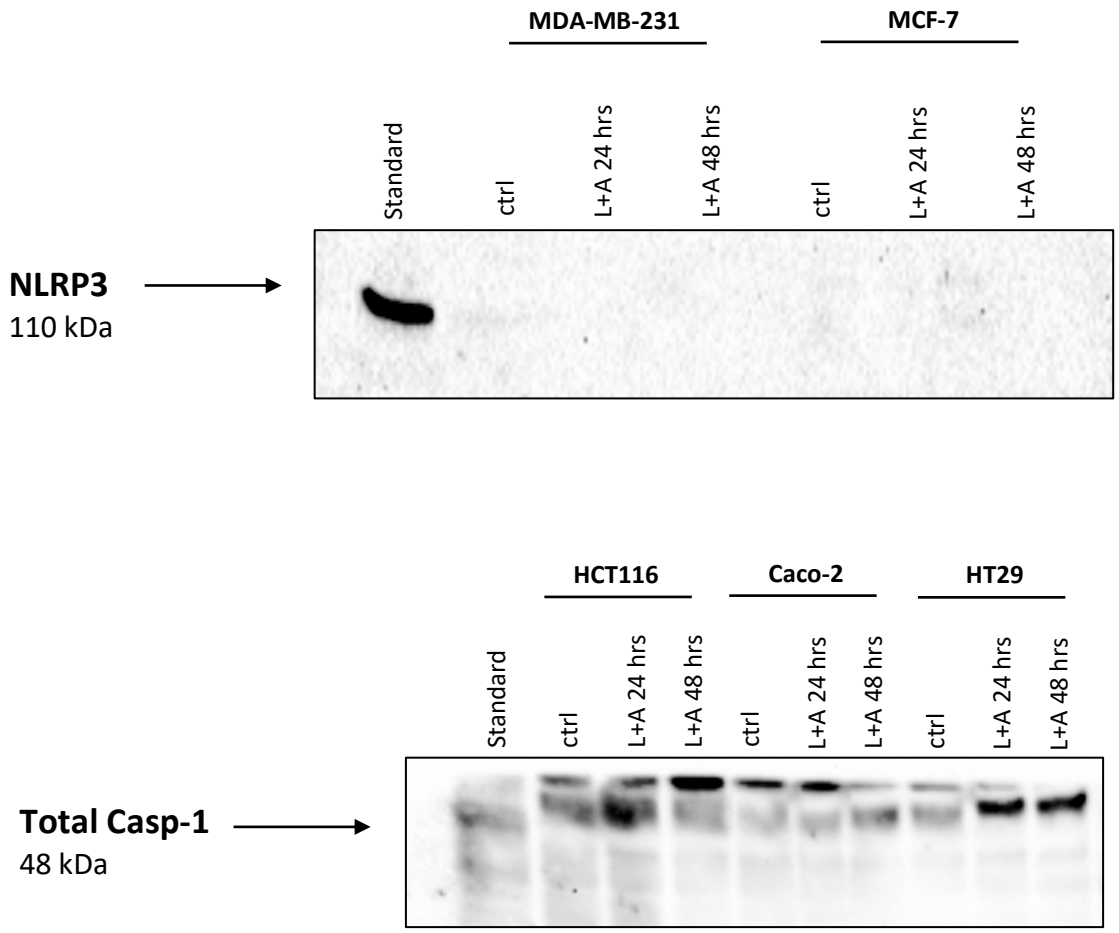

Figure 1.3*:* Western blot analysis to detect NLRP3 inflammasome components in cancer cells. All five cancer cell lines were treated with 1 μg/ml LPS for 24 and 48 hours and ATP (5 mM) for 2 hours (L+A). Proteins were separated by SDS-PAGE and transferred to a nitrocellulose membrane for analysis.

The next step was to determine whether SAA activates the NLRP3 inflammasome, since it has been shown that SAA induces NLRP3 activation without priming stimulation. However, similar to the LPS and ATP treatments, NLRP3 expression was not observed in the breast cancer or colon cancer cells. Total caspase-1 was detected in MDA-MB-231, HCT116 and Caco-2 cells, but no cleaved caspase-1 bands were observed.

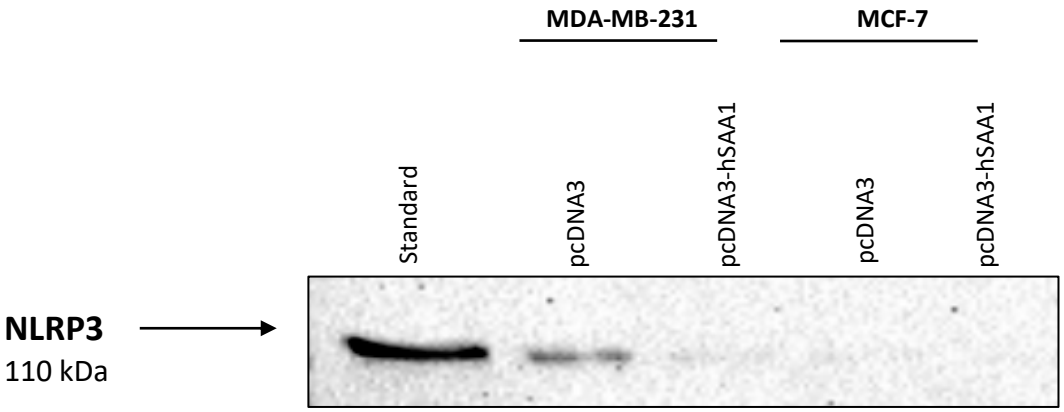

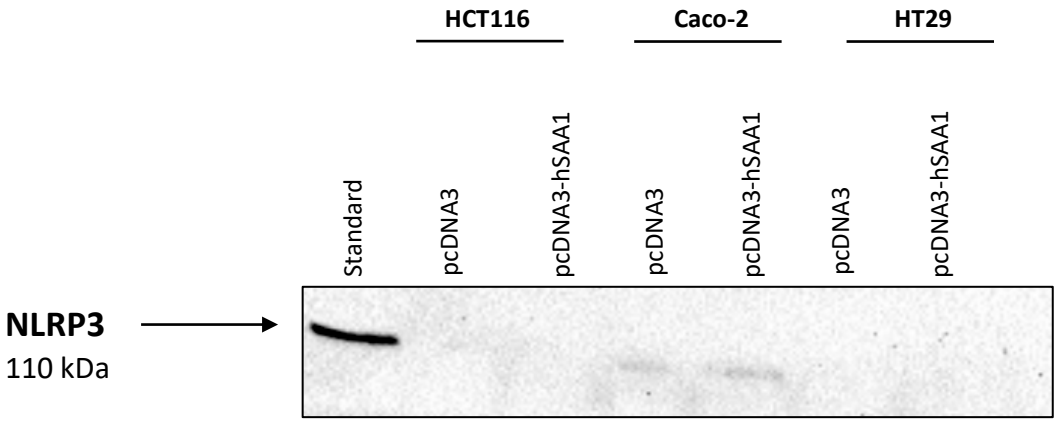

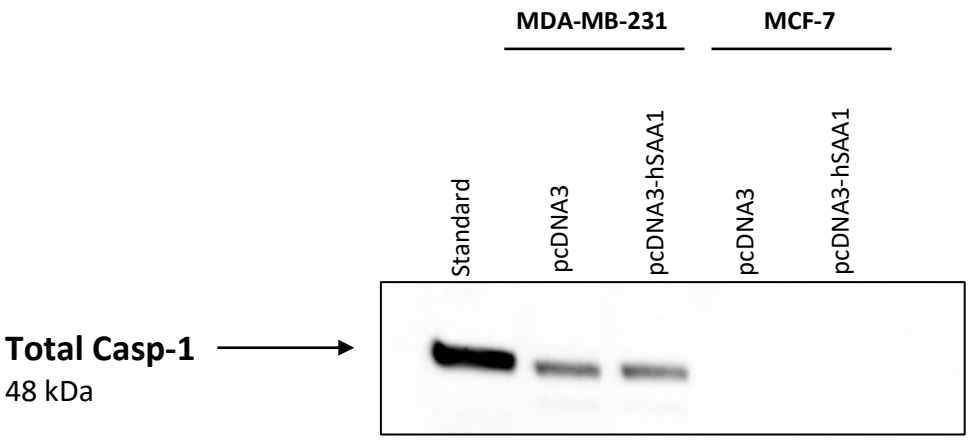

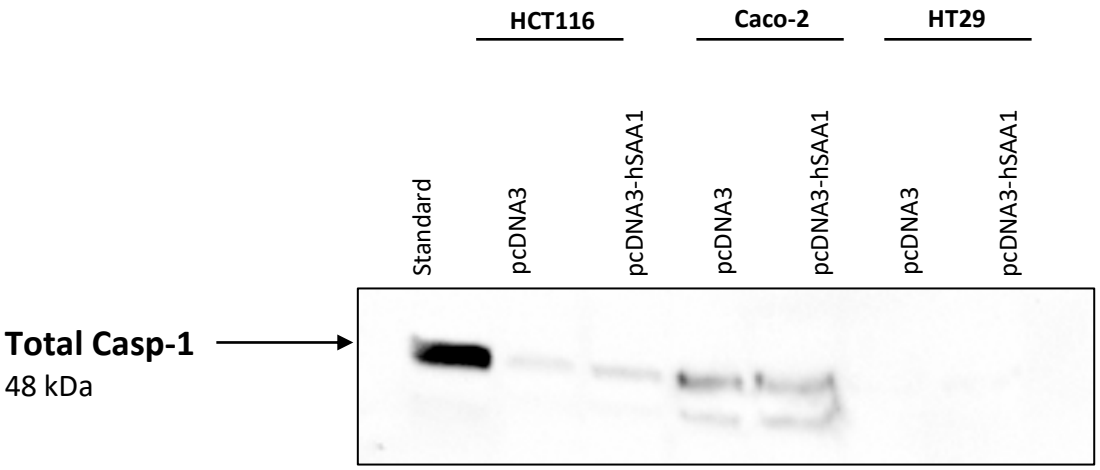

Figure 1.3*:* Western blot analysis to detect NLRP3 inflammasome components in cancer cells after SAA transfection. All five cancer cell lines were transfected with SAA for 72 hours. Proteins were separated by SDS-PAGE and transferred to a nitrocellulose membrane for analysis.

In conclusion, it is possible that these cancer cells lack the components of the NLRP3 inflammasome such as NLRP3 and caspase-1. However, studies have shown that NLRP3 activation does occur in cancer cells. Wang and authors stimulated A549 lung cancer cells with 1 µg/ml LPS for 8 hours with or without 5 mmol/l ATP for the last half an hour. The authors found that many intracellular NLRP3 and ASC colocalizations were present in punctate spot style after the stimulation of LPS+ATP but less NLRP3 and ASC colocalizations were detected in the control group and the LPS or ATP single-treated group. Western blot analysis also showed that the expression of active caspase-1 p10 significantly increased by stimulation of LPS+ATP (Wang *et al*., 2016). It is therefore possible that the protocol for NLRP3 inflammasome activation should be further optimized, specifically for these breast and colon cancer cell lines.